

DISSERTATION

GLUCOCORTICOID-DEPENDENT REGULATION OF MOLECULAR CLOCKS AND
DENDRITIC SPINES IN THE VENTROMEDIAL PREFRONTAL CORTEX

Submitted by

Alex M. Miller

Department of Biomedical Sciences

In partial fulfillment of the requirements

For the Degree of Doctor of Philosophy

Colorado State University

Fort Collins, Colorado

Summer 2022

Doctoral Committee:

Advisor: Stuart Tobet

Jozsef Vigh
Jim Bamburg
Ryan Maresh

Copyright by Alex Michael Miller 2022

All Rights Reserved

ABSTRACT

GLUCOCORTICOID-DEPENDENT REGULATION OF MOLECULAR CLOCKS AND DENDRITIC SPINES IN THE VENTROMEDIAL PREFRONTAL CORTEX

Biological rhythms in the brain and periphery are governed by the suprachiasmatic nucleus of the hypothalamus (SCN) and the SCN's control of rhythmic adrenal glucocorticoid (GC) secretions via the hypothalamic pituitary adrenal (HPA) axis. The daily surge of GC secretions aid in the entrainment of molecular clocks throughout the body which physically, mentally, and metabolically prime an organism to function in accordance with the external light:dark (L:D) cycle. When key events of biological rhythms fail to match up with the external L:D cycle, various pathologies arise in the brain and periphery. To better understand the neural basis of pathologies caused by the disruption of biological rhythms, further investigation of key limbic regulatory brain regions is required. Thus, the studies described in this dissertation examine how biological rhythms in the ventromedial prefrontal cortex (vmPFC) are regulated by GC secretions.

The vmPFC regulates fear acquisition, fear extinction, mood, and HPA axis function. Multiple brain regions exhibit time-of-day dependent variations in learning, long term potentiation (LTP), and dendritic morphology. GCs have been implicated in the regulation of dendritic structure in the context of stress. GCs are also known to regulate molecular clock entrainment via upregulation of *Per1* transcription in a variety of tissues. In the present study, C57BL/6N mice were sacrificed at 3 distinct times of day (ZT3, ZT12, and ZT16, lights off at ZT12) and *Per1* mRNA expression was measured in the infralimbic and prelimbic vmPFC subregions using droplet digital (dd)PCR after recovering from adrenalectomy or sham surgery for 10 days. Sham mice showed *Per1* rhythmicity in both IL and PL, with peak expression occurring at ZT12. Adrenalectomized mice showed reductions in *Per1* amplitude at ZT12 in both

IL and PL, suggesting that the vmPFC molecular clock is entrained by diurnal GC oscillations. Thy1-eGFP mice were used to visualize and quantify dendritic spine density on layer V pyramidal dendrites at ZT 3, 12, and 16. Spine density in both PL and IL exhibited changes between the light (inactive) and dark (active) phases, with peak spine density observed at ZT16 and trough spine density observed at ZT3. These changes in spine density were restricted to changes in long thin and stubby type spines. To determine if changes in spine density is regulated by diurnal GC oscillations, the 11 β -hydroxylase inhibitor metyrapone was administered 2 hours prior to the onset of the active phase (ZT10) daily for 7 days. Metyrapone administration blocked both the diurnal peak of plasma corticosterone and peak spine densities in the IL and PL at ZT16. These results suggest that vmPFC molecular clock gene and dendritic spine diurnal rhythms depend on intact diurnal GC oscillations. These findings establish a link between diurnal GC oscillations, the molecular clock, and synaptic plasticity. Additionally, these findings describe how the vmPFC changes across 24-hour periods, which provides a foundation for further investigation into how biological rhythms in the vmPFC may be altered in the context of circadian disruption, and how specific disease states may arise as a result.

ACKNOWLEDGEMENTS

I am incredibly grateful for my time spent with my late mentor, Dr. Bob Handa. His knowledge and expertise were vast, and he was a kind and generous advisor. Even after I performed poorly on his unit exam in BMS500, he gladly met with me and welcomed me as a rotation student with open arms. He trusted me to work independently, but also gave me valuable guidance whenever I got stuck or asked for help. Even in the darkest parts of my PhD student journey, you believed in me. None of this was easy, and I would not have made it to the finish line without your support. You were an essential part of my path to success as a PhD student, and I wish more than anything that you could be here to see me out. I wish we could all go out to Boyd lake again. You will be dearly missed.

I am also grateful to my committee members, Dr. Stu Tobet, Dr. Jozsef Vigh, Dr. Jim Bamburg, and Dr. Ryan Maresh. They have been available when I need guidance and were very helpful in giving me multiple perspectives regarding my specific project and regarding scientific inquiry in general. Thank you all for staying the course with me throughout this turbulent journey and thank you for helping me see the forest whenever I was focusing too closely on the trees. I would like to thank Dr. Tobet especially for stepping up as my advisor after Dr. Handa passed. By taking in our orphaned lab, you assumed countless additional responsibilities on top of your already packed calendar. Your efforts have not gone unnoticed, and I am grateful for your help in getting me to the finish line. I would also like to thank Dr. Maresh for letting me teach for you. I was lucky to be picked as your first GTA when you were an incoming professor, and I hope to carry the skills I've honed into the next chapter.

I have been lucky to work with an incredibly knowledgeable, supportive, and friendly group of people in the Handa lab during my time here. Thank you to Dr. Mario Oyola, Dr. Ashley Heck, Dr. Allie Holschbach, Dr. Brad Hammond, Dr. Amanda Borrow, and Sara Watson for your time spent training me as a younger graduate student. Thank you to Renata Daniels, Julietta

Sheng, Hayley Templeton, Mina Roueinfar, Emily Castellanos, Natalie Bales, and Theo Fleury for being wonderful and supportive friends and colleagues. A special thank you to Renata Daniels for your abundant support, humor, and creativity. I loved having a musical collaborator to play with to help offset the stress of grad school, and I am grateful that you are in my life.

Thank you to so many of my past teachers and professors for encouraging me to push my limits and realize this goal. Thank you to Mr. Taber, Ms. Zerbonia, and Mr. Huberman. You were some of the first teachers that made me feel intelligent and capable. Thank you to Dr. Bob Tallitsch, Dr. Scott Gehler, Dr. Greg Domski, Dr. Jose Boquin, Dr. Ian Harrington, Dr. Shara Stough, and Dr. Rupa Gordon for helping me realize my passions for biology, neuroscience, and teaching in general. I look up to all of you as excellent role models, and I hope to one day convey the passion and effort that every one of you displayed when I was in your classes.

I would like to acknowledge and sincerely thank every one of my past students that I have had the privilege to teach at CSU. You have taught me countless lessons as I've developed into an educator and scientific communicator, and I am forever grateful for them. Thank you for the much-needed breaks from lab work, and thank you for helping me find my passion.

Thank you to my pets, Reggie, Elisa, Willow, and Charlie. You will never know what I was up to at CSU, but I relied on your love the whole time. Thank you to CSU's lab animal resources for allowing me to adopt my sweet lab cats Elisa and Willow. Other than my degree, those two goofy cats were the best thing to come out of my time at CSU.

Last, but certainly not least, I would like to thank my family members and friends for their enduring support, especially my wife, Meridith. You are my best friend, my adventure buddy, and my closest confidant. You've supported me through some of the lowest lows and biggest triumphs that I've encountered in my life so far, and I simply could not have done this without you. When we stand together, there is no challenge that we can't overcome. I love you and I sincerely thank you for everything that you have done and continue to do for me.

TABLE OF CONTENTS

ABSTRACT.....	ii
ACKNOWLEDGEMENTS.....	iv
LIST OF FIGURES.....	viii
Chapter 1: The Neuroendocrine Control of Biological Rhythms and Dendritic Spines.....	1
1.1 Summary.....	1
1.2 Introduction.....	2
1.3 The Hypothalamic Pituitary Adrenal (HPA) Axis.....	4
1.4 Biological Rhythms.....	9
1.5 The Molecular Basis of Biological Rhythmicity in Mammals.....	11
1.6 The Suprachiasmatic Nucleus, the Brain's Master Clock.....	15
1.7 Neuroendocrine Regulation of Biological Rhythms.....	22
1.8 Dendritic Spines and Synaptic Plasticity.....	28
1.9 Specific Hypotheses and Conclusion.....	36
Chapter 2: Glucocorticoid Regulation of Diurnal Spine Plasticity in the Murine Ventromedial Prefrontal Cortex.....	38
2.1 Summary.....	38
2.2 Introduction.....	39
2.3 Materials and Methods.....	41
2.4 Results.....	48
2.5 Discussion.....	59
2.6 Conclusion.....	63
Chapter 3: Conclusion.....	65
3.1 Summary.....	65
3.2 Conclusions Drawn from the Present Study.....	65
3.3 Significance.....	68
3.4 Limitations of the Present Study.....	72
3.5 Mechanistic Considerations.....	74
3.6 Possible Future Directions.....	76

3.7 Human Relevance.....	78
3.8 Concluding Remarks.....	80
References.....	82
List of abbreviations.....	98

LIST OF FIGURES

Figure 1.1: Anatomy of the HPA Axis.....	8
Figure 1.2: Core clock gene transcriptional-translational feedback loop.....	13
Figure 1.3: SCN control of HPA axis schematic.....	20
Figure 1.4: GCs influence core clock gene transcription.....	23
Figure 1.5 Examples of spine subtype morphologies.....	31
Figure 2.1: vmPFC Per1 transcriptional rhythmicity is disrupted in response to adrenalectomy.....	50
Figure 2.2: Glucocorticoid receptor (GR) is colocalized with eGFP+ vmPFC layer V pyramidal neurons.....	51
Figure 2.3: A diurnal rhythm in spine density is detected in PL layer V pyramidal neurons.....	53
Figure 2.4: A diurnal rhythm in spine density is detected in IL layer V pyramidal neurons.....	55
Figure 2.5: Disruption of CORT rhythmicity via repeated metyrapone injections prior to light offset diminishes spine rhythmicity.....	58-59
Figure 3.1: Graphical Summary of Current Findings.....	66

CHAPTER 1

THE NEUROENDOCRINE CONTROL OF BIOLOGICAL RHYTHMS AND DENDRITIC SPINES

1.1 Summary

Biological rhythms regulate every aspect of physiology and cell function in nearly all forms of life. Humans have spent most of their existence evolving along with natural light cues from the sun in the absence of artificial lighting. Since the invention of artificial lighting, our species has been encountering the unprecedented challenge of adapting to an increasingly modernized world capable of generating abundant light cues at all times of day and night. Despite the staggering amount of past work conducted to understand the nature of timekeeping in living organisms, much is left unknown and unanswered. The ventromedial prefrontal cortex (vmPFC) is important for the appraisal of aversive stimuli, sociability, affective behaviors, and the regulation of the neuroendocrine response to stress. However, the influence of biological rhythms on vmPFC function is largely understudied. This chapter provides a review of biological rhythms in mammals, including descriptions of molecular/genetic mechanisms of timekeeping, the role of the suprachiasmatic nucleus (SCN) in generating and maintaining rhythms synchronized to the light:dark cycle, and the neuroendocrine mechanisms utilized to entrain other biological rhythms to the SCN's master rhythm with special attention paid to the vmPFC. Specifically, the role of rhythmic glucocorticoid (GC) secretions in the maintenance of biological rhythms throughout the body and brain is emphasized. Background on synaptic plasticity and dendritic spine function and regulation is provided, followed by a discussion on long-term potentiation (LTP) and learning as a potential function of the circadian clock. Each of these factors are tied together with an introduction of the emerging story of diurnal rhythms of dendritic spine plasticity in the brain. Finally, gaps in our knowledge of biological rhythms within the

vmPFC are identified and a brief outline of the experimental approaches utilized in this dissertation is provided.

1.2 Introduction

One ever-present aspect of the world in which we live is the cycle between day and night. Nearly all living organisms are influenced by this cycle and exhibit widespread rhythmic changes in function corresponding with the phase of the day night cycle. These daily changes are observable in every domain of life and at every level of biological complexity, ranging from basic cellular metabolic processes like rhythms in redox reactions and gene expression, to higher levels of complexity like the rhythmic regulation of body temperature, tissue and organ function, hormone secretions, locomotor activity, sleep, alertness, and even learning^{1,2}. These widespread changes to cellular function, physiology, and behavior exist to optimize performance and ensure that resources and energy are expended or conserved properly to accommodate the various challenges and environmental variations that accompany different times of day.

For humans, our biological rhythms ensure that we stay active and vigilant during the daytime and conserve energy at night. Biological rhythms permeate nearly all aspects of human life and civilization, ranging from waking up at approximately the same time every morning, daily routines and rituals like a morning fitness regimen, coffee, breakfast, the morning rush hour, 9am-5pm workdays, and the tendency to fall asleep at approximately the same time every night. We can also anecdotally observe the importance of biological rhythms in optimizing human performance in everyday life with examples of slight disturbances to our rhythms, evidenced by complaints of tiredness and increased irritability of co-workers following spring daylight savings clock shifting in the United States, or by witnessing the abnormal sleep and activity rhythms of an individual readjusting to their normal time zone after returning from international travel. Despite these practical examples of how biological rhythms influence our everyday life, so much has yet to be discovered about how biological rhythms influence physiology and behavior, and how the disruption of those rhythms can impact health and wellbeing.

The prefrontal cortex (PFC) is perhaps one of the most enigmatic cortical regions of the brain. Phineas Gage's famous injury sustained from an iron rod piercing his skull gave us our first glimpse into the function of the prefrontal cortex³. After recovering from his injury, Gage had a radically transformed personality. He was previously considered a responsible, intelligent, and well adapted individual. After his injury, he was noted as rude, irreverent of social conventions, prone to mood swings, irresponsible, and unable to hold a job³. Since this famous case, formal study of the PFC has implicated its role in the regulation of many complex behaviors that Gage showed deficits in, including executive function, decision making, impulse inhibition, cognitive flexibility, emotion, social interactions, and many more. In a sense, the human PFC is what makes us uniquely human. Accordingly, as primates have evolved, their PFCs have grown and differentiated beyond those of other mammals, possessing some PFC subregions that are structurally and functionally unique⁴. Humans represent the apex of primate PFC differentiation, with the human PFC constituting approximately 30% of total cortical area⁴. While this PFC differentiation is considered necessary for the emergence of human-specific behaviors and qualities, some PFC subregions are conserved across species.

The rodent ventromedial prefrontal cortex (vmPFC) shares many structural and functional similarities with two PFC subregions in humans⁴⁻⁸. In rodents, the infralimbic (IL) and prelimbic (PL) vmPFC is considered structurally and functionally homologous with Brodmann areas (BA) 25 and 32 in humans^{6,9-12}. The vmPFC is responsible for the regulation of a wide variety of cognitive, emotional, and endocrine processes relevant to stress and affective disorders^{5,13,14}. The roles of diurnal GC signaling and the circadian clock in the regulation of vmPFC structure and function are understudied. My dissertation aims to elucidate how the vmPFC may be influenced by these factors. Investigating the influences of GC signaling and the circadian clock on the rodent vmPFC may provide valuable insights into how circadian disruptions contribute to the etiology of affective disorders in humans.

The first chapter of my dissertation reviews basic mechanisms of timekeeping in mammals, ranging from rhythms in gene expression to the neuronal circuits that regulate the diurnal rhythm of glucocorticoid (GC) secretion. A review of dendritic spines and synaptic plasticity will be provided, emphasizing the role of GC signaling in the regulation of these factors. I also define the emerging roles of diurnal glucocorticoid (GC) signaling and the circadian clock in the regulation of synaptic plasticity and dendritic spine structure in the brain. By discussing common GC-mediated and circadian clock-mediated effects on dendritic morphology and synaptic plasticity in other extensively studied brain regions, I provide a framework for my overarching hypothesis that similar rules also apply to the regulation of the vmPFC. Finally, the chapter concludes with the identification of specific hypotheses and proposed experiments that are addressed in the following chapter.

1.3 The Hypothalamic-Pituitary-Adrenal (HPA) Axis

A brief history of stress and adrenal secretions

In the 1930s, physiologist Hans Selye described a common set of symptoms that appear in rats in response to various modalities of adverse stimuli, ranging from cold exposure, injuries sustained from surgery, excessive exercise, and delivery of sublethal doses of various drugs¹⁵. The common symptoms occur in three distinct stages. The first stage occurs within hours of the initial stimulus, characterized by rapid reductions in the size of lymphatic tissues and liver, decreases in visceral adiposity, loss of muscular tone, a fall in body temperature, and a reduction of chromaffin granules and lipid structures in the adrenal medulla and cortex, respectively. The second stage, occurring ~48 hours after the initial stimulus, is characterized by enlarged adrenal glands with restored lipid structures in the adrenal cortex, thyroid hyperplasia, cessation of body growth, gonadal atrophy, and cessation of lactation in females. Late in the second stage, if animals continue to be exposed to the stimulus, the appearance and function of affected tissues remarkably return to normal. The third stage arises through long

term exposure to the adverse stimulus over the course of months, which causes the animals to present with symptoms that mimic the first stage of symptoms. This pattern of was consistent regardless of stimulus modality, which led Selye to conclude that the symptoms are independent of the stimuli administered and are instead an adaptive response to the damage caused by the various stimuli. Thus, the term “general adaptation syndrome” was coined¹⁵. This “general adaptation syndrome” turned out to be a strikingly accurate description of widespread physiological changes that accompany exposure to stress.

Selye’s work implicated the adrenal and pituitary glands in the regulation of physiological changes associated with the stress response¹⁶. Stressed animals typically show reduction in thymus size. When adrenalectomized, stressed rats appear resistant to reductions in thymus size. Stress-induced thymus reductions are blocked by hypophysectomy, but hypophysectomized rats also display atrophied adrenal glands. These findings demonstrate that stress-induced reductions in thymus size are mediated by both the pituitary and adrenal glands, and that there is a hierarchical organization of the endocrine stress axis¹⁶. Specifically, the pituitary regulates the adrenal response to stress. Accordingly, GCs, steroids released from the adrenal cortex in response to pituitary-released adrenocorticotrophic hormone (ACTH), were isolated in the next decade by Edward Kendall¹⁷. Despite Selye’s apt descriptions of the mammalian stress response and its dependence on pituitary and adrenal function, the factors regulating anterior pituitary secretions remained unclear.

Hypothalamic control of pituitary function

In 1955, the anatomist Geoffrey Harris hypothesized that anterior pituitary hormone secretions are regulated by hypothalamic releasing factors that are secreted into the hypophyseal portal vasculature¹⁸. Harris noted that, while the posterior pituitary is robustly innervated by the paraventricular nucleus (PVN) and supraoptic nucleus (SON) of the hypothalamus, the anterior pituitary lacks well defined innervation and is highly vascularized via

the hypophyseal portal system, a dense network of blood vessels connecting the hypothalamus to the anterior pituitary. He also observed that hypophyseal portal vasculature can readily regenerate after being cut. Harris demonstrated a functional relationship between hypothalamus and anterior pituitary through a series of surgical experiments.

In one experiment, Harris severed the pituitary stalk from the median eminence, a highly vascularized structure linking the hypothalamus to the pituitary. Rat estrus cycles were assessed postoperatively as a readout of pituitary gonadal regulation¹⁹. A vast majority of stalk-sectioned rats had estrus cycles, and one was mated and successfully carried a pregnancy to term. Post-mortem examination of the sectioned pituitary stalk showed regenerated hypophyseal portal vasculature as early as one day after surgery. Harris then sectioned the pituitary stalk and implanted a plate of paper between the severed stalk and the median eminence. Following surgery, implanted rats lacked estrus cycles. Post-mortem examination showed a lack of portal vasculature regeneration¹⁹. In a separate study, Harris further demonstrated hypothalamic-pituitary regulation by hypophysectomizing rats and grafting pituitary tissue taken from other rats into the temporal lobe, within the hypophyseal capsule, or below the median eminence²⁰. All grafted pituitary tissue was vascularized and remained viable regardless of graft location, but only grafts under the median eminence were incorporated into the hypophyseal portal vasculature. Hypophysectomized rats with pituitary grafts in temporal lobe and hypophyseal capsule lacked estrus cycles. Rats with pituitary grafts under the median eminence had intact estrus cycles, were mated, and successfully carried pregnancies to term. Temporal lobe- and hypophyseal capsule-grafted rats displayed atrophied ovaries, adrenals, and thyroid glands. Median eminence-grafted rats displayed no atrophy in ovaries, adrenals, and thyroid glands²⁰. Together, these results support Harris' hypothesis that secretion of anterior pituitary hormones are under control of hypothalamic releasing factors via the hypophyseal portal system.

Harris did not isolate or characterize hypothalamic releasing factors in his lifetime, but he did provide a framework of three requirements that must be met for his releasing factor hypothesis to be established¹⁸. First, the putative releasing factor must be found in the hypophyseal portal vasculature in greater concentrations than systemic blood. Second, the concentration of the releasing factor must change in response to electrical or reflex activation of the hypothalamic nerve tracts that supply the hypophyseal portal system. And third, activity of the anterior pituitary must change in response to varying concentrations of the putative releasing factor¹⁸. The first releasing factor that met all three of Harris' requirements was demonstrated 20 years later with the isolation of gonadotropin-releasing hormone (GnRH)²¹. Then, a decade after the discovery of GnRH, corticotropin releasing hormone (CRH) was finally isolated and characterized²².

Anatomy and physiology of the HPA axis

The HPA axis encompasses a series of neuroendocrine stimulatory pathways and feedback loops involving the hypothalamus, anterior pituitary gland, and adrenal gland (**Fig 1.1**). The HPA axis, at its highest level, comprises a group of neurons that are found within the PVN which synthesize and secrete the hypothalamic releasing factor corticotropin releasing hormone (CRH)²². The release of PVN CRH to the hypothalamo-hypophyseal portal vasculature controls the release of the anterior pituitary hormone adrenocorticotrophic hormone (ACTH) into the general circulation²³⁻²⁵. Circulating ACTH acts upon the zona fasciculata of the adrenal cortex to induce the synthesis of glucocorticoid (GC) hormones, of which cortisol is the predominate form in humans, and corticosterone (CORT) is the predominate form in rats and mice²⁶. From there, newly synthesized GCs diffuse into the general circulation to act on cells that express glucocorticoid receptor (GR). GR ligand binding primarily results in the regulation of gene transcription of a multitude of genes

that have glucocorticoid response elements (GREs) on or near their promoters. The consequences of GC secretion are widespread; virtually every nucleated cell in the body is influenced by GC signaling to some degree.

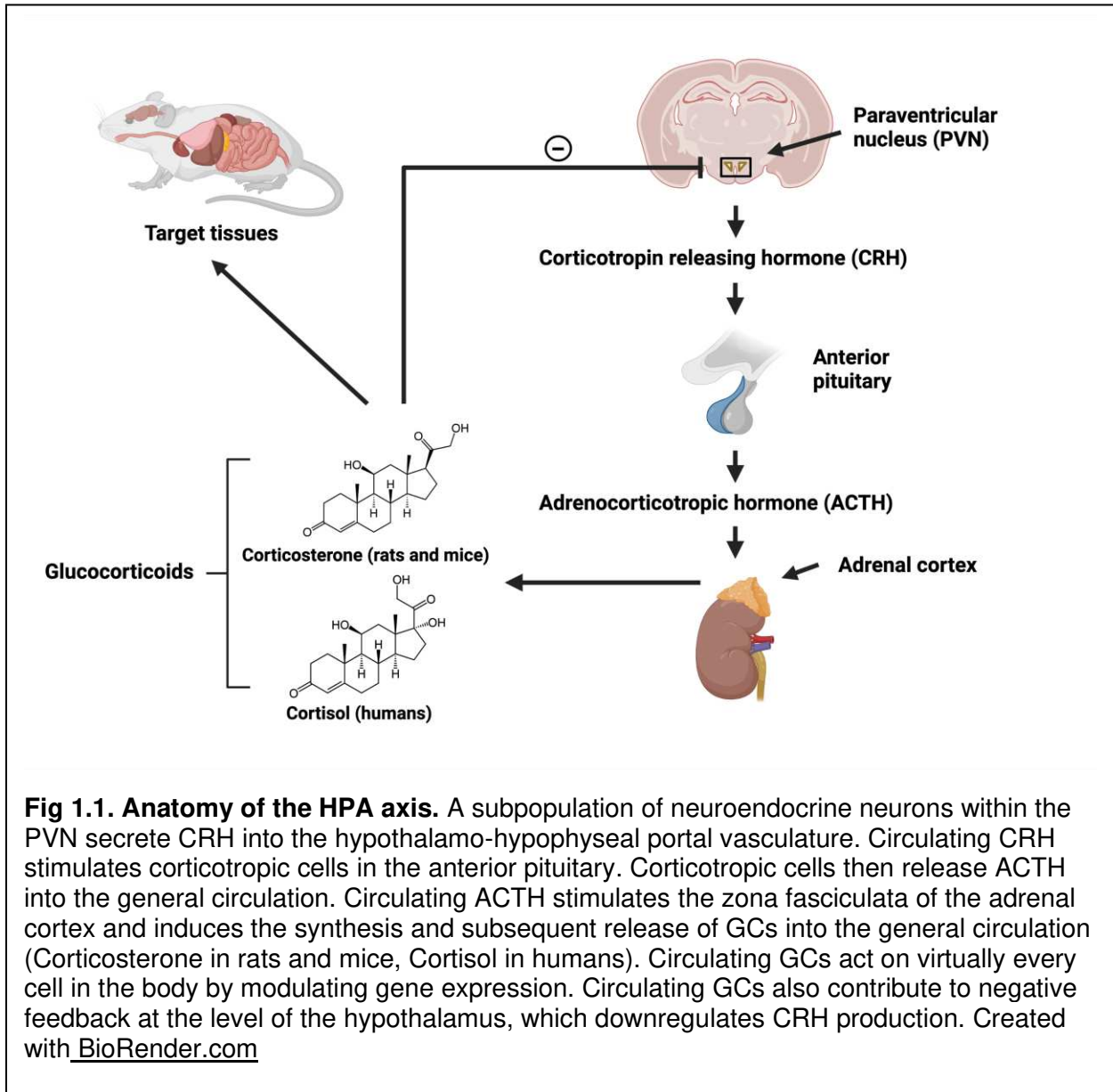


Fig 1.1. Anatomy of the HPA axis. A subpopulation of neuroendocrine neurons within the PVN secrete CRH into the hypothalamo-hypophyseal portal vasculature. Circulating CRH stimulates corticotropic cells in the anterior pituitary. Corticotropic cells then release ACTH into the general circulation. Circulating ACTH stimulates the zona fasciculata of the adrenal cortex and induces the synthesis and subsequent release of GCs into the general circulation (Corticosterone in rats and mice, Cortisol in humans). Circulating GCs act on virtually every cell in the body by modulating gene expression. Circulating GCs also contribute to negative feedback at the level of the hypothalamus, which downregulates CRH production. Created with [BioRender.com](https://www.biorender.com)

Stress is a powerful trigger of CRH release from the hypothalamus²⁷. However, the precise mechanisms of stress appraisal remain unclear. The function of the HPA axis is to adjust homeostatic mechanisms to respond to a potential threat, or stressor. GCs, the main

output of the HPA axis, have a multitude of effects on peripheral and central tissues which aid in an organism's short-term survival. Canonical actions of GCs largely recapitulate Selye's observations of general adaptation syndrome. GC actions include increasing glucose availability, immunosuppression and reduction of inflammation, suppression of the hypothalamic-pituitary-gonadal and hypothalamic-pituitary-thyroid axes, promotion of visceral adiposity, and increasing attention/arousal toward the threatening stimulus^{15,28}. This dissertation focuses on HPA axis-mediated entrainment of biological rhythms, which is arguably as crucial to the day-to-day wellbeing of an organism as adaptations to stress.

1.4 Biological Rhythms

A brief history of chronobiology

Chronobiology, the study of timekeeping and biological rhythmicity in living systems, spans multiple centuries. Perhaps the first written account of biological rhythmicity came from the astronomer Jean Jacques d'Ortous De Mairan in 1729. De Mairan placed a mimosa plant into a dark room for multiple days and observed that, in the total absence of light cues, the plant continued to rhythmically open its leaves at dawn and close them at dusk²⁹⁻³¹. The persistence of rhythmic leaf opening in constant darkness led De Mairan to conclude that the behavior was not simply a response to the presence of light cues from the sun, but instead was driven by a timekeeping mechanism within the organism itself³⁰.

In 1932, biologist Erwin Bünning recorded similar rhythms in bean plant leaf movement in constant light conditions³⁰. Bünning determined that the rhythmic leaf movement had a period of 24.4 hours rather than 24 hours, meaning the rhythm repeated itself daily, but would start approximately 0.4 hours later each day that the plant was in the absence of external timing cues (i.e., zeitgebers). This near-24-hour rhythmicity in the absence of zeitgebers is known as a free-running rhythm. Bünning also found that the periodicity of the bean plant free-running rhythm was heritable. Even though Bünning didn't possess our current knowledge of specific circadian

clock genes or modern genetics in general, this was likely the first account of circadian phenotypes being grounded in genetic factors. Together, these observations allowed him to conclude that rhythmic plant behavior is controlled by a near 24-hour clock that can be entrained by zeitgebers. Additionally, heritability of specific free-running period phenotypes to offspring indicated that the near-24-hour clock is indeed endogenous³⁰.

In the mid-20th century, the field of chronobiology began to flourish, with similar free running rhythms being discovered in insects, mammals, and humans held in constant conditions^{30,31}. Free-running periods have been shown to vary widely between species and even between individuals of the same species, but one common aspect that unifies all species is the nature of their near-24-hour periodicity in the absence of zeitgebers. Thus, the term “circadian” was coined by Franz Halberg in 1959, taken from the Latin phrase “circa diem” which translates to “about a day”³¹. Soon after the term circadian rhythm was coined, a universal set of empirical generalizations about circadian rhythms was published by chronobiologist Collin Pittendrigh in 1960, which still largely serves as the basis of how circadian rhythms are classified today^{30,32}.

Criteria for circadian rhythms

Pittendrigh’s set of empirical generalizations state that circadian rhythms have periods of approximately 24-hours, are ubiquitous in living organisms, are endogenous and self-sustaining, and occur autonomously at both single cell and whole organism levels of organization³².

Circadian rhythms in the absence of zeitgebers exhibit precise free-running periods, and free-running periods vary between species and within individuals of the same species. Free-running periods of circadian rhythms are largely temperature independent, but are entrained by light and can be shifted by a single perturbation to the light:dark (L:D) regime³². To be considered a true circadian rhythm, the rhythm must follow these criteria. The rhythm must exhibit a persistent, near-24-hour free-running period in the absence of zeitgebers. Upon reintroduction to a consistent zeitgeber regime, true circadian rhythms will entrain to the phase of the new cues,

regardless of when they occur on the organism's subjective clock. Unless these criteria have been demonstrated, the near 24-hour rhythm being studied is referred to as a diurnal rhythm. Examples of true circadian rhythms are mouse wheel running behavior and sleep wake cycles. Diurnal rhythms are rhythms that consistently vary with time of day but either do not persist in the absence of time cues or have yet to be demonstrated to do so. Therefore, any near 24-hour rhythm discussed herein that has not been observed to meet these criteria will be classified as a diurnal rhythm.

1.5 The Molecular Basis of Biological Rhythmicity in Mammals

The discovery of clock genes

Elucidation of the genetic basis of circadian rhythmicity started in the early 1970s with a seminal study characterizing fruit fly mutants with abnormal rhythmic behaviors³³. In the study, three distinct fly mutants were found to have deletions spanning varying lengths of a common functional genetic locus. Remarkably, the varying lengths of deletions in the three fly mutants conferred three distinct circadian phenotypes. When investigating locomotor rhythms in constant darkness, one of the mutants exhibited a shortened free-running period (~19 hours), another exhibited a lengthened free-running period (~28 hours), and the mutant with the largest length of deletion lacked rhythmicity entirely, exhibiting sporadic bouts of locomotion around the clock³³. Due to its effects on free-running period length, the affected gene was named *Period*, or *Per*. This study was the first of its kind to directly demonstrate a link between genetic mutations and altered circadian phenotype and served as a jumping off point for the discovery and isolation of other core clock components in the fly and their various homologs in mammals^{34,35}.

Clock gene transcriptional-translational feedback loops

Circadian and diurnal rhythms are present in nearly every tissue in the body³⁶⁻⁴². Within these tissues, rhythms are maintained by a series of transcriptional and translational feedback

loops that give way to timed changes in gene expression, physiology, and behavior⁴³. The best characterized molecular clock rhythm starts with the transcription factors circadian locomotor output cycles kaput (CLOCK) and brain and muscle Arnt-like protein-1 (BMAL1) forming a heterodimer and binding to a palindromic DNA sequence called an enhancer box (E-box) response element (**Fig 1.2**). E-box binding promotes the transcription of the *Period* (*Per*) and *Cryptochrome* (*Cry*) genes. When *Per* and *Cry* protein levels rise, *Per* and *Cry* form a complex with casein kinase (CK) in the cytoplasm and undergo phosphorylation⁴⁴. The phosphorylated *Per*-*Cry*-CK complex translocates into the nucleus and inhibits CLOCK-BMAL1 DNA binding. Specifically, *Cry* binds the CLOCK-BMAL1-E-Box complex to interfere with transactivation, and *Per* displaces CLOCK-BMAL1 from E-box binding⁴³. Together, these actions inhibit further transcription of the *Per* and *Cry* genes. After upregulated *Per* and *Cry* protein levels return to baseline after ubiquitination and subsequent proteasomal degradation, CLOCK and BMAL1 return to DNA binding, which resets the feedback loop. This cycle takes approximately 24 hours to complete⁴³.

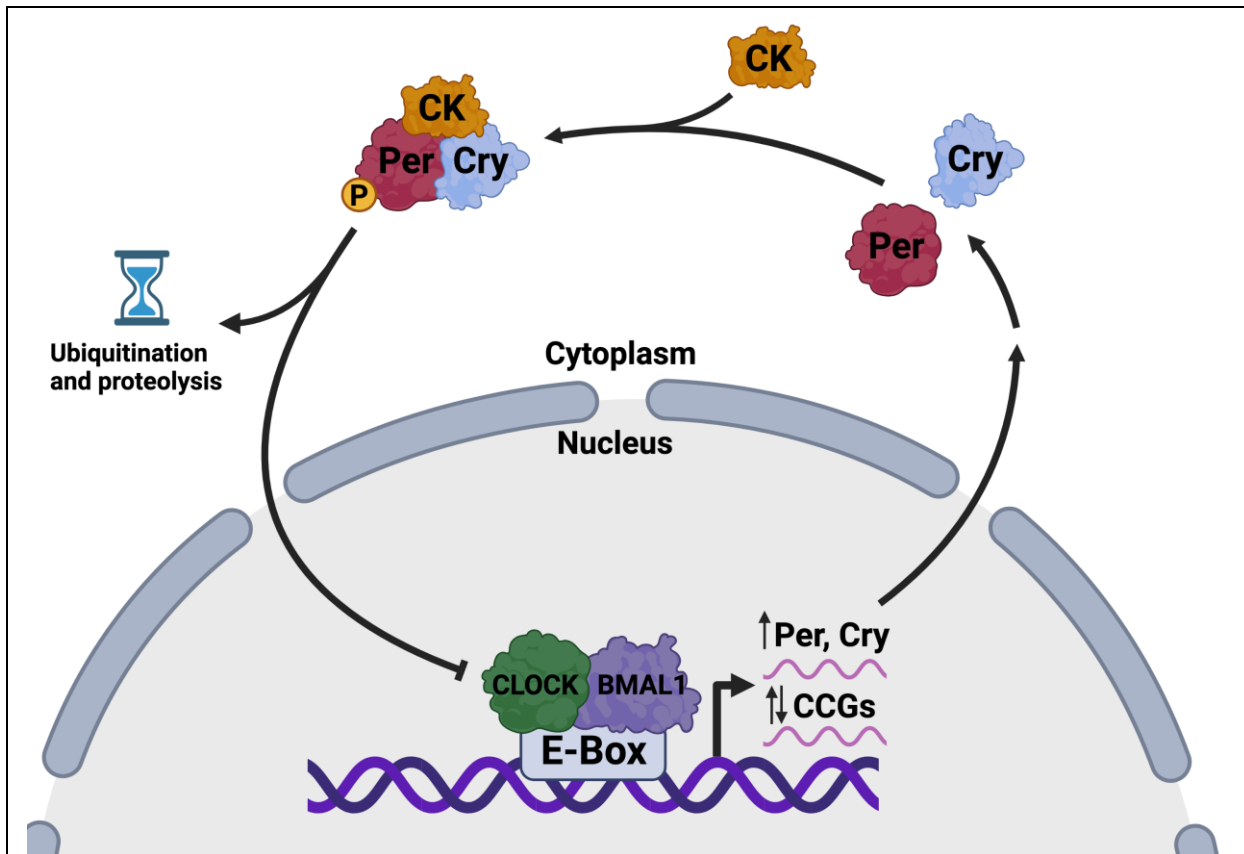


Fig 1.2. Core clock gene transcriptional-translational feedback loop. Transcription factors CLOCK and BMAL1 form a heterodimer and bind to E-Box response elements throughout the genome. E-Box binding upregulates *Per* and *Cry* transcription. E-Box binding also modulates CCG expression. As *Per* and *Cry* protein levels accumulate, they form complexes with CK in the cytoplasm, undergo phosphorylation, and enter the nucleus. Upon nuclear entry, *Per*-*Cry*-CK complexes inhibit CLOCK-BMAL1 DNA binding, which downregulates further *Per* and *Cry* transcription. As *Per* and *Cry* undergo ubiquitination and proteolysis and protein levels drop, CLOCK and BMAL1 return to E-Box binding. This cycle takes approximately 24 hours to complete. Created with [BioRender.com](https://www.biorender.com)

In addition to inducing *Per* and *Cry* expression, CLOCK and BMAL1 influence the expression of other genes, referred to as clock-controlled genes (CCGs). 43% of all protein coding genes exhibit daily rhythms of transcription, largely in an organ specific manner⁴⁵. Many CCGs show peak transcription preceding dawn or dusk⁴⁶. This temporal regulation of CCG expression is responsible for circadian variations of tissue function, which repeats itself

approximately every 24 hours^{43,47}. Importantly, the entrainment of the rise and fall of the CCG expression to transitions between day and night in the external environment is necessary for efficient circadian function.

All circadian clocks have periods of approximately 24 hours, but the period of a circadian clock can be shortened or lengthened within certain limits⁴⁸. For example, mice can entrain to L:D cycles with periods of 23 and 25 hours but cannot entrain to aberrant L:D cycles that have periods above or below that range^{48,49}. Instead, free running rhythms are observed when exposed to L:D cycles beyond the limits of entrainment⁴⁸⁻⁵¹. *CLOCK* mutant mice with a 51 amino acid deletion near the protein's C-terminus can entrain to 20-hour and 28-hour L:D cycles, suggesting that the limitations of period length are ultimately governed by the structure of core clock proteins and their interactions. The period of circadian rhythms can be slightly modified by posttranslational modifications of core clock proteins, which regulate nuclear localization, protein stability, and the time it takes for newly synthesized clock proteins to undergo protein degradation⁵². This allows for the ability of molecular clocks to phase shift and entrain to seasonal variations in the time of light phase onset. But how does the L:D cycle interact with such small scale biochemical and genomic events? How do core clock genes know when to phase shift and entrain to the onset of the light or dark phase? Clock genes alone are completely blind to the external environment, so other signaling factors must be necessary to confer entrainment and appropriate phase shifting in response to changes to external light cues. In mammals, the answer to these questions lies at the base of the hypothalamus.

1.6 The Suprachiasmatic Nucleus, the Brain's Master Clock

The discovery of the suprachiasmatic nucleus as a central circadian regulator

While the first clock gene was being discovered in fruit flies, there was a concurrent race to determine the anatomical localization of a master circadian clock in mammals. The ability for higher level organisms to entrain activity rhythms to the L:D cycle and show persistent rhythmicity in the form of free running rhythms in the absence of zeitgebers led researchers to believe that there must be a central circadian clock to coordinate such organized rhythms. Indeed, master circadian clocks had been demonstrated in the optic lobes of insects and the pineal gland of birds, but the localization of the mammalian clock proved elusive³⁰.

The journey to finding the mammalian brain's master circadian clock started in the retina. Knowing that circadian rhythms are entrained by L:D cues, tract tracing studies were performed to visualize the efferent projections from the retina into the brain in rats⁵³. The studies showed fibers terminating in known visual processing centers such as the lateral geniculate nucleus and superior colliculus, but a smaller population of efferent fibers were shown terminating in the anterior hypothalamus, immediately dorsal to the optic chiasm⁵³. Informed by these tracing experiments, two different groups simultaneously conducted lesion studies on the suprachiasmatic nucleus (SCN) to determine its putative role in driving circadian rhythmicity. The first group delivered electrolytic lesions to the SCN and observed a total loss in locomotor activity rhythms and rhythmic drinking, two behaviors that are often restricted to the dark phase in rats⁵⁴. The second group physically ablated the SCN and observed a loss of rhythmic glucocorticoid secretions, which typically precede the dark phase in rats⁵⁵. Each of the measured rhythms entirely lost rhythmicity in response to SCN lesion, implicating the SCN as a critical regulator of light-entrained circadian rhythms and the generation of persistent near-24-hour free running periods of behavior in the absence of zeitgebers.

Mechanisms and pathways of photoentrainment

The SCN is the master circadian pacemaker of the mammalian brain⁵⁴⁻⁵⁶. The nucleus serves as the starting point for the entrainment of other clock rhythms in the brain and throughout the body, which are entrained to oscillate in accordance with the external L:D cycle. To accomplish this, the SCN itself needs to be entrained via projections from the retina. It was previously assumed that the SCN received L:D cues from rod or cone-mediated photoreceptor pathways. This assumption was challenged when photoentrainment of rod and cone-lacking mice was unchanged compared to wild type mice⁵⁷. Only complete enucleation of rod and cone-lacking mice was sufficient to ablate photoentrainment, suggesting the existence of a non-rod, non-cone photoreceptor in the eye that drives photoentrainment⁵⁷. The SCN receives innervation via the retino-hypothalamic tract from a population of retinal ganglion cells known as intrinsically photosensitive retinal ganglion cells (ipRGCs). IpRGCs are a unique population of ganglion cells that express the photopigment melanopsin and are the only retinal ganglion cell type that has been demonstrated to be sensitive to light independent of rod and cone photoreceptor signaling^{58,59}. IpRGCs fire in accordance with the L:D cycle, and primarily project to the SCN.

Retinorecipient SCN neurons are stimulated by glutamatergic ipRGCs via α -amino-3-hydroxy-5-methyl-4-isoxazolepropionic acid (AMPA) and *N*-methyl-D-aspartate receptor (NMDA) receptor activation. Prolonged AMPA and NMDA receptor ligand binding allows calcium to enter the cytoplasm through NMDA receptors, which subsequently activates the Calmodulin CaM-Kinase pathway and results in the downstream phosphorylation of cyclic AMP (cAMP) Response Element Binding protein (CREB)⁶⁰. Phosphorylated CREB then binds to cAMP response elements (CREs) within the genome to induce the expression of *Per* genes, among others⁶¹. As a result, retinorecipient SCN neurons entrain internal clock rhythms to oscillate in phase with the L:D cycle. From there, the SCN relays its rhythmic clock activity to the rest of the

body via a combination of neural and endocrine pathways, which results in the entrainment of central and peripheral molecular clocks, ensuring that all SCN-controlled rhythms oscillate with periods matching the 24-hour L:D cycle⁵⁶.

The SCN is composed of two subregions delineated as the core and the shell. Neurons expressing the neuropeptides vasoactive intestinal polypeptide (VIP) and gastrin releasing peptide (GRP) reside in the core, and neurons expressing the neuropeptide arginine vasopressin (AVP) reside in the shell⁶². Additionally, γ -aminobutyric acid (GABA) is expressed by nearly all SCN neurons. Interaction between these neuropeptide-expressing subpopulations of neurons confers rhythmicity within the SCN, so much so that dissociated SCN neurons and organotypic SCN slice cultures maintain precise rhythms of molecular clock feedback loops at the network level and the cellular level⁶³⁻⁶⁵. SCN neurons have also been shown to exhibit circadian rhythms of action potential propagation in culture⁶⁶.

SCN core VIP and GRP neurons confer rhythmicity within the SCN network. VIP and GRP neurons are the primary targets of retino-hypothalamic projections⁶⁷. VIP and GRP neurons primarily project to subpopulations within the SCN⁶⁸. VIP and VIP receptor VPAC₂ knockout mice display mixed circadian phenotypes, with ~two thirds of mutants having arrhythmic activity patterns and ~one third of mutants having significantly shortened free running periods when exposed to constant darkness⁶⁹. In both VIP and VPAC₂ knockouts, many SCN neurons lack rhythmic firing patterns. In VIP knockouts, rhythmic SCN firing patterns are rescued by application of the VPAC₂ agonist Ro 25-1553⁶⁹. These data implicate VIP signaling as a necessary component for proper photoentrainment of locomotor activity rhythms and for the entrainment of rhythmic firing within the SCN network itself. Exogenous GRP administered to the SCN immediately before exposure to constant darkness produces significantly larger phase advances in free-running locomotor activity rhythms in constant darkness⁷⁰. This phase

shifting effect is shown to be a result of *Per1* induction in the SCN through activation of the CREB pathway⁷⁰. These results suggest GRP signaling contributes to entrainment of the SCN network during changes in photoperiod.

SCN shell AVP neurons are primarily responsible for the entrainment of extra-SCN clock rhythms. Remarkably, most non-SCN central and peripheral molecular clock oscillations maintain phase synchrony with the molecular clock oscillations in the SCN shell, but not the SCN core⁵⁶. Shell neurons largely receive afferent projections from core VIP neurons, with very few reciprocal AVP projections to the core⁶⁸. VIP-mediated induction of clock gene transcription in AVP neurons is not well understood, but it has been proposed that VIP upregulates *Per* transcription through a pathway involving Extracellular signal-related kinase (ERK) signaling and possibly the CREB pathway⁷¹. Shell AVP neurons project to numerous hypothalamic structures and are responsible for driving several rhythmic behaviors. For example, AVP neurons are responsible for rhythmic drinking behaviors via projections to the organum vasculosum lamina terminalis (OVLT), as optogenetic silencing of OVLT neurons expressing the AVP receptor V1aR cease rhythmic drinking⁷². SCN AVP projections facilitate rhythmic feeding behaviors through projections to oxytocin (OT)-expressing neurons within the paraventricular nucleus (PVN)⁷³. GABAergic neurons within the SCN (unspecified neuropeptide phenotype) project to CRH-expressing neurons within the PVN to regulate wakefulness and activity rhythms⁷⁴. In the light (inactive) phase, CRH neurons receive GABAergic inhibition from the SCN, which is alleviated during the dark phase, allowing increased CRH neuronal activity. Severing projections from the SCN to the PVN in slice cultures resulted in a loss of rhythmic reductions in CRH neuron activity during the subjective day, causing the subjective day activity pattern of CRH neurons to resemble firing patterns observed during the subjective night⁷⁴.

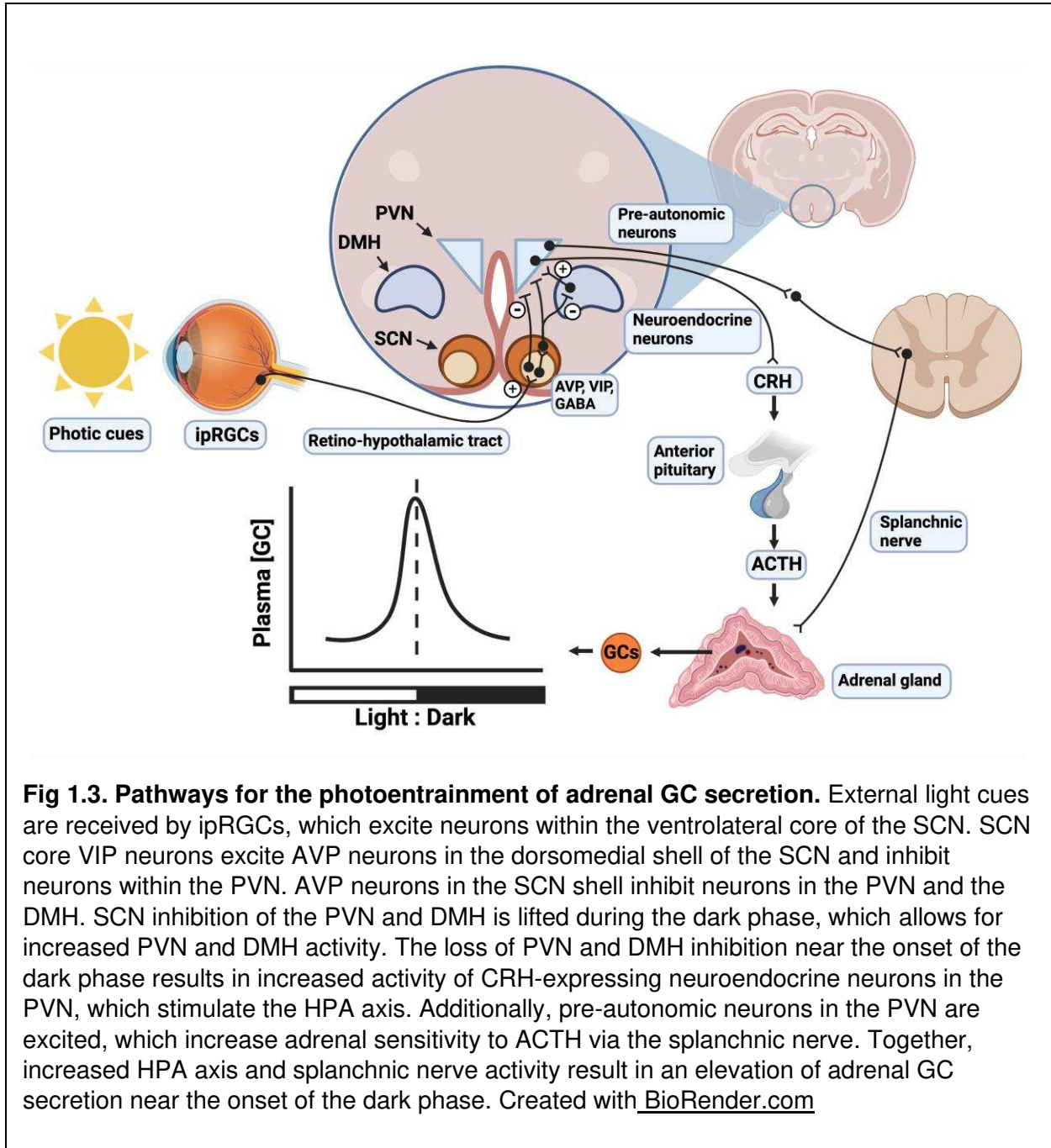
The SCN does not directly project to the vmPFC⁷⁵. Instead, the SCN reaches the vmPFC through a multi-synapse pathway involving the paraventricular thalamic nucleus (PVT)⁷⁶. Stereotaxic injections of a mixture of the transsynaptic retrograde tracer pseudorabies

virus (PRV) and the retrograde tracer cholera toxin β subunit (CTb) into the infralimbic (IL), prelimbic (PL), and anterior cingulate (ACC) vmPFC subregions produce different results depending on the region injected. When investigating the retrograde tracing pattern of IL injections, the SCN showed significantly more PRV-infected neurons than the PL or ACC injections. Additionally, there was robust CTb staining in the PVT of the IL injected rats, suggesting that the SCN-IL pathway must relay through the PVT. The same retrograde tracing experiment was performed on rats with bilateral PVT lesions, which prevented PRV labeling in the SCN⁷⁶. This study suggests that the IL receives significantly more input from the SCN than the PL and ACC, but the functional consequences of these region-specific afferent projections has not been examined. Despite these findings, the molecular clocks of the IL, PL, and ACC have been shown to oscillate in phase with one another, exhibiting peak expression of *Per1* and *Per2* mRNA between ZT12-18 (early active/dark phase) and baseline expression at ZT0 (onset of the inactive/light phase)⁴¹. These findings appear to contrast with one another. If only the IL receives substantial SCN input, one could assume that the IL molecular clock would, in some way, be different compared to the neighboring vmPFC subregions. Thus, molecular clock synchrony among the different vmPFC subregions is likely not grounded in afferent projection patterns. Instead, vmPFC molecular clocks rely on a common, bloodborne entrainment cue: circulating GCs.

Photoentrainment of the diurnal rhythm of GCs

Perhaps the most important aspect of SCN control for my dissertation is the circadian control of rhythmic GC secretions via SCN modulation of PVN CRH neurons (**Fig 1.3**). As previously mentioned, one of the first SCN lesion studies demonstrated that the diurnal pattern of GC release depends on the SCN⁵⁵. When the SCN is lesioned, rats lose the diurnal rhythm of GC secretion. Enucleation did not result in a loss of the diurnal rhythm of GC secretion, but

instead caused peak GC secretions to occur several hours after dark phase onset, suggesting that the HPA axis is dependent on the endogenous free-running rhythm of the SCN rather than retinal cues⁵⁵.



The SCN is believed to exert control over the PVN through AVP, VIP, and GABAergic signaling. SCN-derived AVP is primarily released in the light phase^{77,78}. Administration of AVP V₁ receptor antagonist directly to the PVN greatly increases plasma CORT within 30 minutes of administration during the light phase, but not during the dark phase^{77,79}. When AVP is delivered directly to the PVN during the diurnal rise of plasma CORT, peak CORT secretion is blocked⁷⁷. AVP is also highly expressed within the PVN itself, which makes SCN-derived AVP difficult to pinpoint as the sole source of AVP-mediated PVN regulation. PVN-derived AVP can be released within the PVN itself, which inhibits ACTH and CORT secretion⁸⁰. However, this phenomenon has only been demonstrated to occur in response to acute stress, possibly serving as a mechanism of rapid HPA axis negative feedback⁸⁰. PVN-derived AVP does not show a diurnal pattern of release, suggesting that intra-PVN AVP release may solely be a response to stress rather than a diurnal regulator⁷⁸.

Optogenetic stimulation of SCN VIP neurons during the diurnal rise of plasma CORT blocks the peak of CORT secretion, but stimulation during the early light phase has no effect on CORT secretion⁸¹. Stimulation of SCN VIP neurons also reduces Ca²⁺ fluorescence in CRH neurons expressing Ca²⁺ sensor jRCaMP1b. In organotypic slice cultures containing SCN and PVN, daily optogenetic stimulation of SCN VIP neurons result in larger phase shifts in *Per2* expression rhythms in CRH neurons compared to *Per2* expression rhythms of non-stimulated controls⁸¹.

Although the precise neurocircuitry is not fully resolved, the dorsomedial nucleus of the hypothalamus (DMH) also influences the diurnal rhythm of PVN CRH neuronal activity. Neurons within the SCN shell project to the DMH⁸². Like SCN lesion studies, DMH lesions abolish the diurnal rhythm of GC secretion⁸³. Given that DMH lesions spare the SCN, these results suggest that the SCN's control of the PVN is mediated through SCN projections to interneurons within the DMH⁸³. Additionally, direct application of the GABA_A receptor antagonist bicuculline methiodide (BMI) to the DMH results in rapid elevations in plasma ACTH within five minutes of

application and CORT within 30 minutes post-application⁸⁴. This suggests that removal of tonic GABAergic inhibition of the DMH results in the excitation of PVN CRH neurons, and subsequent HPA axis activation⁸⁴. However, this is ultimately an assumption, as no current study directly demonstrates a diurnal rhythm of tonic GABAergic inhibition on DMH neurons.

Together, these data suggest that CRH secretion and DMH activity are under inhibitory influence of the SCN during the light phase. Near the transition between the light and dark phase, SCN inhibition of the DMH is reduced. Concurrently, AVP and VIP-mediated inhibition of PVN CRH secretion is reduced. Collectively, these events result in PVN CRH secretion, followed by a diurnal surge of GC secretion. The functional consequences of the diurnal GC secretion are vast and important for the entrainment of non-SCN clocks, which will be discussed further in the following section.

1.7 Neuroendocrine regulation of biological rhythms

SCN regulation of the HPA axis plays a vital role in the maintenance of biological rhythms throughout the body. As discussed in the previous section, rhythmic PVN activity is regulated by rhythmic SCN activity. In mice, SCN VIP and AVP-expressing neurons inhibit CRH release in the light phase. SCN inhibition is reduced near the onset of the dark phase, which results in increased CRH release and subsequent HPA axis activation. Timed HPA axis activation results in a diurnal pattern of GC secretion which peaks near the onset of the dark phase. Due to the ubiquity of GR, GC signaling has the potential to regulate every tissue system of the body. Accordingly, the diurnal pattern of GC secretion drives widespread changes in gene expression throughout the body, which serves to prime the organism for the various challenges accompanying the active phase.

GCs aid in the entrainment of individual cellular clocks throughout the body^{41,42,85}. This is due to GC ability to enhance *Per* gene expression by acting through a GRE immediately upstream of the *Per1* gene's transcription start site, and an overlapping GRE and E-box region within the *Per2* promoter^{41,86,87} (**Fig 1.4**). Because of this functional overlap with core clock gene-mediated induction of *Per* genes, rhythmic GC secretions can regulate core clock gene transcriptional rhythms as well as the amplitude and timing of CCG expression in the periphery and brain^{41,42,85,88}.

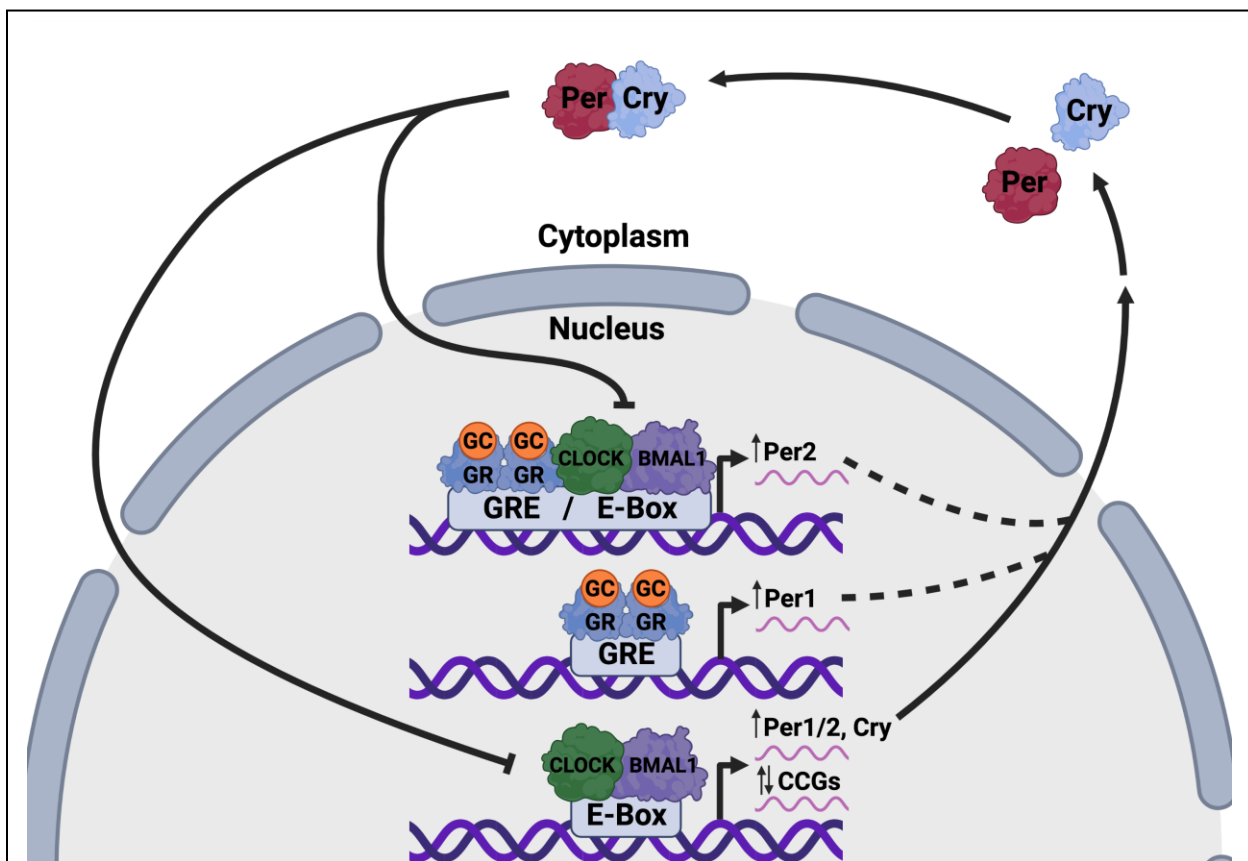


Fig 1.4. GCs influence core clock gene transcription. After GC binding, GR forms a homodimer which enters the nucleus and binds to GREs throughout the genome to modulate gene expression. A GRE exists upstream of the *Per1* transcription start site. An overlapping GRE and E-Box response element exists within the *Per2* promoter. Presence of GREs within *Per* promoter regions enable GR to upregulate *Per* transcription independently of CLOCK and BMAL1 DNA binding. Created with [BioRender.com](https://www.biorender.com)

GC signaling as a peripheral entrainment cue

Per rhythmicity is modulated by GC signaling in a many peripheral tissues. In *Per2::Luciferase* (LUC) reporter mice, rhythms in *Per2* bioluminescence are present in kidney, liver, and submandibular glands⁸⁹. In a *Per2::LUC* mouse with a dominant negative mutation in the *CLOCK* gene, bioluminescence rhythms are blunted and peak bioluminescence is phase shifted from the peaks of the non-clock mutant. Dexamethasone (DEX), a synthetic GC, injected into *Per2::LUC* mice at ZT4 (early active phase) daily for 3 days causes submandibular gland peak bioluminescence to phase shift from vehicle treated mice, resulting in peaks occurring earlier in the day. Interestingly, this DEX-mediated phase shift in *Per2* expression does not occur in liver or kidney. In *Per2::LUC* clock mutants, ZT4 DEX injections result in increases in submandibular gland *Per2::LUC* amplitude and a similar pattern of phase shifting as non-clock mutants, resulting in peaks occurring at the same time as DEX-treated non-clock mutants⁸⁹. These results highlight a role for GC signaling as an entrainment cue that can modulate the expression pattern of *Per2* transcription independently of the core clock gene *clock* in a tissue dependent manner. GCs added to both rat and mouse fibroblasts, and mouse marrow stromal cells in vitro confer rhythmic clock gene expression^{88,90,91}. GC-mediated *Per1* expression and phase shifting is observed in the kidney, visceral adipose tissue, spleen, heart, and liver^{88,92}. In the liver, DEX injections phase shift *Per1* and *BMAL1* expression rhythms, and, in a separate experiment, adrenalectomy has been shown to abolish liver *Per1* rhythmicity^{88,92}. In a mouse that specifically lacks GR in hepatocytes, DEX injection does not result in the phase shifting of *Per1* or *BMAL1* expression, which suggests that GR expression in the liver is required for GC-mediated phase shifting of hepatic clock rhythms⁸⁸.

GCs are involved in controlling the timing of CCG transcription. Diurnal GC signaling regulates ~60% of the liver transcriptome³⁷. In SCN-lesioned mice, hepatic CCG expression loses rhythmicity. In SCN-lesioned mice receiving DEX, CCG expression profiles synchronize to the DEX treatment regimen³⁷. The intestines maintain circadian rhythms of salt and nutrient

transporter expression⁹³. Many rhythmically expressed intestinal transporter genes have reduced expression, or are phase shifted in response to adrenalectomy⁴². Although no organ was specifically investigated in this study, increased leptin levels and an increase in glucose tolerance are reported in mice with a genetic deletion spanning the GRE in the *Per2* promoter, suggesting that interactions between GCs and *Per2* are involved in the regulation of glucose homeostasis⁹¹. Taken together, these various results link GC signaling the regulation of core clock gene and CCG expression throughout the periphery. Additionally, these results highlight that GC-mediated effects on clock gene expression vary depending on the target tissue.

The timing of food intake also serves as an important entrainment cue in the periphery⁹⁴. If mice are restricted to feeding in the light phase rather than following their typical nocturnal feeding schedule, the kidney and liver molecular clock rhythms phase shift while the SCN molecular clock stays entrained to the L:D cycle⁹⁵. The light phase feeding schedule is accompanied by an aberrant diurnal rhythm of GC secretion, displaying a peak GC secretion near the onset of the dark phase and a separate peak near the early light phase. Surprisingly, food-entrained peripheral clock phase shifting occurs in both sham and adrenalectomized mice, but at different rates. Within two days of entrainment to the altered feeding schedule, peripheral clocks of adrenalectomized mice phase shift by 8-12 hours, while sham mice phase shift by ~4 hours. Similarly, in mice that lack GR in hepatocytes, transitioning to the light phase feeding schedule induces rapid phase shifting in GR-lacking hepatic clocks when compared to the slower phase shifting of wild-type hepatic clocks. After a week of light phase-exclusive feeding, peripheral clocks of sham and adrenalectomized mice have similar phases⁹⁵. These results suggest that changes in feeding schedule can phase shift peripheral clocks independently of the SCN and GC rhythms, but the rate at which food-entrained phase shifting occurs is ultimately regulated by GC signaling.

GC signaling as a central entrainment cue

While the SCN can directly influence the photoentrainment of other brain regions via direct projections, the SCN does not directly regulate all brain regions that possess rhythmicity. Instead, much like the periphery, the SCN utilizes the diurnal rhythm of GC secretion to assist in the regulation of molecular clock rhythms in the brain. The exception to this statement is the SCN, which lacks GR after postnatal day 16 and is therefore unable to directly respond to GC signaling and displays persistent molecular clock rhythms after adrenalectomy^{41,96}. Like the periphery, GC-mediated effects on clock entrainment in the brain vary depending on the specific region or nucleus studied.

Some brain regions appear to not be solely dependent on diurnal GC signaling for the maintenance of their molecular clock rhythms³⁹. In the cerebellum, *Per1* and *Per2* mRNA expression differs between ZT3 and ZT15, with peak expression of both genes occurring at ZT15. Cerebellar clock gene rhythmicity is abolished by lesioning the SCN but is rescued with diurnal CORT replacement. Strangely, cerebellar clock gene rhythmicity is present in adrenalectomized animals with an intact SCN³⁹. These results suggest the presence of additional mechanisms of control for the maintenance of cerebellar clock gene rhythms, which are perhaps aided by the diurnal rhythm of GC secretion. In hippocampus, cornu ammonis (CA)1, CA3, and dentate gyrus subregions have similar timing of core clock gene rhythms in intact animals⁹⁷. Adrenalectomy abolishes *Per1* and *Per2* rhythmicity in all subregions except for CA3, which has a persistent *Per1* rhythm after adrenalectomy. DEX treatment after adrenalectomy produces mixed results. DEX rescues *Per1* and *Per2* rhythmicity in the dentate gyrus, but only *Per2* rhythmicity is rescued in CA1 and CA3, suggesting the presence of GC-independent mechanisms for the entrainment of some hippocampal rhythms⁹⁷. In the basolateral amygdala (BLA), the *Per2* protein expression rhythm is entirely opposite to the neighboring central amygdala (CEA) *Per2* expression rhythm⁹⁸. In BLA, peak *Per2* expression is observed at ZT1, and trough expression is observed at ZT13. In CEA, peak *Per2* expression is

observed at ZT13, and trough expression is observed at ZT1. Despite their anatomical proximity, the *Per2* rhythm in the BLA is the only rhythm that persists in response to adrenalectomy⁹⁸. Additionally, GR knockout mice still possess a *Per2* rhythm in the BLA⁸⁵. Together, these data suggest that the BLA *Per2* rhythm is entrained independently of GC signaling.

Other brain regions display a clear dependence on GC signaling for driving molecular clock rhythms. Unlike the neighboring BLA, the *Per2* rhythm within the CEA is abolished in response to adrenalectomy⁹⁸. Moreover, GR knockout mice lack *Per2* rhythmicity in the CEA, but *Per2* rhythmicity is still present in the BLA⁹⁹. These data indicate that the CEA molecular clock is GC-dependent. In the oval nucleus of the bed nucleus of the stria terminalis (BNSTov), rhythmic expression of *Per2* peaks at ZT12 and reaches trough expression between ZT18 and ZT0. BNSTov *Per2* rhythmicity is blocked by adrenalectomy⁸⁵. GR knockout mice also lack *Per2* rhythmicity in the BNSTov, which suggests that *Per2* rhythmicity in the BNSTov is entrained by GC signaling⁹⁹.

GCs influence the phase of clock gene expression in both the IL and PL vmPFC subregions, as well as other PFC subregions like the anterior cingulate cortex (ACC) and the ventral orbital cortex (VO)⁴¹. Expression of *Per1* and *Per2* is elevated in the early dark phase (between ZT12-18) and is reduced during the light phase, with trough expression of *Per1* and *Per2* both occurring at ZT0. Adrenalectomy shifts *Per1* and *Per2* rhythms to reach peak transcription later in the L:D cycle, whereas daily exogenous GC administration 1 hour prior to the onset of the dark phase (ZT11) rescues the phase of *Per1* and *Per2* expression. Daily GC administration to adrenalectomized rats in the early light phase (ZT1) abolishes rhythmic clock gene expression entirely, causing *Per1* and *Per2* levels to remain near trough expression values across the L:D cycle, suggesting that appropriately timed GC oscillations are important for the entrainment and maintenance of molecular clock rhythms within the vmPFC. A curious aspect of the PFC's molecular clock rhythms is that that they appear to phase shift in the absence of GC

signaling, still showing distinct peak and trough *Per* mRNA expression, but occurring several hours earlier or later depending on the core clock gene studied⁴¹. All previously mentioned non-SCN brain regions either oscillate independently of GCs, as seen in the Cerebellum, BLA, and some hippocampal subregions, or simply do not oscillate when GCs are removed, as seen in the CEA, BNSTov.

1.8 Dendritic spines and synaptic plasticity

A brief history of dendritic spines

In 1873, the Italian histologist Camillo Golgi invented a method of labeling nervous tissue¹⁰⁰. The new method called for immersion of nervous tissue that had been previously cured with potassium or ammonium dichromate into a solution of silver nitrate. Golgi's stain resulted in dark black labeling of neuronal cell bodies, axons, and dendritic arbors. This stain allowed investigators to witness intact neurons and glia in a histological preparation for the first time, which was revolutionary the young discipline of neuroscience. With his new method, Golgi extensively studied the nervous system and generated detailed illustrations of various cell types throughout the brain.

Despite Golgi's great attention to detail as an illustrator, his first depictions of neurons lacked something very important. If nobody questioned Golgi's assumptions of anatomical accuracy back then, perhaps I would not be writing this dissertation today. Golgi's first illustration of dendritic arbors *lacked dendritic spines*¹⁰⁰. The reason for this was because Golgi, and many of his contemporaries, dismissed spines as an artifact produced by the Golgi stain. Dendritic spines were assumed to be needle-like crystallizations of silver chromate, so no attention was paid to them. In 1887, the Spanish histologist Santiago Ramón y Cajal became captivated by the Golgi stain and utilized it extensively, publishing several works and illustrations that laid the foundation for the field of modern neuroscience. In contrast to Golgi's illustrations, Cajal's illustrations included dendritic spines. In Cajal's second publication, he

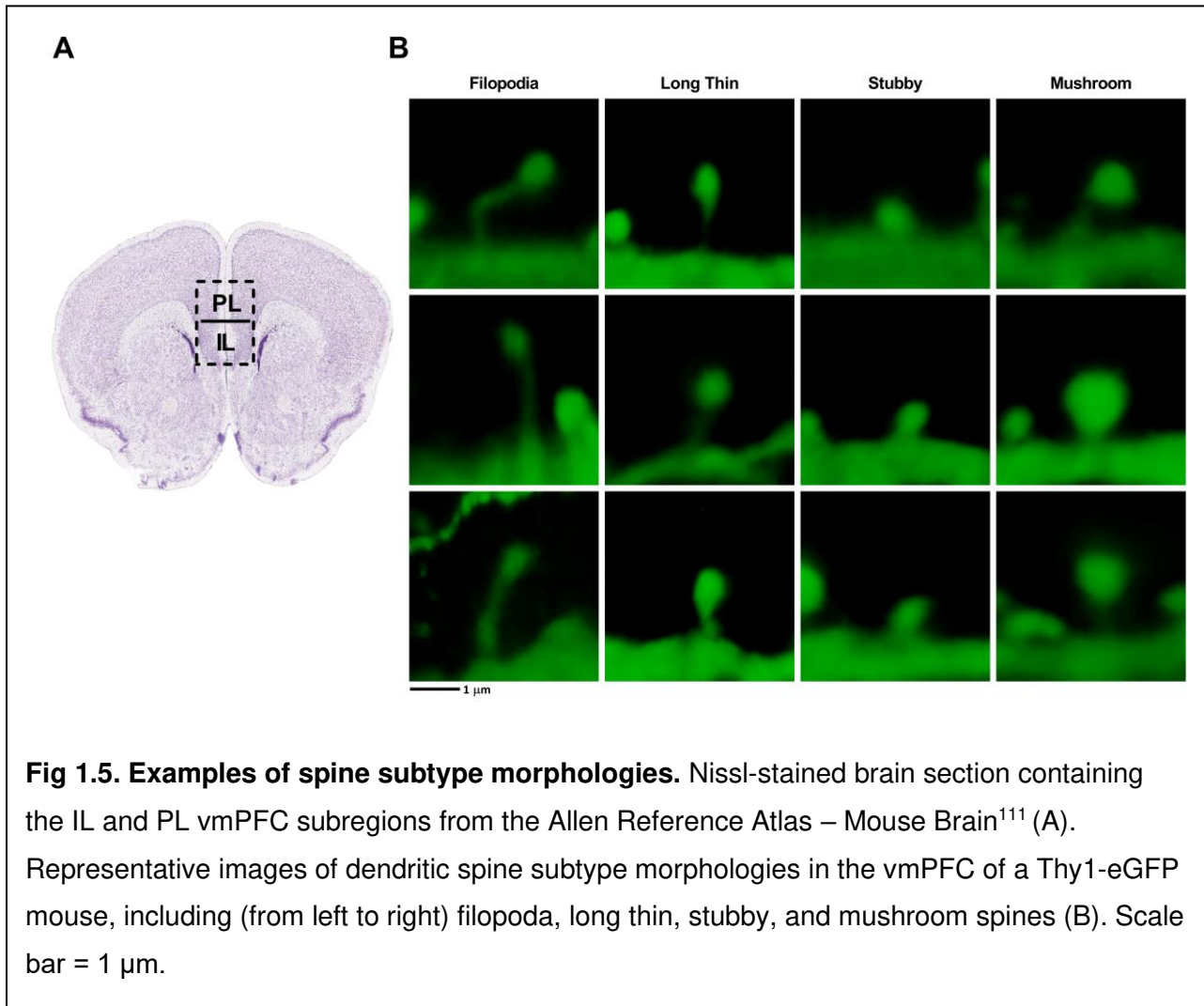
formally described and named dendritic spines while writing about the dendritic arbors of Purkinje cells in the cerebellum. He argued that spines were anatomical features of neurons due to their consistent localization on dendritic arbors and consistent absence on axon initial segments, cell bodies, and proximal segments of dendrites¹⁰¹. Despite this, Cajal's contemporaries still disagreed about the existence of dendritic spines. Skepticism on dendritic spines was lifted after Cajal and other histologists were able to demonstrate consistent dendritic spine staining with methylene blue, which indicated that spines were not an artifact of the Golgi method. After reports of spine staining with methylene blue spread throughout the scientific community, it became widely accepted that dendritic spines were indeed an anatomical feature of neurons. Even Golgi was convinced, as his following publications included illustrations of dendritic spines¹⁰⁰.

Cajal made several strikingly accurate predictions regarding the structure and function of dendritic spines¹⁰¹. Noting that higher level vertebrates possessed greater spine density than lower vertebrates, he supposed that spines had some correlation with intelligence. Visualizing axon terminals in close contact with spines led him to predict that spines received input from individual axons. Additionally, he predicted that spines were dynamic and could expand and retract in response to learning and behavior in living organisms. Perhaps of greatest importance to my dissertation, Cajal even predicted that spines could connect and disconnect in response to activity and inactivity that accompanies the cycle between day and night¹⁰¹.

Dendritic spine morphology

Dendritic spines are small, actin-rich postsynaptic membrane protrusions which contain most excitatory synapses within the mammalian brain and are implicated as the morphological basis of learning and memory. Spines are typically categorized into 4 main subtypes based on their morphology: Filopodia, thin, stubby, and mushroom¹⁰² (**Fig 1.5**).

Filopodia represent immature spine precursors, where mushroom spines represent a stable, fully mature spine. Long thin and stubby spines are subclassifications of spines that are often considered morphological intermediates between nascent filopodial spines and fully mature mushroom spines. *In vivo* imaging studies of somatosensory cortical pyramidal neurons suggest that mushroom-like spines are persistent, meaning that they exhibit stable morphologies over long periods of time¹⁰³. All non-mushroom spine subtypes are transient, exhibiting dynamic morphologies and are often formed and pruned daily. Due to the highly dynamic nature of dendritic spines, it is important to consider spine morphology as a spectrum rather than strictly adhering to defined classifications without lacking intermediate morphologies^{103–107}. Filopodia are abundant in the young brain during critical stages of spinogenesis. Throughout life, filopodia undergo rapid extension and retraction as they search for synaptic partners^{108,109}. Once a suitable presynaptic partner is found, a subset of filopodia mature into other spine subtypes, while others are pruned. Stubby, thin, and mushroom spines contain postsynaptic densities (PSDs), which are characterized by thickened bands of postsynaptic membrane found within synaptic junctions when observed with electron microscopy. Postsynaptic densities contain essential molecular components for synaptic plasticity and structural changes¹¹⁰.



Long-term potentiation and long-term depression regulate spine structure

Long term potentiation (LTP) is a term that represents a series of postsynaptic signaling events that occur following high frequency excitation of a synapse^{112,113}. In a glutamatergic synapse, the postsynaptic membrane expresses AMPA and NMDA receptors. At rest, NMDA receptors hold a magnesium ion that blocks sodium and calcium permeability. During high frequency stimulation, the NMDA magnesium block is removed, which allows sodium and calcium to enter the cell upon NMDA receptor ligand binding. From there, calcium is bound by calmodulin. Calcium-bound calmodulin then interacts with CaM-Kinase, which phosphorylates

and activates many downstream targets. In brief, CaM-Kinase pathway activation results in the increased expression of AMPA receptors in the postsynaptic membrane. Increased postsynaptic AMPA receptor expression results in a long-lasting increase in the postsynaptic response to glutamate¹¹². Long term depression (LTD) is a long-lasting reduction in the postsynaptic response to glutamate driven by a net reduction of postsynaptic AMPA receptor expression. In contrast to LTP, LTD is often induced by patterns of low frequency stimulation¹¹³.

Early studies utilizing electron microscopy show that, after 30 seconds of rapid electrical stimulation of afferent fibers, dendritic spines within the dentate gyrus increase in size by 38%, and PSD surface area significantly increases^{104,105}. LTP induction is also associated with cofilin localization to dendritic spines and remodeling of the actin cytoskeleton¹¹⁴. These reports suggest a role for long-term potentiation (LTP) in driving morphological changes in dendritic spines through reorganization of the actin cytoskeleton. Conversely, long-term depression (LTD) correlates with the shrinkage of spines¹¹⁵. Interestingly, GABA uncaging experiments suggest LTD-induced spine shrinkage only takes place when GABA is bioavailable to spines, implicating a role for inhibitory neurotransmission in the pruning of spines¹¹⁶. Simply put, the growth and pruning of dendritic spines may reflect increases and decreases in synaptic input to a given neuron, respectively. In addition to LTP/LTD related spine dynamics, glucocorticoids are known effectors of dendritic spine dynamics, displaying multiple dose and time-dependent effects on dendritic spine morphology.

Glucocorticoids influence synaptic plasticity and dendritic morphology

The rodent hippocampal CA1 region and vmPFC undergo dendritic remodeling in response to chronic stress and chronic GC administration^{117–123}. The hippocampus is an evolutionarily conserved structure that predates the neocortex and is perhaps the most well studied structure in the context of learning, LTP, and dendritic spines¹²⁴. Although the hippocampus is not entirely comparable to the neocortex, it shares some structural key

similarities. The hippocampus has multiple layers, including a pyramidal cell layer. Much like the neocortex, pyramidal neurons within the hippocampus are covered in dendritic spines and highly express GR^{125,126}. Because of this, reviewing GC-mediated effects on hippocampal spine dynamics may be valuable for understanding possible conserved mechanisms in neocortical structures like the vmPFC. Sholl analysis is a measure of dendritic branching and complexity, done by counting dendritic intersections with a superimposed array of evenly spaced concentric circles. Rats receiving three weeks of CORT injections show significant reductions in dendritic branching and Sholl intersections in CA1 pyramidal neurons^{123,127}. Additionally, chronic CORT administration reduces CA1 dendritic spine density¹²³. Similarly, chronic restraint stress reduces IL layer II/III pyramidal neuron dendritic branching and Sholl intersections¹¹⁸. Dendritic spine density on layer II/III IL pyramidal neurons is also reduced by chronic restraint stress¹¹⁸. In the PL, chronic restraint stress reduces dendritic branching, number of Sholl intersections, and spine density on layer II/III pyramidal neurons^{121,122}. In mice, a sex difference has been reported where chronic variable stress (CVS) reduces dendritic spine density on apical dendrites of IL layer V pyramidal neurons in males but not in females¹¹⁹. This correlates with increased depressive-like behaviors which can be rescued by daily administrations of GR antagonist RU486 during CVS¹¹⁹. These results implicate GCs as regulators of IL dendritic spines following stress. Aside from deleterious effects of chronic GC exposure on dendritic spines, it has also been shown that acute exposure to GCs can rapidly stimulate spine growth in hippocampus and motor cortex, demonstrating that different dosages and durations of GC exposure can exert opposite effects on spine dynamics^{128,129}.

A functional correlate of the GC-dependent effects on dendritic spines may be seen in changes of synaptic strength as assessed by electrophysiological experiments. GCs display duration-dependent trends when assessing stress-induced changes in synaptic strength^{130,131}. In PFC, both acute stress and acute CORT administration increase excitatory post-synaptic current (EPSC) amplitude and total protein levels of NMDA and AMPA receptor subunits as

early as 1-hour post-stress. Acutely stressed mice showed improved working memory when subjected to the delayed alternation T-maze assay. Stress-induced effects on EPSC amplitude and T-maze performance are blocked by administration of GR antagonist RU486¹³⁰. In addition to changes in synaptic protein expression and improved behavioral outcomes, acute stressor exposure temporarily increases PL dendritic spine density¹³⁷. Chronic stress leads to the opposite effects¹³¹. Five days of repeated restraint stress is sufficient to reduce EPSC amplitude as well as NMDA and AMPA receptor subunit expression. Chronically stressed mice show diminished performance in working memory tasks. These effects are also blocked by GR antagonism¹³¹. Together, these data indicate that acute GC exposure promotes excitatory neurotransmission and cognitive performance, where chronic GC exposure diminishes both.

Differences between the apparent spine-promoting effects of acute GC exposure and the spine-deleterious effects of chronic GC exposure are not always clear. The effects of stress and/or GC exposure varies depending on the brain region or subregion studied¹³². BLA dendritic length and Sholl intersections both increase in response to chronic stress¹²⁷. Acute and chronic stress both increase BLA dendritic spine density¹³². Chronic stress also increases dendritic spine density on medium spiny neurons in the nucleus accumbens (NAc)¹³². Interestingly, chronic stress-mediated changes to hippocampal dendrites have been shown to vary between hippocampal subregions^{123,133}. As mentioned previously, CA1 dendritic spine density is reduced following chronic stress, but the neighboring CA3 subregion displays an increase in dendritic spine density following chronic stress^{123,133}. These results demonstrate that while some brain regions appear to display clear differences in dendritic spine density in response to acute and chronic stress exposure, the same cannot be assumed for other brain regions.

Diurnal rhythms in synaptic plasticity

In mice, hippocampal CA1 pyramidal neurons and pyramidal neurons in the cerebral cortex show changes in dendritic spine density across the L:D cycle^{126,134}. For hippocampus,

CA1 pyramidal neurons of mice on a 12:12 L:D show peak dendritic spine density begins to increase at ZT10 and reaches peak spine density 1 hour after the onset of the dark phase (ZT13). After reaching peak density in the early dark phase, CA1 spine density remains slightly elevated for 7 hours (until ZT19) before dropping to baseline for the remainder of the dark phase. Baseline spine density persists during the light phase. This diurnal rhythm of spine density is negated by adrenalectomy 7 days prior or by blocking GC synthesis with a single metyrapone injection 4 hours prior to euthanasia¹²⁶. Corresponding with these changes in spine density, hippocampal slices collected during the dark phase show increased excitatory postsynaptic potential (EPSP) slopes in response to LTP induction when compared to slices collected during the light phase, suggesting a circadian influence on LTP¹³⁵. Moreover, knockout of the clock gene BMAL1 is sufficient to impair LTP induction and reduce spatial memory in the Morris water maze¹³⁶. These results indicate that dendritic spine dynamics and LTP both change across the L:D cycle.

In the cerebral cortex of mice placed on a 12:12 L:D schedule, pyramidal neurons show peak spine density in the early dark phase (ZT14) and trough spine density in the early light phase (ZT2)¹³⁴. In rats, IL layer II/III pyramidal neurons show a diurnal rhythm of dendritic length and branching¹¹⁸. Layer II/III pyramidal neurons display greater increased dendritic branching and number of Sholl intersections in the early dark phase (ZT14) when compared to neurons measured in early light phase (ZT3)¹¹⁸. In addition to dendritic branching, peak dendritic spine densities on basilar and apical dendrites were observed at ZT14 and trough values at ZT3¹¹⁸. In the motor cortex, mice exposed to a rotarod motor learning task show significantly more new spine growth on layer V pyramidal neurons when training sessions coincide with the diurnal peak of GCs¹³⁷. Less spine growth is observed when mice are trained during trough GC concentrations. Additionally, spine growth is reduced when the diurnal peak of GCs is blocked¹³⁷. Together, these reports demonstrate that diurnal spine density rhythms exist in multiple brain regions, with additional evidence of GC regulation.

While a unified mechanism for observations of diurnal rhythms of dendritic spine density throughout the brain has yet to be proposed, it is suggested by reports on stress and diurnal GC rhythms correlating with rhythms of dendritic spine density that GC signaling is a major candidate for driving changes in dendritic spines. In hippocampal slice cultures, CORT application increases dendritic spine density in CA1 within an hour, but concurrent application of CORT and protein synthesis inhibitor cycloheximide blocks the increase in spine density¹²⁶. CORT and transcriptional inhibitor actinomycin D increase spine density¹²⁶. Similarly, CORT applied directly to the motor cortex increased spine formation within 90 minutes of application, which was also observed with concurrent CORT and actinomycin D treatment¹³⁸. Cortical application of CORT conjugated to membrane-impermeable bovine serum albumin also resulted in increased spine formation¹³⁸. Together, these findings suggest that acute exposure to GCs, like the diurnal peak of GC secretion, upregulates dendritic spine density via membrane associated GR activation and genomic mechanisms may not be necessary.

1.9 Specific Hypotheses and Conclusion

The maintenance of biological rhythms in mammals is a tightly regulated process responsible for the optimal functioning of virtually every tissue in the body. Mammalian biological rhythmicity involves rhythmic gene expression governed by core clock protein interactions, photoentrainment of SCN clock rhythms by ipRGC responses to external L:D cues, and the subsequent entrainment of central and peripheral clocks through the diurnal rhythm of GC secretion. GC signaling entrains core clock gene rhythms by inducing *Per* expression in the periphery and in some brain regions, which ultimately causes CCG expression patterns to occur at the proper times of day.

The diurnal rhythm of GC secretion is required for the proper timing of core clock gene expression across the L:D cycle in the rat vmPFC. In the mouse vmPFC, the regulation of core clock gene expression by the diurnal rhythm of GC secretion has yet to be demonstrated. The

diurnal rhythm of GC secretion is an important regulator for rhythmic gene expression in several other brain regions, including the CEA, oval nucleus of the bed nucleus of the stria terminalis (BNSTov), and cerebellum. Because the diurnal rhythm of GC signaling is important for regulating molecular clocks in multiple brain regions including the rat vmPFC, I hypothesize that diurnal rhythm of GC secretion also regulates the mouse vmPFC molecular clock.

GCs are heavily implicated in the regulation of dendritic spine dynamics. Acute GC exposure promotes synaptic potentiation and spine growth, while chronic GC exposure results in reductions in dendritic spines. The vmPFC is highly sensitive to GC-induced dendritic remodeling during stress, but the role of the diurnal rhythm of GC secretion in the regulation of dendritic remodeling in the vmPFC is unclear. In other brain regions like the motor cortex and the hippocampus, the diurnal rhythm of GC secretion drives a diurnal rhythm of dendritic spine density on pyramidal neurons. Due to the ubiquitous expression of GR in the brain, and common trends of the diurnal rhythm of GC secretion driving diurnal rhythms of dendritic spine density on pyramidal neurons in other brain regions, I hypothesize that pyramidal neurons within the mouse vmPFC also possess a GC-regulated diurnal rhythm of dendritic spine density.

In the following chapter, I seek to determine whether the mouse PL and IL vmPFC subregions exhibit rhythmic transcription of the core clock gene *Per1* across the L:D cycle after disrupting the diurnal rhythm of GC secretion via adrenalectomy. Then, I measure dendritic spine density in the PL and IL during the early light (inactive) phase, during the onset of the dark phase, and during the early dark (active) phase. Finally, I determine whether vmPFC dendritic spine density changes across the L:D cycle after disrupting the diurnal rhythm of GC secretion by inhibiting the synthesis of CORT via administration of metyrapone prior to the onset of the dark phase.

CHAPTER 2:
GLUCOCORTICOID REGULATION OF DIURNAL SPINE PLASTICITY IN THE MURINE
VENTROMEDIAL PREFRONTAL CORTEX

2.1 Summary

The ventromedial prefrontal cortex (vmPFC) regulates fear acquisition, fear extinction, mood, and HPA axis function. Multiple brain regions exhibit time-of-day dependent variations in learning, long term potentiation (LTP), and dendritic morphology. Glucocorticoids have been implicated in the regulation of dendritic structure in the context of stress. Glucocorticoids are also known to regulate molecular clock entrainment via upregulation of *Per1* transcription. In the present study, C57BL/6N mice were sacrificed at 3 distinct times of day (ZT3, ZT12, and ZT16, lights off at ZT12) and *Per1* mRNA expression was measured in the infralimbic and prelimbic vmPFC subregions using droplet digital (dd)PCR after recovering from adrenalectomy or sham surgery for 10 days. Sham mice showed *Per1* rhythmicity in both IL and PL, with peak expression occurring at ZT12. Adrenalectomized mice showed reductions in *Per1* amplitude at ZT12 in both IL and PL, suggesting that the vmPFC molecular clock is entrained by diurnal glucocorticoid oscillations. Thy1-eGFP mice were used to visualize and quantify dendritic spine density on layer V pyramidal dendrites at ZT 3, 12, and 16. Spine density in both PL and IL exhibited changes between the light (inactive) and dark (active) phases, with peak spine density observed at ZT16 and trough spine density observed at ZT3. These changes in spine density were restricted to changes in long thin and stubby type spines. To determine if changes in spine density is regulated by glucocorticoid oscillations, the 11 β -hydroxylase inhibitor metyrapone was administered 2 hours prior to the onset of the active phase (ZT10) daily for 7 days. Metyrapone administration blocked both the diurnal peak of plasma corticosterone and peak spine densities in the IL and PL at ZT16. These results suggest that vmPFC molecular clock gene and dendritic spine diurnal rhythms depend on intact diurnal glucocorticoid oscillations.

2.2 Introduction

Glucocorticoids (GCs) are released from the adrenal cortex in response to perceived environmental stressors and function to prime an organism to ensure homeostasis and survival. Activation of the hypothalamic-pituitary-adrenal (HPA) axis results in GC secretion (cortisol in humans, corticosterone (CORT) in mice and rats). The HPA axis is controlled by many factors, including negative feedback via direct GC action at the level of the paraventricular nucleus of the hypothalamus (PVN) and GC action on limbic regulatory regions like the ventromedial prefrontal cortex (vmPFC)¹³⁹⁻¹⁴¹. Notably, the HPA axis is regulated by the suprachiasmatic nucleus of the hypothalamus (SCN), the brain's master clock¹⁴². GC secretions follow a diurnal rhythm that is set by the SCN¹⁴². In the SCN, arginine vasopressin and vasoactive intestinal polypeptide-expressing neurons receive photic information from the retina⁶⁷. SCN neurons project to neuroendocrine and pre-autonomic neurons in the PVN^{67,82,143}. Projections to neuroendocrine neurons modulate corticotropin releasing hormone (CRH)-expressing neurons within the PVN, which stimulates adrenocorticotropin hormone (ACTH) release from the pituitary^{81,82}. Projections to pre-autonomic neurons regulate adrenal sensitivity to ACTH via the adrenal splanchnic nerve¹⁴⁴. The diurnal rhythm of GC secretion mirrors the organism's external light:dark (L:D) cycle, with highest levels observed at the onset of the active period, and lowest levels observed during the inactive period. Accordingly, in diurnal rodents, GC concentrations peak during light phase onset, whereas in nocturnal rodents, GC concentrations peak during the onset of the dark phase. SCN input to PVN is required for L:D-synchronized GC release since ablation of the SCN abolishes GC rhythmicity¹⁴⁵.

The diurnal rhythm of GCs is responsible for the synchronization of both peripheral clocks and several neural clock rhythms to coordinate a vast array of physiological responses to time of day. Diurnal GC secretion synchronizes molecular clock gene feedback loops in many peripheral tissues such as lung, kidney, cornea, liver, skeletal muscle, intestine, and others^{36-38,42}. In addition to molecular clock synchronization in the periphery, several brain regions

including cerebellum, central nucleus of the amygdala (CEA), oval nucleus of the bed nucleus of the stria terminalis (BNSTov), and vmPFC have been shown to have GC-entrained molecular clocks^{39–41,85}.

Neuronal characteristics, such as dendritic branching and spine density exhibit diurnal changes in multiple brain regions of the rodent. In rats sampled during the active phase, there are more dendritic branch points and a greater dendritic spine density in layer 2/3 pyramidal neurons of the infralimbic area (IL) when compared to rats sampled during the inactive (light) phase¹⁴⁶. Rat hippocampal CA1 pyramidal neurons also show an increased dendritic spine density during the active phase¹²⁶. This diurnal change of dendritic spine density was abolished after adrenalectomy (ADX) and rescued with exogenous CORT administration suggesting that glucocorticoids (GCs) are involved in driving hippocampal rhythms in spine plasticity¹²⁶. In the motor cortex, training mice in a motor learning task during peak diurnal plasma CORT led to significantly more new spine growth and significantly improved motor performance when compared to mice trained at trough plasma CORT¹⁴⁷. Taken together, these findings suggest an important role for GCs in rhythmic spine turnover and spine growth across the L:D cycle.

Neurons in the IL and prelimbic (PL) vmPFC subregions are involved in working memory, decision making, emotion, fear conditioning, and regulation of the HPA axis^{13,139}. In rats, vmPFC neurons exhibit a diurnal pattern of function in a fear extinction paradigm¹⁴⁸. Specifically, rats subjected to a fear extinction learning paradigm in the inactive phase (zeitgeber time (ZT)16, with ZT12 representing the onset of the dark phase and ZT0 representing onset of the light phase) show optimal fear extinction recall when compared to rats tested in the light phase (ZT4). These time-of-day effects in fear extinction recall are abolished in rats with ShRNA-mediated *Per1/Per2* knockdown delivered to the vmPFC, indicating that fear extinction recall is mediated by local vmPFC molecular clock machinery. Moreover, ADX'd rats subjected to the same fear extinction paradigm show a deficit in fear extinction recall at ZT16

when compared to sham operated rats tested at ZT16, indicating that intact adrenal output is also required for this circadian pattern of vmPFC-mediated fear conditioning¹⁴⁸.

Although evidence suggests that the diurnal rhythm of CORT secretion is a contributor to dendritic spine changes over the L:D cycle in other brain regions, the presence of diurnal dendritic spine rhythmicity in the mouse vmPFC has yet to be demonstrated. The objectives of the current study are to determine whether vmPFC spine rhythmicity is present in the mouse vmPFC and to assess GC involvement in regulating dendritic structure and core clock gene *Per1* transcriptional oscillations across the L:D cycle.

2.3 Materials & Methods

Animals

Animals in these studies were housed in the laboratory animal research facility at Colorado State University. Male C57BL/6N (RRID:IMSR_CRL:027) mice from Charles River Laboratories (Wilmington, MA) were delivered at 6-8 weeks of age. The Thy1-eGFP (RRID:IMSR_JAX:007788) colony was maintained heterozygously by breeding female Thy1-eGFP mice with noncarrier C57BL/6N mice. Mice were weaned at 21 days of age and group housed in a temperature/humidity-controlled room on a 12:12 L:D cycle (lights on at 06:00 (ZT0), off at 18:00 (ZT12)). Food and water were available *ad libitum*. All experimental protocols were conducted in accordance with the National Institutes of Health Guidelines for the Care and Use of Animals and approved by the Colorado State University Institutional Animal Care and Use Committee and the Department of the Navy, Bureau of Medicine and Surgery (BUMED) (NRD-949).

Blood collection

For terminal blood sample collection, mice were deeply anesthetized using isoflurane. If mice were decapitated, trunk blood was collected following decapitation. If mice were perfused,

blood was drawn from the right atrium prior to perfusion. Blood was collected into EDTA-coated blood collection tubes (BD Vacutainer, Franklin Lakes, NJ). Blood was centrifuged at 2000 rpm for 10 minutes at 4°C and plasma was pipetted off and stored in separate tubes at -20°C until assayed.

Microdissection, RNA isolation, and droplet digital PCR (ddPCR)

Flash frozen brains were sectioned at -16°C into 300µm-thick sections containing the IL and PL using a CM3050 S cryostat (Leica; RRID:SCR_016844). IL (Bregma 1.53mm, 1.41mm) and PL (Bregma 1.69mm, 1.53mm) tissue samples were obtained from two sections per animal using a micropunch made from stainless-steel type 304 tubing with an internal diameter of 0.991 (Small Parts Inc., Miami Lakes, FL). Tissue punches were frozen and stored at -80°C until RNA extraction. RNA was isolated from IL and PL punches using the RNeasy mini kit (Qiagen, Germantown, MD) according to the manufacturer's instructions. Total RNA was reverse transcribed to yield cDNA using iScript Reverse Transcriptase Super Mix (Bio-Rad, Hercules, CA). ddPCR was then used to measure *Per1* cDNA copies as number of molecules. This approach has been demonstrated to yield increased sensitivity and decreased variability compared to other qPCR methods^{149–151}. The ddPCR reaction mix was prepared by the addition of cDNA to an EvaGreen supermix (10µL; Bio-Rad) combined with forward (0.7µL) and reverse (0.7µL) primers and nuclease-free water up to a total volume of 20µL. *Per1* primer sequences are as follows:

Per1 mRNA forward 5'-TGTCGGTCACCAGTCAGTGT-3'

Per1 mRNA reverse 5'-CCAGGCAGGTCTTCCATC-3'

To generate droplets, 20µL of PCR reaction mix and 70µL of droplet generation oil were added to appropriate wells in the DG8 Cartridge for the QX200 droplet generator and was loaded into the automated droplet generator (Bio-Rad QX200 Droplet Digital PCR System, RRID:SCR_019707). After generation, droplets were transferred to a 96-well plate and sealed

using a PX1 PCR plate sealer. PCR amplification of *Per1* in each individual droplet was conducted in a C1000 Touch Thermal Cycler. The following protocol was used: 95°C for 10 minutes (one cycle), 95°C for 30 seconds, and then 60°C for 1 minute (40 cycles), 4°C for 5 minutes (one cycle), 90°C for 5 minutes (one cycle), and hold at 4°C. The ramp rate was set at 2°C/s, the sample volume at 40 µL, and the heated lid at 105°C. After amplification, the plate was inserted into the QX200 Droplet Reader (Bio-Rad QX200 Droplet Digital PCR System, RRID:SCR_019707), and the absolute template expression in copies per microliter was quantified using QuantaSoft software.

Radioimmunoassay (RIA)

CORT was measured using RIA as previously described¹⁵² (limit of detection = 4.45 ng/mL). Plasma samples were diluted 1:25 in 0.01M phosphate buffered saline (PBS) (pH = 7.4). CORT binding globulin was denatured by heating samples at 65C for 1 hour. A standard curve ranging from 2.5pg to 750pg CORT (Steraloids, Newport, RI) was run alongside all assay tubes. All samples and standards were incubated with CORT antiserum (1:1200, Cat# 7120016, RRID:AB_2801269, MP Biomedicals, Solon, OH) and ³H corticosterone (Perkin Elmer, Boston, MA) overnight at 4C. Unbound CORT was removed by adding dextran-coated charcoal and centrifuging for 15 min at 3000rpm and 4C. The supernatant containing bound CORT was decanted into plastic scintillation vials, mixed with 4mL liquid scintillation cocktail (Ecoscint Ultra, National Diagnostics, Atlanta, GA), and counted using a Tri-Carb 2900TR (Packard Tri-Carb 2900TR Liquid Scintillation Analyzer, RRID:SCR_018610, PerkinElmer, Waltham, MA). Sample CORT concentrations were determined via comparison to a standard curve (2.5-750pg) and data was analyzed using Graphpad Prism Software (GraphPad Prism, RRID:SCR_002798, San Diego, CA). The intra-assay variance was 9.4% and was determined using internal quality controls measured throughout the assay. All samples from a single experiment were run in a single assay.

Enzyme-Linked Immunosorbent Assay (ELISA)

Plasma CORT was determined in duplicate with an ELISA kit (Arbor Assays Cat# K014-H1, RRID:AB_2877626, limit of detection = 7.7pg/mL, mean intra-assay CV = 8.5%) per manufacturer guidelines.

Adrenalectomy

ADX procedures were performed as previously described^{141,153}. To remove the primary source of circulating CORT, adult mice were anesthetized with isoflurane (2-4% in O₂) and were given a 4mg/kg meloxicam SR injection subcutaneously. Mice were subjected to bilateral ADX followed by a subcutaneous injection of 0.9% saline solution (0.3mL). ADX'd mice were also given 0.9% saline in drinking water to maintain osmotic balance. To verify a reduction in plasma CORT, trunk blood was collected at the time of euthanasia (as described above) then assayed for CORT via RIA.

Tissue collection for confocal imaging and immunohistochemistry

Mice were deeply anesthetized with isoflurane (5% isoflurane in O₂) and transcardially perfused with 0.01M PBS (pH = 7.4), followed by 0.1M phosphate buffered 4% paraformaldehyde (PFA) (pH = 7.4). Brains were post-fixed in PFA for 24 hours and then stored in 0.1M phosphate buffered 30% sucrose at 4C. Brains were subsequently sectioned at 40µm using a Leica CM3050 S cryostat (Leica Biosystems, Buffalo Grove, IL) and mounted onto charged glass slides (Superfrost Plus, Fischer Scientific, Pittsburg, PA) with Prolong Diamond Antifade mounting media (Invitrogen, Waltham, MA) for confocal imaging.

Glucocorticoid receptor (GR) immunohistochemistry (IHC)

GR IHC was performed on free-floating 35µm thick coronal sections containing IL and PL. 5 x 10 minute washes were performed in 0.01M PBS (pH = 7.4). Blocking of nonspecific antibody binding was performed in 4% normal goat serum (NGS) in PBS for 1 hour prior to incubation in primary antibody solution (0.01M PBS with 0.1% Triton-X (PBST)), 4% NGS, and primary antibody). The primary antibody used was a previously validated rabbit anti-GR antibody (1:500 dilution; Thermo Fisher Scientific, Waltham, MA, Cat# PA1-511A, RRID:AB_2236340)¹⁵⁴. Sections were incubated in primary antibody solution overnight. Then, 3 x 10 minute washes were performed in PBST before secondary antibody incubation. The secondary antibody used was a biotinylated goat anti-rabbit antibody (1:200; Vector Laboratories, Burlingame, CA, Cat# BA-1000, RRID:AB_2313606) and sections were incubated for 1 hour. Sections were then washed 3 x 10 minutes in PBST and incubated in tertiary streptavidin solution, containing Alexa Flour-555 (1:200; Thermo Fisher Scientific, Waltham, MA) for 1 hour. 2 x 10 minute washes were performed in PBS, followed by incubation with TO-PRO™-3 Iodide (1:1000; Thermo Fisher Scientific, Waltham, MA) nucleic acid counterstain solution for 10 minutes. Finally, sections were washed 5 x 10 minutes in PBS and were mounted and cover slipped using ProLong Diamond Antifade mounting media.

Confocal microscopy- spine imaging

Spine images were collected with a ZEISS LSM 880 confocal microscope (Zeiss LSM 880 with Airyscan Confocal Laser Scanning Microscope, RRID:SCR_020925, Oberkochen, Germany) using a 40x/1.3 numerical aperture Oil DIC Plan-APOCHROMAT objective lens and ZEN black acquisition software. Imaging parameters were 40x objective, 1.5x zoom, 2% laser intensity for 488nm (eGFP), 6 speed, 2 averaging, Pinhole = 1 airy unit (AU) and were kept consistent for all eGFP imaging. Z-stacks were 20-30µm thick and the z interval was set to 0.14µm (equal to 1 pixel) to allow 3D rendering.

Dendritic spine quantification and analysis

Confocal z-stacks were subsequently analyzed in 3 dimensions using Bitplane IMARIS 8.4.2 software (Imaris, RRID:SCR_007370). Twelve unique IL dendritic segments with an average length of 21.9 μ m were randomly selected and analyzed per brain region. Dendritic segments beyond tertiary branch points were selected at random for analysis, whereas primary and secondary dendritic branches were excluded from the analysis for uniformity of each sample. Spines were digitally reconstructed and manually counted by an investigator blinded to experimental condition. Spine subtypes were classified using the IMARIS filament tracer plugin (FilamentTracer, RRID:SCR_007366). The criteria for each spine subtype are as follows: Filopodia = length greater than 2 μ m, Thin = length less than 2 μ m, Stubby = length less than 1 μ m, Mushroom = length less than 2 μ m and head width greater than two times the neck width. Spine counts from each segment for each brain were averaged together to give a representative mean for each mouse in the sample and means for each mouse were used in all statistical analyses. Spine counting and subtype classification was performed using the filament tracer plugin on IMARIS and subtypes were analyzed in the same fashion as data for total spine counts. Example images of spine subtype morphologies are provided in **Fig 1.5**.

Statistics

Statistical analyses were performed in GraphPad Prism 9.0 (GraphPad Prism, RRID:SCR_002798). A p-value < 0.05 was considered significant. Unpaired student's t-test was used to compare IL and PL GR/eGFP colocalization. One-way ANOVA was used to assess the effect of time of day on dendritic spine density in the PL and IL. Two-way ANOVA was used to assess the effects of time of day and ADX on *Per1* transcription. Two-way ANOVA was also used to assess the effects of time of day and metyrapone administration on dendritic spine density in the PL and IL. For spine subtype analysis, two-way ANOVA was used to assess the

effects of time of day and spine subtype on overall spine density. Bonferroni *post hoc* tests were used to compare groups in all ANOVA designs when qualified by significant main effects or significant interactions.

Experiment 1. Effect of plasma GC depletion via ADX on vmPFC *Per1* rhythmicity

Intact C57BL/6N males aged 2-4 months (n = 4 to 6 per group) were bilaterally ADX'd under isoflurane anesthesia and given 0.9% saline as drinking water to maintain osmolarity. Sham operated mice were given tap water. 10 days after surgery, animals were decapitated at ZT3, 12, or 16 (ZT0 denotes lights on, ZT12 denotes lights off) within 2 minutes of cage disturbance and brains were removed, flash frozen in 2-methyl butane on dry ice at -40°C and stored at -80°C until sectioning and tissue dissection for quantification of *Per1* mRNA by ddPCR. Immediately following decapitation, trunk blood was collected plasma was stored until assayed for CORT via RIA.

Experiment 2. Diurnal rhythm of dendritic spine density on ventromedial prefrontal cortex layer V pyramidal neurons

Intact Thy1-eGFP males aged 2-4 months (n = 5 to 6 per group) were transcardially perfused at ZT3, 12, or 16 and brains were stored and sectioned for confocal imaging and dendritic spine quantification (described above).

Experiment 3. Colocalization of glucocorticoid receptor with layer V vmPFC eGFP labeling in the Thy1-eGFP mouse

Intact Thy1-eGFP males aged 2-4 months (n = 4) were subjected to 60 minutes of restraint stress to allow for CORT-GR binding and subsequent nuclear translocation of GR. Immediately following restraint, mice were perfused, and brains were stored and sectioned. Brain sections were then immunolabeled for GR and all eGFP+ pyramidal neurons present in IL

and PL were imaged to assess % colocalization. The following formula was used to calculate % eGFP/GR colocalization: % colocalization = (# of cells containing both eGFP and GR) / (Total # of eGFP cells in the brain region) x 100.

Experiment 4. Effect of plasma GC depletion via daily metyrapone injections on vmPFC spine rhythmicity

Intact Thy1-eGFP males aged 2-4 months (n = 7 per group) were subjected to 7 daily injections of vehicle (0.9% saline) or 50mg/kg metyrapone (MedChemExpress, Monmouth Junction, NJ) administered prior to dark phase onset at ZT10. After metyrapone administration on day 7, blood samples were taken via cardiac puncture and mice were perfused at ZT3, 12, and 16. Brains were stored and subsequently sectioned for confocal imaging and dendritic spine quantification. Blood samples were collected in chilled EDTA coated tubes. Blood was then centrifuged at 4°C, and plasma was removed and stored at -20°C until it was assayed for CORT via ELISA.

2.4 Results

vmPFC *Per1* transcriptional rhythmicity was disrupted in response to ADX

To assess the effect of ADX on the circadian pattern of CORT release, plasma from sham and ADX mice were assessed for CORT at ZT3, 12, and 16. The chosen timepoints for plasma sampling reflect circadian trough (ZT3), peak (ZT12), and early active phase (ZT16) CORT concentrations in sham animals (**Fig 2.1A**). Two-way (Surgery x Time of day) ANOVA showed a significant effect of Surgery [$F(1,24) = 38.70$; $p < 0.0001$] and time of day [$F(2,24) = 39.95$; $p < 0.0001$] on plasma CORT concentration. Additionally, a significant surgery x time of day interaction was found [$F(2,24) = 11.03$; $p < 0.001$]. Bonferroni *post hoc* analysis was performed to examine the effect of surgery at different times of day. Compared to sham, ADX reduced plasma CORT at ZT12 ($p < 0.0001$) and ZT16 ($p < 0.01$), but not ZT3 (**Fig 2.1A**).

To assess the influence of ADX on *Per1* mRNA rhythmicity, we compared ADX *Per1* copies/ul cDNA with sham surgery groups at ZT3, 12, and 16 in both the PL and IL. For PL, two-way (Surgery x Time of day) ANOVA showed significant main effects of Surgery [$F(1,23) = 24.89$; $p < 0.0001$] and time of day [$F(2,23) = 8.002$; $p < 0.01$]. A significant interaction was also found [$F(2,23) = 6.35$; $p < 0.01$]. *Post hoc* analysis showed that ADX significantly reduced PL *Per1* mRNA levels at ZT12 ($p < 0.0001$) and ZT 16 ($p < 0.05$), but not ZT3, reflecting changes in plasma CORT concentrations in response to ADX (**Fig 2.1B**). For IL, two-way (Surgery x Time of day) ANOVA revealed a significant interaction [$F(2,23) = 5.82$; $p < 0.01$]. *Post hoc* analysis showed that ADX reduced IL *Per1* mRNA levels at ZT 12 ($p < 0.05$), but not ZT3 or ZT16 (**Fig 2.1C**).

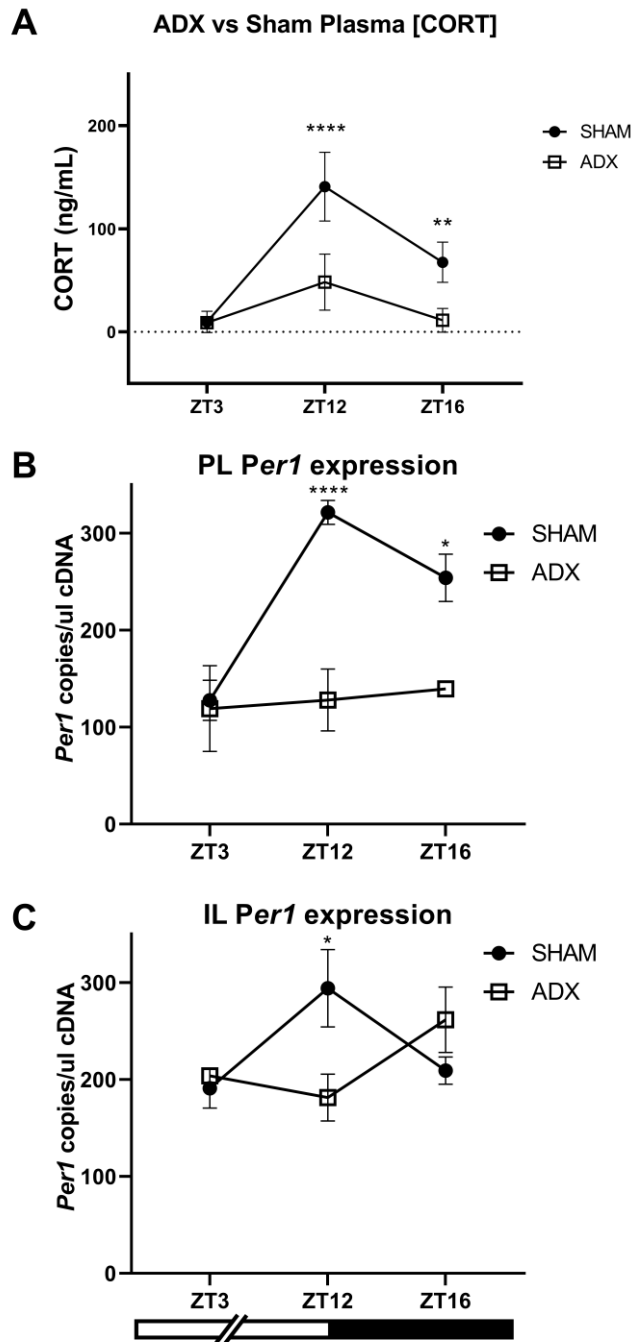
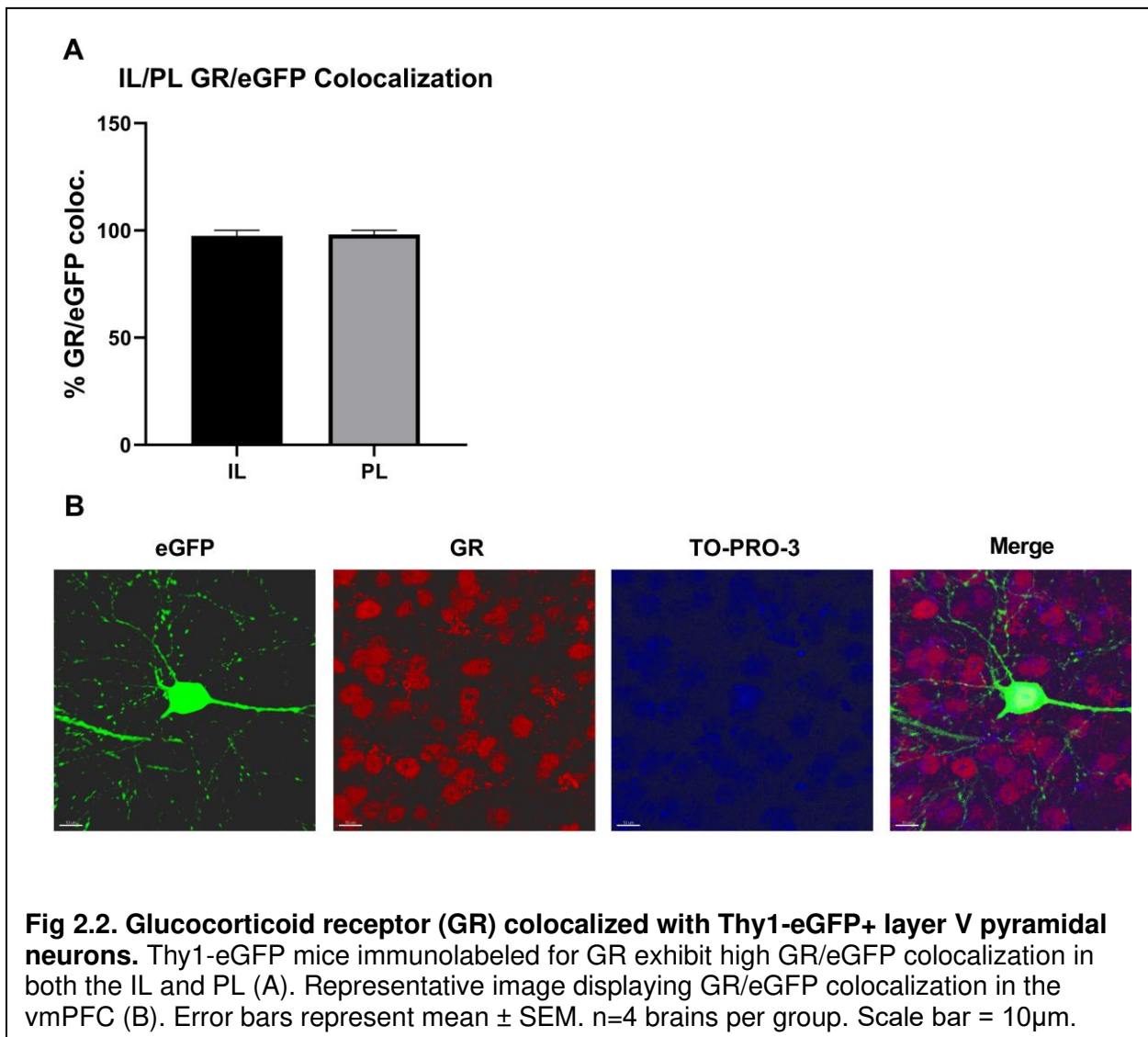


Fig 2.1. Adrenalectomy (ADX) disrupts rhythmic *Per1* mRNA expression in both IL and PL. C57/BL6N mice were subjected to ADX or SHAM surgery and sacrificed 10 days later at ZT3, 12, or 16. IL and PL *Per1* expression was measured by ddPCR. ADX decreased plasma [CORT] at ZT12 and ZT16 (A). ADX decreased IL *Per1* expression at ZT12 (B). ADX decreased PL *Per1* expression at both ZT12 and 16 (C). Error bars represent mean ± SEM. n=4-5 brains per group. * p<.05, ** p<.01, **** p<.0001. White/black bar denotes L:D cycle.

Glucocorticoid receptor (GR) was colocalized with eGFP+ vmPFC layer V pyramidal neurons

To verify GR expression in eGFP expressing IL and PL layer V pyramidal neurons, we compared eGFP/GR colocalization between IL and PL subregions. Unpaired t-test showed no significant difference in the colocalization of GR and eGFP in the IL and PL. Notably, both subregions exhibited high levels of colocalization, with IL showing $97.5 \pm 2.5\%$ colocalization and PL showing $98.08 \pm 1.925\%$ colocalization of GR with eGFP (**Fig 2.2A**). A representative Thy1-eGFP+ neuron that colocalizes with GR is shown in **Fig 2.2B**.



A diurnal rhythm in spine density was detected in PL layer V pyramidal neurons

The chosen timepoints for dendritic spine sampling reflect circadian trough (ZT3), peak (ZT12), and early active phase (ZT16) plasma CORT concentrations (**Fig 2.1A**). One-way ANOVA revealed a significant effect of time of day on dendritic spine density in the PL [$F(2,12) = 5.49$; $p < 0.05$] (**Fig 2.3**). *Post hoc* analysis revealed that brains collected at ZT16 had significantly higher spine density when compared to both ZT3 and ZT12 ($p < 0.05$ for ZT3 vs ZT16, $p < 0.05$ for ZT12 vs ZT16) (**Fig 2.3A**). To further investigate changes in the dendritic spine subtype composition across the L:D cycle, Two-way (Spine subtype x Time of day) ANOVA revealed a significant main effect of both spine subtype [$F(3,44) = 320.7$; $p < 0.0001$] and time of day [$F(2,44) = 3.72$; $p < 0.05$]. A significant spine subtype x time of day interaction was found [$F(6,44) = 9.86$; $p < 0.0001$]. *Post hoc* analysis revealed that long thin spines are upregulated at ZT16 compared to both ZT3 and ZT12 ($p < 0.0001$ for ZT3 vs ZT16, $p < 0.0001$ for ZT12 vs ZT16). Stubby spines are slightly reduced at ZT16 when compared to ZT12 ($p < .01$) (**Fig 2.3B**). Example profiles of spines are shown in **Fig 1.5**.

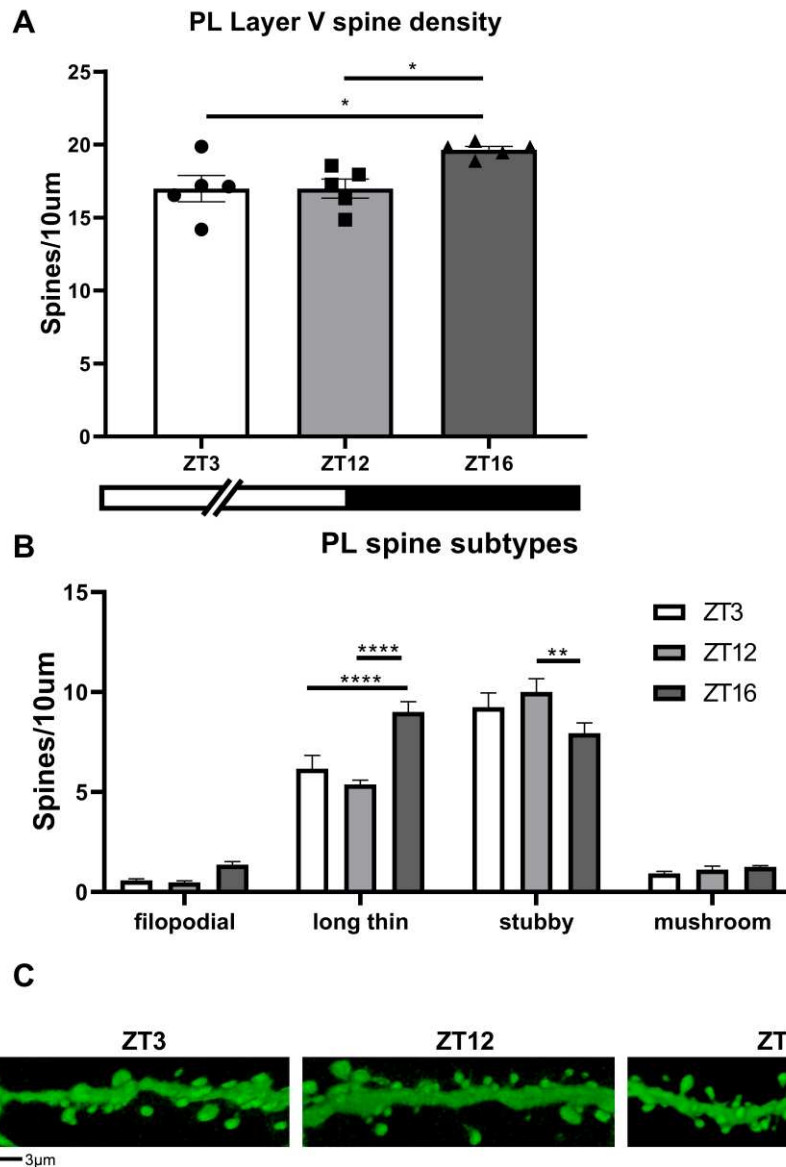


Fig 2.3. PL layer V pyramidal neurons exhibit a diurnal rhythm of dendritic spine density. Thy1-eGFP mice were sacrificed at ZT3, ZT12, and ZT16. Prelimbic area (PL) layer V pyramidal neuron spine density exhibits a diurnal rhythm (A). PL spine subtype distribution exhibits a diurnal rhythm in PL layer V pyramidal dendrites, showing increased long thin spine number at ZT16, and decreased stubby spine density at ZT16 (B). Representative images of dendritic spine segments at ZT3, 12, and 16 (C). Error bars represent mean \pm SEM (n= 5 brains per group, 60 segments per group). * $p < .05$, ** $p < .005$, **** $P < .0001$. White/black bar denotes L:D cycle. Scale bar = 3µm.

A diurnal rhythm in spine density was detected in IL layer V pyramidal neurons

To assess IL dendritic spine rhythmicity across the day, we sampled layer V IL dendrites at ZT3, 12, and 16. One-way ANOVA revealed a significant effect of time of day on dendritic spine density in the IL [$F(2,13) = 32.84$; $p < 0.0001$]. *Post hoc* analysis showed that brains collected at ZT12 and ZT16 had higher spine density when compared to ZT3 ($p < 0.001$ for ZT3 vs ZT12, $p < 0.0001$ for ZT3 vs ZT16). Additionally, ZT16 was found to have higher spine density when compared to ZT12 ($p < 0.05$) (**Fig 2.4A**). To further investigate changes in dendritic spine subtype composition across the L:D cycle, two-way (Spine subtype x Time of day) ANOVA revealed a significant main effects of both spine subtype [$F(3,52) = 253.9$; $p < 0.0001$] and time of day [$F(2,52) = 22.85$; $p < 0.0001$]. An interaction was also found [$F(6,52) = 7.086$; $p < 0.0001$]. *Post hoc* analysis revealed that spine rhythmicity was restricted to changes within the long thin and stubby subtype pools. Specifically, ZT16 showed increased long thin spine density when compared to both ZT3 and ZT12 ($p < 0.0001$ for ZT16 vs ZT3, $p < 0.001$ for ZT16 vs ZT12). Additionally, both ZT12 and ZT16 showed increased stubby spine density when compared to ZT3 ($p < 0.0001$ for ZT12 vs ZT3, $p < 0.0001$ for ZT16 vs ZT3) (**Fig 2.4B**).

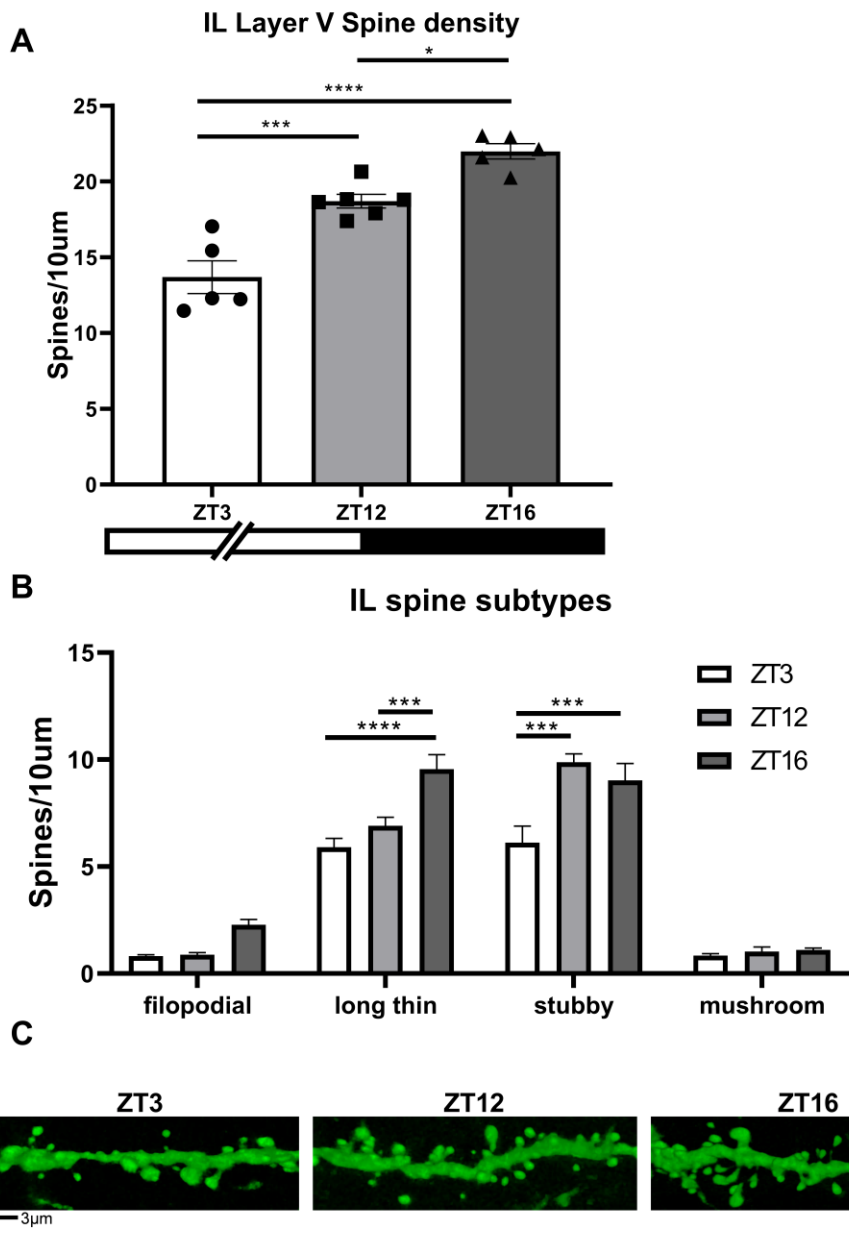


Fig 2.4. IL layer V pyramidal neurons exhibit a diurnal rhythm of dendritic spine density. Thy1-eGFP mice were sacrificed at ZT3, ZT12, and ZT16. Infralimbic area (IL) layer V pyramidal neuron spine density exhibits a diurnal rhythm (A). Spine subtype distribution exhibits a diurnal rhythm in IL layer V pyramidal dendrites, showing increased stubby spine density at ZT12, and increased long thin spine density at ZT12 and ZT16 (B). Representative images of dendritic spine segments at ZT3, 12, and 16 (C). Error bars represent mean \pm SEM (n= 5-6 brains per group, 60-72 segments per group). * p<.05, *** p<.001, **** P<.0001. White/black bar denotes L:D cycle. Scale bar = 3µm.

Disruption of CORT rhythmicity via repeated metyrapone injections prior to light offset diminishes vmPFC spine rhythmicity

To assess the influence of daily ZT10 metyrapone administration on the diurnal pattern of CORT release, we compared metyrapone-injected plasma CORT with vehicle-injected plasma CORT at ZT3, 12, and 16. Two-way (Metyrapone x Time of day) ANOVA revealed a significant effect of time of day [$F(2,36) = 13.68$; $p < 0.0001$] as well as an interaction [$F(2,36) = 16.17$; $p < 0.0001$]. *Post hoc* analysis revealed that metyrapone-injected mice had significantly reduced plasma CORT at ZT12 when compared to vehicle-injected mice ($p < 0.001$) (**Fig 2.5A**). To assess the influence of metyrapone administration on vmPFC dendritic spine rhythmicity, we compared PL and IL dendritic spine density and subtype composition between metyrapone and vehicle-injected mice at ZT3 and 16. Sampling time points were chosen due to previously observed robust differences in dendritic spine density between ZT3 and ZT16 in both PL and IL subregions (**Fig 2.2, Fig 2.3**).

For PL, metyrapone administration blocked diurnal changes in spine density. Two-way (Metyrapone x Time of day) ANOVA revealed significant effects of both time of day [$F(1,24) = 33.19$; $p < 0.0001$] and metyrapone [$F(1,24) = 32.68$; $p < 0.0001$] on PL spine density. Additionally, a significant metyrapone x time of day interaction was found [$F(1,24) = 26.55$; $p < 0.0001$]. *Post hoc* analysis showed that vehicle-injected mice exhibited PL spine rhythmicity ($p < 0.0001$ for veh ZT3 vs veh ZT16). In contrast, metyrapone-injected mice showed no difference in spine density between ZT3 and ZT16. Vehicle-injected mice at ZT16 showed significantly higher spine density when compared to metyrapone-injected mice at ZT16 ($p < 0.0001$) (**Fig 2.5B**). To assess spine subtype composition across timepoints, two-way (Spine subtype x time of day) ANOVAs were conducted for vehicle and metyrapone-injected groups. For vehicle groups, significant effects of spine subtype [$F(3,48) = 235.6$; $p < 0.0001$] and time of day [$F(1,48) = 14.24$; $p < 0.0001$] were found. Consistent with previous observations, *post hoc* analysis showed that PL spine rhythmicity in vehicle-injected mice is restricted to long thin

spines ($p < 0.01$) (**Fig 2.5C**). Conversely, for metyrapone-injected groups, no significant effect of time of day was found, indicating that spine subtype composition remained unchanged.

For IL, metyrapone administration blocked diurnal changes in spine density. two-way (Metyrapone x Time of day) ANOVA revealed significant effects of both time of day [$F(1,24) = 92.13$; $p < 0.0001$] and metyrapone [$F(1,24) = 45.38$; $p < 0.0001$] on IL spine density. A significant interaction was found [$F(1,24) = 73.04$; $p < 0.0001$]. *Post hoc* analysis showed similar trends to the PL, in that vehicle-injected mice showed IL spine rhythmicity ($p < 0.0001$ for veh ZT3 vs veh ZT16). Metyrapone-injected mice showed no change in spine density between ZT3 and ZT16. Again, vehicle-injected mice at ZT16 showed significantly higher spine density when compared to metyrapone-injected mice at ZT16 ($p < 0.0001$) (**Fig 2.5D**). two-way (Spine subtype x time of day) ANOVA of vehicle-injected groups showed significant effects of spine subtype [$F(3,48) = 208.2$; $p < 0.0001$] and time of day [$F(1,48) = 58.50$; $p < 0.0001$]. An interaction was also found [$F(3,48) = 7.64$; $p < 0.001$]. *Post hoc* analysis showed that IL spine rhythmicity in vehicle-injected mice is restricted to long thin ($p < 0.0001$) and stubby ($p < 0.001$). For metyrapone-injected groups, no time of day effect was found (**Fig 2.5E**).

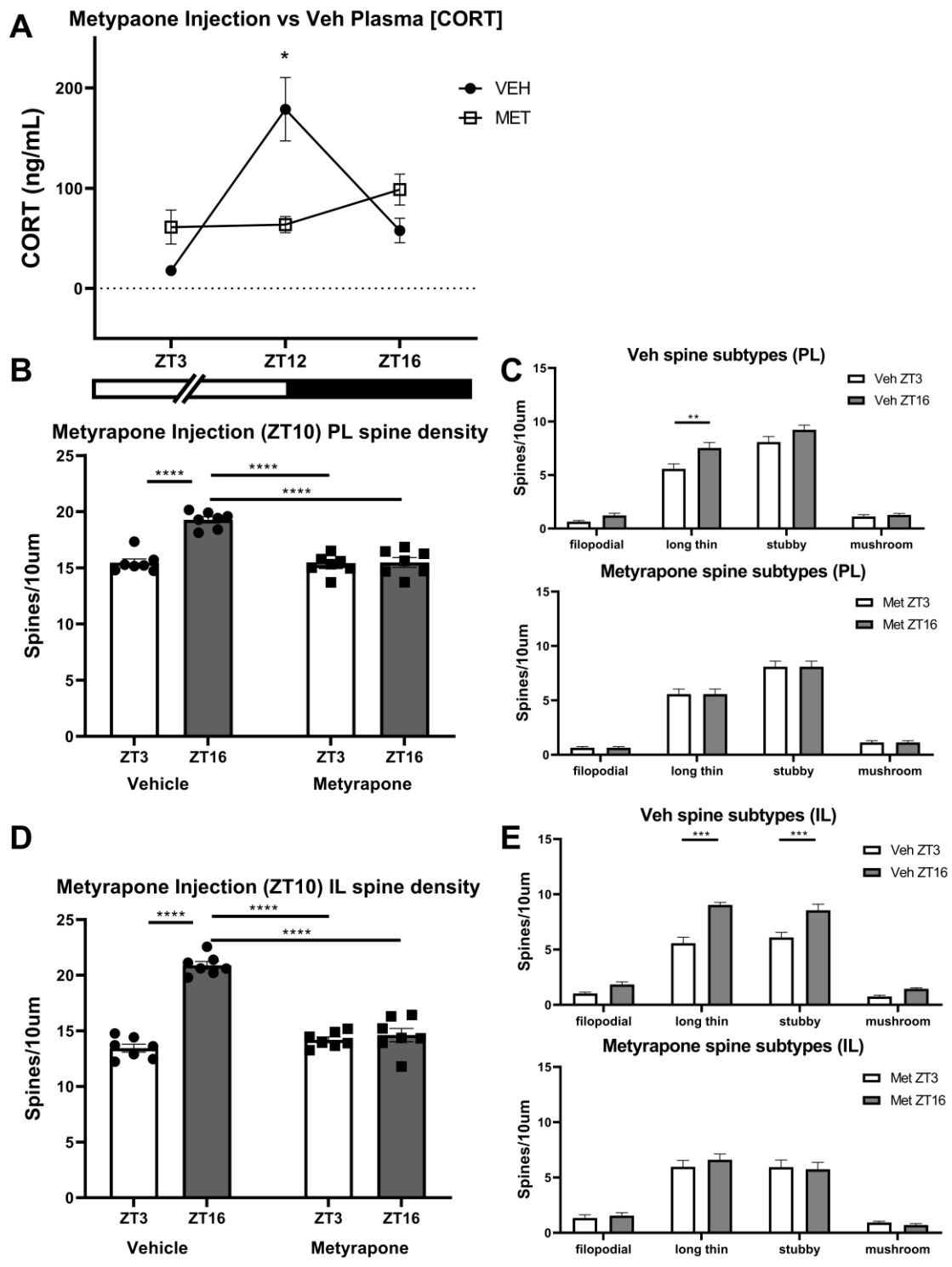


Fig 2.5. Repeated metypaone injections block the diurnal peak of corticosterone and diminish layer V vmPFC spine rhythmicity.

Fig 2.5. Repeated metyrapone injections block the diurnal peak of corticosterone and diminish layer V vmPFC spine rhythmicity. Thy1-eGFP mice were given daily 50mg/kg metyrapone injections at ZT10 for 7 days and were sacrificed at ZT3, ZT12, and ZT16. Metyrapone injections reduced plasma [CORT] at ZT12 (A). Vehicle-injected PL spine density exhibits a diurnal rhythm, but metyrapone-injected PL spine density lacks rhythmicity (B). Vehicle-injected PL spine subtype distribution exhibits a diurnal rhythm, showing increased long thin spine density at ZT16, but metyrapone-injected PL spine subtype distribution lacks rhythmicity (C). Vehicle-injected IL spine density exhibits a diurnal rhythm, but metyrapone-injected IL spine density lacks rhythmicity (D). Vehicle-injected IL spine subtype distribution exhibits a diurnal rhythm, showing increased long thin and stubby spine density at ZT16, but metyrapone-injected IL spine subtype distribution lacks rhythmicity (E). White/black bar denotes L:D cycle.

2.5 Discussion

Overall, this study demonstrates that layer V pyramidal neurons in the mouse PL and IL exhibit diurnal rhythms of dendritic spine rhythmicity, which is dependent on a functional diurnal GC secretory pattern that predicts active phase onset. The data showed that disruption of GC secretions via ADX alter core clock gene *Per1* expression in IL and PL. These findings compliment a growing body of literature indicating that dendritic morphology is influenced by circadian rhythms^{17,27,28}. This study also shows that the diurnal rhythm of GC secretion is a regulator of dendritic plasticity in the vmPFC^{17,29}.

The loss of rhythmic *Per1* transcription in the PL and IL in response to ADX in the current study shows interactions between GC rhythmicity and *Per1* transcription in the mouse vmPFC. GC-dependent synchronization of molecular clock and clock-controlled gene rhythmicity had been demonstrated in other brain regions, including the rat vmPFC, BNSTov, CEA, as well as several peripheral organs^{41,42,85,88,98}. GC-dependent synchronization of molecular clock rhythms is not a universal phenomenon and varies depending on brain region, cell type, and tissue studied. Within the amygdala, the basolateral amygdala (BLA) and CEA nuclei exhibit opposite rhythms of clock gene expression. The CEA is the only nucleus in the amygdala where molecular clock rhythms are altered in response to adrenalectomy; the BLA molecular clock rhythm persists in the absence of GCs⁹⁸. The present results suggest that the

Per1 transcriptional rhythms in the IL and PL are relatively uniform in that both vmPFC subregions show ablated rhythmicity in response to GC disruption. However, among the timepoints sampled, the PL from ADX mice exhibited reductions in *Per1* mRNA at both ZT12 and 16, whereas the IL from ADX mice only showed reduced *Per1* mRNA at ZT12. This slight difference between regions could be in part due to differences in afferent projections to the IL and PL. Specifically, the IL receives projections from an SCN-paraventricular thalamus-IL pathway that could be responsible for relaying time-of-day cues to the IL independent of GC status. In comparison, the PL lacks substantial afferent input from this pathway⁷⁶.

The present study demonstrates a robust diurnal rhythm of dendritic spine density on layer V pyramidal neuron basilar dendrites in both PL and IL vmPFC subregions. Diurnal dendritic spine rhythmicity has been previously demonstrated in CA1 pyramidal neurons in rat hippocampus as well as the mouse cortex, although the specific cortical region was not specified^{126,134}. Additionally, diurnal dendritic spine rhythmicity has been shown in rat IL Layer II/III pyramidal neurons¹⁴⁶. To our knowledge, this is the first report of dendritic spine rhythmicity in layer V IL and PL pyramidal neurons. The distinction between layer II/III and layer V pyramidal neurons is significant, as each pyramidal cell layer of cortex exhibits unique projection patterns and targets^{155–157}. Layer II/III pyramidal neurons in the vmPFC typically project to other cortical regions, with previously demonstrated projections to somatosensory cortex, auditory cortex, and retrosplinal granular cortex¹⁵⁶. Layer II/III pyramidal neurons can also project to subcortical regions like the posterior thalamus, ventral striatum, and BLA^{156,157}. Layer V pyramidal neurons in both IL and PL project to numerous subcortical regions, with some common projection targets and some unique to each subregion. Shared projections between IL and PL layer V pyramidal neurons include limbic regulatory regions like the septum, periaqueductal grey, BLA, and autonomic regulatory regions like the rostral and caudal ventrolateral medulla. IL layer V pyramidal neurons have significantly more projections to the parabrachial nucleus and nucleus tractus solitarius, where PL layer V pyramidal neurons have

significantly more projections to the VS, dorsal raphe, and the spinal cord¹⁵⁷. Although data on selective activation layer II/III and layer V vmPFC pyramidal neurons is lacking, these distinct projection patterns suggest that the different vmPFC cortical layers are functionally divergent.

IL and PL diurnal spine rhythms in the current study arose from changes within the long thin and stubby spine pools, while the mushroom spine pool remained stable across all timepoints. Long thin and stubby spines are subclassifications of spines that may be morphological intermediates between nascent filopodial spines and fully mature mushroom spines. *In vivo* imaging studies of somatosensory cortical pyramidal neurons suggest that mushroom-like spines are persistent, meaning that they exhibit stable morphologies over long periods of time¹⁰³. All non-mushroom spine subtypes are transient, exhibiting dynamic morphologies and are often formed and pruned between daily imaging sessions. Due to the highly dynamic nature of dendritic spines, it is important to consider spine morphology as a spectrum rather than strictly adhering to defined classifications without lacking intermediate morphologies^{103–107}. As the diurnal rhythm in spine density progresses over the course of a day, non-mushroom vmPFC spines likely switch between subtype classifications, while concurrently forming new spines and pruning existing spines as shown previously^{103,106,107}. Although our fixed tissue approach lacks the temporal resolution to observe spine subtype-switching as shown in in-vivo studies, these data provide evidence that the total number of non-mushroom type spines fluctuates on layer V vmPFC dendrites over the course of a day.

IL and PL dendritic spine densities in the current study were found to be dependent on GC secretion. Metyrapone administered two hours prior to light offset daily for seven days was sufficient to block the ZT16 active phase increase in spine density. GC-mediated effects on vmPFC dendritic spine remodeling and synaptic strength have been extensively studied in the context of stress^{119–121,130,131,146,158–160}. Overarching trends in the field suggest that the vmPFC is highly GC-responsive, exhibiting changes in dendritic spine density and synaptic strength in a dose-dependent manner^{120,121,130,160–162}. The influence of diurnal GC secretion on dendritic spine

dynamics is an emerging topic of investigation. All existing reports of diurnal dendritic spine rhythmicity show peak spine density in the active phase, which is preceded by the diurnal peak of GC secretion^{126,146}. Our findings follow this same trend, with increased spine density observed at ZT16 in both PL and IL subregions. In hippocampal CA1 pyramidal neurons, the diurnal peak of spine density is blocked by inhibition of CORT synthesis via metyrapone administered prior to dark phase onset¹²⁶. Our findings demonstrate a similar effect, suggesting that vmPFC and CA1 spine rhythmicity are both driven by the timed diurnal peak of GC secretion.

A limitation of the current study is that we do not demonstrate a mechanism for how spines are upregulated by diurnal GC secretion. Several possible mechanisms exist to explain GC action on vmPFC diurnal spine rhythmicity, including classical genomic action of GR, GR's entraining influence of the vmPFC molecular clock, or rapid cell signaling downstream of membrane associated GR ligand binding. In hippocampal slice cultures, CORT application increased dendritic spine density within an hour, but concurrent application of CORT and protein synthesis inhibitor cycloheximide blocked the increase in spine density¹²⁶. CORT and transcriptional inhibitor actinomycin D increased spine density¹²⁶. Similarly, CORT applied directly to motor cortex increased spine formation within 90 minutes of application, which was also observed with concurrent CORT and actinomycin D treatment¹³⁸. Cortical application of CORT conjugated to membrane-impermeable bovine serum albumin also resulted in increased spine formation¹³⁸. Together, these findings suggest that acute exposure to GCs, like the diurnal peak of GC secretion, upregulates dendritic spine density via membrane associated GR activation and genomic mechanisms may not be necessary.

Recent behavioral findings also point to the vmPFC molecular clock as a regulator of vmPFC-dependent learning behaviors. In rats, vmPFC-dependent fear extinction behavior exhibits a diurnal rhythm, with optimal fear extinction recall shown by rats tested at ZT16 when compared to rats tested at ZT4¹⁴⁸. Selective shRNA-mediated knockdown of *Per1* and *Per2* in

the vmPFC ablates this time-of-day difference in behavior. Additionally, adrenalectomized rats lack fear extinction recall at ZT16, but the behavioral phenotype is rescued through a combination of CORT supplementation via drinking water and acute CORT administration post-training¹⁴⁸. These findings suggest that vmPFC-dependent learning and behavior is regulated through a coordination between diurnal GC rhythmicity and a functional vmPFC molecular clock. Although this departs from molecular clock regulation of vmPFC function, similar trends of molecular clock-dependent function have been demonstrated in hippocampus. Mice lacking core clock gene *BMAL1* demonstrate impaired hippocampal dependent learning and memory and diminished excitatory postsynaptic potential slope in response to LTP induction, suggesting that optimal hippocampal learning requires a functional molecular clock¹³⁶. However, the above vmPFC and hippocampus studies did not assess changes in dendritic spine dynamics in response to clock gene disruption, so the functional consequences of clock gene disruption on dendritic spine rhythmicity remain elusive.

Our findings suggest that disruption of the diurnal rhythm of GC secretion alters core clock gene expression and spine rhythmicity in the vmPFC, but the functional contribution of clock gene expression on vmPFC dendritic spine rhythmicity is unclear. To assess the potential influence of the molecular clock on vmPFC dendritic spine rhythmicity, a necessary future direction would be to assess vmPFC dendritic spine rhythmicity in a clock mutant animal supplemented with an exogenous GC rhythm, as clock mutants globally lacking *Per* display no diurnal rhythm in GC secretion^{163,164}. If a spine rhythm is absent in a clock mutant receiving diurnal GC supplementation, this would indicate intact molecular clock function as a regulator of spine rhythmicity.

2.6 Conclusion

This study demonstrates that mouse layer V vmPFC pyramidal neurons exhibit a diurnal rhythm of dendritic spine density and morphology in the transition from the inactive (light) phase

to the active (dark) phase. We also show that vmPFC *Per1* mRNA rhythms and dendritic spine rhythms are driven by diurnal GC oscillations. This work provides important morphological evidence that complements a growing body of existing work demonstrating that time of day is a significant factor when considering performance in learning and behavioral tasks^{136,147,148}.

CHAPTER 3: CONCLUSION

3.1 Summary

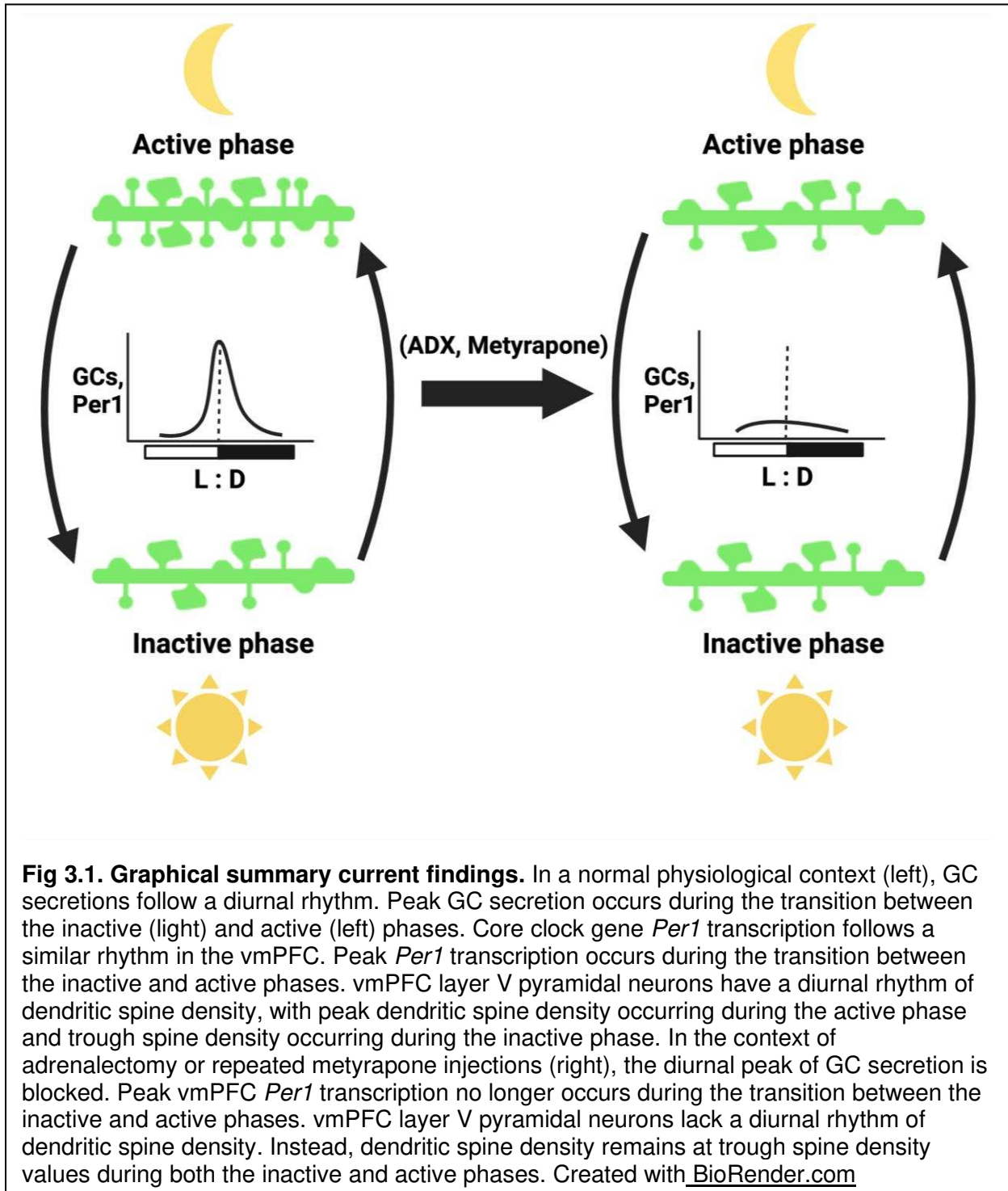
The present study is perhaps the first to demonstrate glucocorticoid dependent dendritic spine rhythmicity in the mouse ventromedial prefrontal cortex. However, the interplay between biological rhythms and dendritic spine dynamics is still not well understood and further investigation is required. This chapter provides a discussion on the main takeaway messages of the present study. Then, limitations of the experimental techniques utilized in the study are considered. Mechanisms are proposed for diurnal GC modulation of dendritic spines. Discussion of future directions and follow-up studies that could expand on the experiments conducted in this dissertation is provided. The findings presented are then discussed in the context of shift work, jet lag, and other forms of circadian disruption relevant to the human experience. Finally, concluding remarks are given.

3.2 Conclusions drawn from the present study

Overarching conclusions

This current work provides modest insights into how diurnal GC secretions are important for the regulation of the mouse IL and PL vmPFC and adds more evidence to the emerging story of diurnal rhythms of dendritic spine plasticity in the brain. This study demonstrates that when the diurnal rhythm of GC secretion is altered, rhythms in gene expression and dendritic structure are affected in the vmPFC. A graphical summary of the current findings is outlined in

Fig 3.1.



GCs and the vmPFC molecular clock

The diurnal rhythm of GC secretion confers changes in both IL and PL *Per1* expression between the light and dark phases. These results suggest that the IL and PL, while functionally distinct, have similar molecular clock rhythms that depend on GC signaling for proper entrainment to the L:D cycle. This contrasts with other brain regions like the hippocampus and the amygdala, which show subregion-specific effects of GC-influenced molecular clock entrainment^{97,98}. The functional consequences of GC entrained molecular clocks in the vmPFC, or any brain region previously demonstrated to possess GC entrained molecular clocks, is unclear. While the data in chapter 2 show that *Per1* expression changes in the absence of GC signaling, any claims about how the molecular clock governs vmPFC structure and function require further investigation.

GCs and diurnal rhythms of vmPFC spine density

My results demonstrate robust diurnal rhythms of dendritic spine density on layer V pyramidal neurons in both the PL and IL vmPFC, which are both regulated by the diurnal rhythm of GC secretion. Diurnal rhythms of dendritic spine density have been demonstrated elsewhere in the brain^{126,134,137,146}. Diurnal rhythms of dendritic spine density have been demonstrated in CA1 pyramidal neurons in the rat hippocampus and in pyramidal neurons in the mouse cerebral cortex, although the specific cortical region was not specified^{126,134}. A diurnal rhythm of dendritic spine density has also been shown in rat IL Layer II/III pyramidal neurons¹⁴⁶. To my knowledge, the present study is the first report of a diurnal rhythm of dendritic spine density in layer V IL and PL pyramidal neurons, and the first study to report such findings in the vmPFC of a mouse.

3.3 Significance

Rats and mice as model organisms

The distinction between rat and mouse is important because while both species share similar neuroanatomical features, they are not always equivalent model organisms. For example, mice and rats display different social behaviors and food seeking behaviors¹⁶⁵. In a sociability test where a novel mouse or rat is placed behind a cage at one end of an arena and a novel object is placed behind a cage on the opposing side of the arena, Sprague-Dawley rats tend to interact with the novel rat significantly more than C57/BL6 mice interact with the novel mouse. When the novel object is replaced with food, rats preferentially interact with the novel rat, while mice tend to interact with the novel mouse and food equally. After 24 hours of fasting, mice preferentially interact with the food, while rats interact with the social stimulus and food equally¹⁶⁵. Rats also display superior performance in the Morris water maze, a common behavioral assay for spatial learning¹⁶⁶. Together, these results suggest that rats and mice are not always comparable in the context of behavior.

Interestingly, hippocampal CA1 pyramidal neurons share many similarities between species¹⁶⁷. Sprague-Dawley rats and C57/BL6 mice have comparable dendritic length, surface area, spine length, and spine density on CA1 pyramidal neurons¹⁶⁷. Unfortunately for this study, vmPFC dendritic morphology has not been formally compared between rats and mice. However, both species exhibit similar GC-mediated alternations in dendritic spine density in the context of stress and GC exposure, which is extensively documented^{119–121,160,162}. While rats and mice are not always equivalent model organisms for studying behavior, they share some similarities when assessing dendritic spine structure and density at rest and in response to GC exposure, suggesting that both model organisms can be useful for the study of GC-mediated effects on vmPFC dendritic morphology.

Differences between layer II/III and Layer V in the vmPFC

The current study demonstrates a diurnal rhythm of dendritic spine density on vmPFC pyramidal neurons in layer V. A diurnal rhythm of dendritic spine density has been previously reported in layer II/III pyramidal neurons¹⁴⁶. The distinction between vmPFC layer II/III and layer V is significant, as each pyramidal cell layer of cortex exhibits unique projection patterns and targets^{155–157}. Layer II/III pyramidal neurons in the vmPFC predominately project to other cortical regions like the somatosensory cortex, auditory cortex, and retrosplinal granular cortex¹⁵⁶. Layer II/III pyramidal neurons can also project to subcortical regions like the posterior thalamus, ventral striatum, and BLA^{156,157}. Layer V pyramidal neurons in both IL and PL project to numerous subcortical regions, with some common projection targets and some unique to each subregion. Shared projections between IL and PL layer V pyramidal neurons include limbic regulatory regions like the septum, periaqueductal grey, BLA, and autonomic regulatory regions like the rostral and caudal ventrolateral medulla. IL layer V pyramidal neurons have significantly more projections to the parabrachial nucleus and nucleus tractus solitarius, where PL layer V pyramidal neurons have significantly more projections to the VS, dorsal raphe, and the spinal cord¹⁵⁷. Although data on selective activation layer II/III and layer V vmPFC pyramidal neurons is lacking, these distinct projection patterns suggest that the different vmPFC cortical layers are functionally divergent. While a diurnal rhythm of dendritic spine density has been reported in IL layer II/III pyramidal neurons, the present study adds IL and PL layer V pyramidal neurons to the catalogue of vmPFC layers and subregions that show structural changes across the L:D cycle. With my novel finding in mind, perhaps future studies can identify and assess potential time-of-day differences in autonomic function and behavior governed by specific circuits involving vmPFC layer V pyramidal neurons.

IL and PL functional differences

The distinction between the IL and PL subregions is important because each subregion exhibits distinct functions^{168–170}. In the context of fear conditioning and fear extinction learning, the PL and IL play opposite roles. Direct cortical infusions of GABA_A receptor agonist muscimol (MUS) to the PL block freezing behaviors in response to a tone previously associated with a foot shock. Conversely, MUS infusions to the IL result in increased freezing behaviors in response to repeated tone presentations and impaired fear extinction memory¹⁶⁸. Stimulation via microelectrode implanted in the PL increases freezing behaviors during tone presentation, but IL microelectrode stimulation led to less freezing behaviors during tone presentation¹⁶⁹. Together, these results indicate that the PL is necessary for the expression of conditioned fear, while the IL is necessary for proper fear extinction learning¹⁶⁸.

The vmPFC regulates the neuroendocrine response to stress with some subregion-specific roles. Rats receiving excitotoxic ibotenic acid lesions in the PL increase in c-Fos expression and CRH mRNA accumulation in the PVN after acute restraint stress¹⁷⁰. Additionally, PL-lesioned animals have enhanced ACTH and CORT secretion in response to acute restraint stress. Rats receiving excitotoxic lesions in the IL also increase c-Fos expression in the PVN, but only in pre-autonomic neurons¹⁷⁰. These results suggest that both the PL and IL regulate the PVN in some capacity, but each subregion regulates distinct subpopulations of neurons within the PVN. The PL appears to regulate neuroendocrine neurons which govern the release of CRH and subsequent HPA axis activation. In contrast, the IL regulates preautonomic neurons, which regulate autonomic nervous system activity. However, the type of lesion or modality of inactivation matters when assessing the role of the vmPFC in HPA axis regulation. Lentiviral-packaged small interfering (si)RNA targeting vesicular glutamate transporter 1 (vGlut1) reduces glutamatergic output of infected neurons while sparing complex networks of interneurons and glia within the region. In contrast, excitotoxic lesions utilizing ibotenic acid are less specific and indiscriminately cause cell death. Lentiviral-mediated vGlut1 siRNA injected into the IL

enhances ACTH and CORT secretion in response to acute restraint stress¹⁷¹. Accordingly, Channelrhodopsin-2 (ChR2)-mediated optogenetic stimulation of the IL reduces CORT secretion in response to acute restraint stress, suggesting that the IL is also involved in HPA axis regulation¹⁷².

In accordance with IL lesions enhancing c-fos expression in PVN preautonomic neurons, the IL has been shown to regulate the diurnal rhythm of heart rate and many other cardiovascular measures. Specifically, IL vGlut1 knockdown causes reduced elevations in heart rate during the active phase¹⁷³. IL vGlut1 knockdown reduces systolic and diastolic blood pressure in non-stressed rats but enhances heart rate elevations in response to acute restraint stress. In rats exposed to chronic stress, IL vGlut1 knockdown increases systolic and diastolic blood pressure and enhances heart rate elevations in response to acute restraint stress¹⁷³. Taken together, glutamatergic neurons in the IL appear to regulate the autonomic nervous system in basal conditions, but also play a key role in gating autonomic output in response to stress.

The IL is also implicated in the regulation of affective behaviors. The forced swim test is a measure of passive and active coping behaviors in response to inescapable swim stress. Time spent immobile while floating in the forced swim test arena is generally considered passive coping, while struggling and attempting to escape is considered active coping. IL vGlut1 knockdown reduces immobility and increases activity in the forced swim test¹⁷⁴. The shock probe burying test is another measure of active coping behavior. In the test, a shock probe is placed within the cage. Attempts to contact and bury the probe are considered active coping behaviors, while immobility is considered passive coping. Like the forced swim test results, IL vGlut1 knockdown reduces immobility and increases number of contacts with the shock probe in the shock probe burying test¹⁷⁴. Together, these results demonstrate IL involvement in the regulation of affective behavior. Specifically, the IL appears to drive passive coping behaviors in

response to stressors as reducing IL glutamatergic output caused reductions in passive coping behaviors.

My current findings do not identify or measure specific behaviors or neuroendocrine functions governed by layer V pyramidal neurons in the PL and IL. My data only suggest that dendritic spine plasticity in the PL and IL changes across 24-hour periods. Ultimately, the functional implications of a diurnal rhythm of dendritic spine density in the PL and IL are unclear and require further investigation. These previously conducted studies provide insights into the specific functions of the PL and IL, and several have yet to be investigated for diurnal variation. Could the diurnal rhythm in vmPFC spine density regulate diurnal changes in affective behaviors like forced swim test immobility? Could the diurnal rhythm of IL spine density be a structural underpinning of the diurnal rhythm in heart rate or fear extinction behaviors? These are interesting possibilities to consider, but these questions are unable to be answered by my dissertation.

3.4 Limitations of the present study

The most significant limitation of the present study is low temporal resolution in experiments investigating changes across the L:D cycle. The timepoints of ZT3, 12, and 16 were selected based on literature demonstrating that diurnal rhythms in spine density reach peak spine density during the early active phase and trough spine density during the early inactive phase^{126,134,146}. Similarly, *Per* transcriptional rhythms in the vmPFC and other cortical regions have been shown to reach peak transcription either during the onset of the active phase or during the early active phase^{41,134}. Thus, three timepoints reflecting these periods were selected due to convenience. Although the chosen timepoints were sufficient for showing changes in vmPFC dendritic spine density and *Per1* transcription in the present study, the omission of other timepoints leaves significant gaps when interpreting the findings. One of the core criteria for circadian rhythms is their ability to free run in the absence of a zeitgeber³². Any

free running phase shifts that may occur in *Per1* transcription or dendritic spine density in the absence of diurnal GC secretions is not captured with the three timepoints chosen. With the limited timepoints chosen, I conclude that the rhythms investigated depend on GC signaling, but I am unable to determine the extent of GC influence. The current data suggest that disrupting diurnal GC secretions stops diurnal rhythmicity of dendritic spine density and *Per1* transcription entirely. If this is indeed true, these findings would be like *Per* rhythms in the CEA, BNSTov, and some hippocampal subregions, which stop rhythmic *Per* expression after GC disruption^{85,97,99}. However, in the rat vmPFC, adrenalectomy results in phase shifted rhythms in *Per* transcription. *Per* transcription shows changes in amplitude comparable to sham-operated rats, but the time at which peak transcription occurs is shifted by several hours⁴¹. It could be argued that this also happens in the mouse vmPFC, but the current study limits our view of *Per1* transcription across the L:D cycle. Diurnal rhythms of dendritic spine density have only been demonstrated in a handful of reports, which fall into the same error of low temporal resolution as this dissertation^{126,134,146}. Much like rhythms of *Per* transcription, if the diurnal rhythm in spine density in the vmPFC is capable of free running in the absence of diurnal GC secretions, the design of the present study prevents us from making that conclusion.

Another limitation of the current study is that only one core clock gene, *Per1*, was measured across the L:D cycle. As discussed in chapter 1, the core clock gene transcriptional-translational feedback loop depends on the expression of other core clock genes *CLOCK*, *BMAL1*, and *Cry*. *Per* transcription was selected as a variable because GCs have only been implicated in the regulation of *Per* transcription. In the rat vmPFC, adrenalectomy phase shifts *BMAL1* transcription in addition to *Per* transcription⁴¹. It is unclear if this also happens in the mouse, or if the other clock components continue to oscillate despite changes in *Per1* transcription brought on by adrenalectomy.

3.5 Mechanistic considerations

Membrane action or genomic action?

The present study implicates the diurnal rhythm of GC secretion in the regulation of dendritic spines in the vmPFC, but the mechanism that GCs utilize to exert these effects is unclear. GCs could be acting through classical genomic mechanisms driven by GRs binding to GREs in the genome and modulating gene expression. Alternatively, GCs could be acting through intracellular signaling cascades initiated at the membrane, which occur independently of genomic changes. In the case of GC-mediated diurnal rhythms of dendritic spine density, there are several pieces of evidence supporting non-genomic mechanisms for the diurnal regulation of dendritic spines.

Genomic and non-genomic GC action can be alluded to by comparing the time course for GC-mediated effects to take place. Generally, intracellular signaling cascades occur rapidly, within minutes to hours after stimulation. Genomic effects can take hours to days to be fully observable. Acute stress exposure has been shown to increase EPSC amplitude and upregulate NMDAR and AMPAR receptor subunit expression in the vmPFC as early as 1-hour post-stress¹³⁰. Acute stress is also shown to enhance working memory via enhanced T-maze performance¹³⁰. Conversely, chronic stress exposure results in the opposite outcomes¹³¹. Specifically, repeated stressor exposure results in downregulation of vmPFC NMDAR and AMPAR subunit expression as well as diminished working memory-related behavior. Notably, reductions in NMDAR and AMPAR subunit expression can only be observed after 3-5 days of chronic GC exposure¹³¹. These studies do not directly point to non-genomic and genomic actions, but instead demonstrate that short term GC exposure and long-term GC exposure produce opposite effects with different temporal dynamics. The results outlined in chapter 2 demonstrate that dendritic spines are elevated at ZT12 and ZT16 in the IL and at ZT16 in the PL. ZT12 corresponds with the diurnal peak of GC secretion, as demonstrated in **Fig 2.1** and

Fig 2.5. Elevations of vmPFC dendritic spine density 4 hours after the diurnal peak of GC secretion are most aligned with the time course of non-genomic GC action, but the experiments in chapter 2 do not address this distinction.

In hippocampal slice cultures, CORT application increases dendritic spine density in CA1 within an hour, which is also observed when CORT and transcriptional inhibitor actinomycin D are applied¹²⁶. Similarly, CORT applied directly to the motor cortex increases spine formation within 90 minutes of application. A similar effect on dendritic spine formation is observed with concurrent CORT and actinomycin D treatment¹³⁸. Cortical application of CORT conjugated to membrane-impermeable bovine serum albumin also increases dendritic spine formation¹³⁸. Together, these findings suggest that acute exposure to GCs, like the diurnal peak of GC secretion, upregulates dendritic spine density via membrane associated GR activation independently of gene transcription.

Implicated signaling cascades

In hippocampal slice cultures, multiple kinases appear to be necessary for facilitating spine formation after acute GC exposure. Specifically, CORT application combined with a protein kinase A (PKA) inhibitor, a protein kinase C (PKC) inhibitor, an extracellular signal-related kinase (ERK) inhibitor, or a LIM kinase (LIMK) inhibitor each block CORT-mediated spine formation¹²⁶. In contrast, CORT application combined with c-Jun N-terminal kinase (JNK) inhibitor results in increased spine formation, suggesting that pathways involving JNK are not involved in CORT-mediated spine formation¹²⁶. In the motor cortex, 20 minutes of CORT application is sufficient to increase LIMK phosphorylation¹³⁷. In cultured cortical pyramidal neurons, CORT application also increases LIMK and cofilin phosphorylation. CORT-mediated LIMK and cofilin phosphorylation are both blocked by GR antagonism¹³⁷. Phospho-LIMK phosphorylates and inactivates cofilin, which is a key protein involved in severing actin filaments¹⁷⁵. A common theme of the four kinases involved in GC-mediated spine growth in

hippocampal slice cultures is that they all, in some way, influence the actin cytoskeleton^{137,176-178}. PKA has been shown to directly phosphorylate LIMK, independently of Rho and Rac GTPases and their downstream effectors¹⁷⁷. PKC has been shown to phosphorylate MARCKS and GAP43, which are two membrane bound proteins that cause phosphatidylinositol 4,5-bisphosphate (PIP2) release and subsequent accumulation of actin modifying proteins¹⁷⁶. PKC also phosphorylates and inhibits the actin capping protein adducin. Adducin caps actin filaments and incorporates spectrin into actin networks, which tethers filamentous actin (F-actin) to the cell membrane. Inhibition of adducin reduces F-actin capping and spectrin-actin binding, which results in increased exposure of F-actin barbed ends and allows for actin polymerization and membrane protrusion¹⁷⁶. ERK phosphorylation has been shown to recruit Arp2/3 to membrane protrusions. Arp2/3 is an actin nucleator, which generates branched actin networks capable of producing membrane protrusions¹⁷⁸. Together, the downstream activation of these kinases promotes actin polymerization, F-actin branching, and membrane protrusion as well as actin filament stabilization through the phosphorylation of cofilin. Each of these processes appear to be necessary for acute CORT-mediated spinogenesis. While these kinases have only been implicated in hippocampal slice cultures and, to a far lesser extent, motor cortex, their downstream regulation of the actin cytoskeleton is a very plausible mechanism for diurnal CORT-mediated spinogenesis in the vmPFC.

3.6 Possible future directions

Perhaps the biggest remaining unknown after doing this work is whether core clock gene oscillations play any role in regulating diurnal rhythms of dendritic spine density. Clock genes have been implicated in the proper functioning of both the vmPFC and hippocampus. The rat vmPFC exhibits an adrenal-dependent and molecular clock-dependent circadian pattern of function in a fear extinction paradigm¹⁴⁸. Rats subjected to fear extinction in the dark phase show enhanced fear extinction recall when compared to rats tested during the light phase.

These time-of-day effects on fear extinction recall are abolished by adrenalectomy, with adrenalectomized (ADXd) rats showing reduced fear extinction recall in the dark phase when compared to sham-operated dark phase rats. Interestingly, this deficit in dark phase fear extinction recall is also observed in rats with shRNA-mediated *Per1/Per2* knockdown within the vmPFC, demonstrating that time-of-day differences in fear extinction recall are mediated by local vmPFC molecular clock machinery¹⁴⁸. These data show that the diurnal rhythm of GC secretion and rhythmic expression of clock genes both modify vmPFC-dependent behaviors. Mice lacking core clock gene *BMAL1* demonstrate impaired hippocampal dependent learning and memory and diminished excitatory postsynaptic potential slope in response to LTP induction, suggesting that optimal hippocampal learning also requires a functional molecular clock¹³⁶. However, the above vmPFC and hippocampus studies did not assess changes in dendritic spine dynamics in response to clock gene disruption, so the functional consequences of clock gene disruption on dendritic spine rhythmicity remain elusive.

To assess the potential influence of the molecular clock on vmPFC dendritic spine rhythmicity, a necessary future direction would be to measure vmPFC dendritic spine density across the L:D cycle in a clock mutant animal that has been supplemented with an exogenous GC rhythm. The reason for the exogenous GC rhythm is because mutants globally lacking *Per* display no diurnal rhythm in GC secretion^{163,164}. If a spine rhythm is absent in a clock mutant receiving diurnal GC supplementation, this would indicate intact molecular clock function as a regulator of spine rhythmicity.

Another future direction would be to assess changes in vmPFC dendritic spine density and *Per1* expression across the L:D cycle in females. The present study only assessed males. Males and females display a multitude of sex differences throughout the brain^{141,153,179–181}. In the hippocampus, males and females display different dendritic spine dynamics in response to acute restraint stress¹⁸¹. After acute stress, males show increased dendritic spine density in CA1 pyramidal neurons, while females display estrus cycle-dependent effects. Specifically,

females stressed during estrus, when circulating estradiol is higher, display increased spine density. Females stressed on diestrus, when circulating estradiol is low, display reductions in dendritic spine density¹⁸¹. The vmPFC exhibits some sexually divergent functions^{172,182}. Females display estrus cycle-dependent differences in fear extinction behaviors. Specifically, rats trained during proestrus, when circulating estradiol is high, have enhanced fear extinction recall compared to rats trained on metestrus, when circulating estradiol is low¹⁸². ChR2-mediated optogenetic stimulation of the IL increases sociability in males, but not females¹⁷². Additionally, stimulation of the IL reduces CORT secretion in response to acute restraint stress in males, but not in females. When exposed to a novel environment, IL stimulation reduces heart rate and mean arterial pressure in males but increases heart rate in females¹⁷². Together, these results suggest that the male and female vmPFC differentially regulate social behavior, fear extinction, and the neuroendocrine and autonomic responses to stress. The full extent of the functional differences between the male and female vmPFC are unclear, and sex differences in GC-mediated changes in vmPFC dendritic spine density have yet to be assessed.

In my experience, the Thy1-eGFP mouse model shows a potential sex difference in eGFP labeling, with females exhibiting dense varicosities of eGFP positive fibers in the vmPFC and males lacking said pattern. The female-specific eGFP varicosities lack spines and display no clear connection with pyramidal neuron dendrites within the vmPFC. Ultimately, the presence of these varicosities makes spine imaging and analysis nearly impossible. If any future investigator seeks to assess changes in vmPFC spine density across the L:D cycle in females, the Thy1-eGFP mouse may not be the best tool for such inquiry.

3.7 Human relevance

Circadian rhythms are important for health and wellbeing, but the extent of their influence is often hard to directly observe in a healthy individual. The importance of proper circadian alignment is often seen in individuals exposed to chronic circadian disruption, which is

a general term used to describe when biological rhythms fail to align with the external L:D cycle. In humans, the effects of circadian disruption can be demonstrated through differences between shift workers and daytime workers. As of 2017, 16% of the US workforce engages in shift work outside of normal daytime hours, totaling approximately 24.8 million individuals¹⁸³. Circadian rhythms are regulators of a wide array of physiological processes, including neuronal function^{184,185}. Thus, the disruption of circadian rhythms contributes to a variety of disease states^{184,185}.

The present study demonstrates the importance of a functional diurnal rhythm of GC secretion when regulating rhythmic expression of clock genes and synaptic plasticity in the vmPFC. Shift work is associated with an increase of cortisol in hair, which is a biomarker for long term elevations in plasma cortisol¹⁸⁶. Shift work is also associated with a reduced diurnal peak of cortisol secretion¹⁸⁷. While adrenalectomy and metyrapone administration are not perfect models of shift work, we can use the present study to gain some insights into how vmPFC-analogous regions may be changing during human circadian disruption.

Shift work increases the incidence of ischemic stroke, obesity, high triglycerides, and lower HDL cholesterol^{188–190}. Shift work also increases the risk of hypertension, cardiovascular disease-related mortality, diabetes, non-alcoholic fatty liver disease, and cancers^{191–196}. In addition to pathologies in the periphery, shift work negatively impacts mental health and executive function. Shift work has been associated with lower performance on cognitive tests, lower job productivity, and higher risk for workplace accidents or injuries^{197,198}. Shift work has also been identified a significant risk factor for depression and mood disorders^{185,190,199,200}. Although each of these disease states are distinct, they are all, in some way, regulated by the SCN and are exacerbated when the individual's external environment and behaviors fail to synchronize with key events of that clock. Despite this link between circadian rhythm and health, there is a gap in our understanding about how important limbic regulatory brain regions change across 24-hour periods, and how those brain regions may contribute to dysregulated

physiological states in the context of circadian disruption. The present study provides evidence that helps narrow this gap in our understanding. The vmPFC has been shown to regulate the autonomic nervous system, the HPA axis, and affective behaviors relevant to depression and mood disorders^{140,148,171–174}. My data show that synaptic plasticity in the vmPFC changes across the day and is dependent on GC signaling. While no definitive conclusions can be made about how the diurnal rhythm in vmPFC dendritic spine density confers changes in the function of downstream projection targets, it is important to consider that many of the above disease states mentioned above have been shown to be regulated by the vmPFC.

Gaining a more complete understanding of the circadian regulation of the brain can provide clues to clinicians regarding the optimal time to administer treatments and therapies. In human memory studies, cortisol administered prior to a learning task enhances performance during subsequent memory tests²⁰¹. In a clinical setting, patients presenting with panic disorder and agoraphobia receive greater therapeutic gains from exposure therapy if sessions occur earlier in the active phase²⁰². Greater therapeutic gains are associated with higher salivary cortisol levels at the time of therapy²⁰². Human experimental models of fear extinction learning have also been shown to be more effective when behavioral sessions occur in the morning rather than the evening²⁰³. Although we can't observe human dendrites in the same way as our animal models, perhaps these time-of-day dependent effects of learning and behavioral therapy are grounded in a common mechanism of glucocorticoid-mediated daily rhythms of dendritic spine dynamics and can be utilized for the benefit of those suffering from vmPFC-mediated psychiatric disorders like posttraumatic stress disorder (PTSD).

3.8 Concluding remarks

Altogether, this dissertation adds substantial evidence to support the emerging concept of diurnal rhythms of dendritic spine density within the brain. I have demonstrated that the IL and PL vmPFC both show changes in dendritic spine density and subtype morphology across

the L:D cycle, and I have demonstrated that these changes depend on the diurnal rhythm of GC secretion. I also demonstrate that rhythmic expression of the core clock gene *Per1* is dependent on the diurnal rhythm of GC secretion. I speculate that GC-mediated diurnal rhythms of dendritic spine density are not restricted to the vmPFC, hippocampus, and motor cortex and will continue to be discovered, which may help humanity gain a further understanding of the intricacies of biological rhythms and how they impact the brain's structure and function, and how time of day may be an important factor when considering medical interventions to a variety of disease states. By seeking a more complete understanding of how circadian rhythms regulate physiology, we will be able to better understand factors that regulate mental health and well-being. With this further understanding, we will hopefully be able to provide better tools and treatments necessary for the proper adaptation to our increasingly light polluted, circadian disrupted modern world.

REFERENCES

1. Wulund L, Reddy AB. A brief history of circadian time: The emergence of redox oscillations as a novel component of biological rhythms. *Perspectives in Science*. 2015;6:27-37. doi:10.1016/j.pisc.2015.08.002
2. Czeisler CA, Gooley JJ. Sleep and circadian rhythms in humans. *Cold Spring Harbor Symposia on Quantitative Biology*. 2007;72:579-597. doi:10.1101/sqb.2007.72.064
3. Damasio H, Grabowski T, Frank R, Galaburda AM, Damasio AR. The Return of Phineas Gage: Clues About the Brain from the Skull of a Famous Patient. *Science (1979)*. 1994;264:1102-1105. www.sciencemag.org
4. Carlén M. What constitutes the prefrontal cortex? *Science (1979)*. 2017;358:478-482. <http://science.sciencemag.org/>
5. Barker JM, Taylor JR, Chandler LJ. A unifying model of the role of the infralimbic cortex in extinction and habits. *Learning & Memory*. 2014;21(9):441-448. doi:10.1101/lm.035501.114
6. Osaka N, Osaka M, Morishita M, Kondo H, Fukuyama H. A word expressing affective pain activates the anterior cingulate cortex in the human brain: An fMRI study. *Behavioural Brain Research*. 2004;153(1):123-127. doi:10.1016/j.bbr.2003.11.013
7. Berlim MT, McGirr A, van den Eynde F, Fleck MPA, Giacobbe P. Effectiveness and acceptability of deep brain stimulation (DBS) of the subgenual cingulate cortex for treatment-resistant depression: A systematic review and exploratory meta-analysis. *Journal of Affective Disorders*. 2014;159:31-38. doi:10.1016/j.jad.2014.02.016
8. Mayberg HS, Liotti M, Brannan SK, et al. Reciprocal limbic-cortical function and negative mood: Converging PET findings in depression and normal sadness. *Depression: The Science of Mental Health*. 2013;6(May):245-253. doi:10.1176/ajp.156.5.675
9. Alexander L, Clarke HF, Roberts AC. A focus on the functions of area 25. *Brain Sciences*. 2019;9(129):1-33. doi:10.3390/brainsci9060129
10. Kitayama N, Quinn S, Bremner JD. Smaller volume of anterior cingulate cortex in abuse-related posttraumatic stress disorder. *Journal of Affective Disorders*. 2006;90:171-174. doi:10.1016/j.jad.2005.11.006
11. Yang M, Tsai SJ, Li CSR. Concurrent amygdalar and ventromedial prefrontal cortical responses during emotion processing: a meta-analysis of the effects of valence of emotion and passive exposure versus active regulation. *Brain Structure and Function*. 2020;225(1):345-363. doi:10.1007/s00429-019-02007-3
12. Devinsky O, Morrell MJ, Vogt BA. Contributions of anterior cingulate cortex to behaviour. *Brain*. 1995;118:279-306. <http://brain.oxfordjournals.org/>

13. David R. Euston, Aaron J. Gruber and BLM. The Role of Medial Prefrontal Cortex in Memory and Decision Making. *Neuron*. 2012;29(6):1057-1070. doi:10.1016/j.neuron.2012.12.002.The
14. Jessica M. McKlveen, Brent Myers and JPH. The Medial Prefrontal Cortex: Coordinator of Autonomic, Neuroendocrine, and Behavioral Responses to Stress. *Physiol Behav*. 2015;27(6):446-456. doi:10.1111/jne.12272.The
15. Selye H. A Syndrome produced by Diverse Nocuous Agents. *Nature*. 1936;138(l):32.
16. Selye H. Thymus and Adrenals in the Response of the Organism To Injuries and Intoxications. *British Journal of Experimental Pathology*. 1936;17(3):234–248.
17. Simoni RD, Hill RL, Vaughan M. The Isolation of Thyroxine and Cortisone: the Work of Edward C. Kendall. *Journal of Biological Chemistry*. 2002;277(21):21-22. doi:10.1016/s0021-9258(20)85219-3
18. Watts AG. The structure of the neuroendocrine hypothalamus: The neuroanatomical legacy of Geoffrey Harris. *Journal of Endocrinology*. 2015;226:T25-T39. doi:10.1530/JOE-15-0157
19. Harris GW. OESTROUS RHYTHM. PSEUDOPREGNANCY AND THE PITUITARY STALK IN THE RAT. *Journal of Physiology*. 1950;111(3):347-360.
20. Harris GW, Jacobsohn D. Functional grafts of the anterior pituitary gland. *Proceedings of the Royal Society B*. 1951;139:263-276.
21. Schally A v., Arimura A, Kastin AJ, et al. Gonadotropin-releasing hormone: One polypeptide regulates secretion of luteinizing and follicle-stimulating hormones. *Science (1979)*. 1971;173:1036-1038. doi:10.1126/science.173.4001.1036
22. Vale W, Spiess J, Rivier C, Rivier J. Characterization of a 41-residue ovine hypothalamic peptide that stimulates secretion of corticotropin and β -endorphin. *Obstetrical and Gynecological Survey*. 1982;37(5):334. doi:10.1097/00006254-198205000-00013
23. Fortier BYC, Harris GW, Mcdonaldt IR. The effect of pituitary stalk section on the adrenocortical response to stress in the rabbit. *Journal of Physiology*. 1957;136:344-363.
24. de Groot J, Harris GW. Hypothalamic control of the anterior pituitary gland and blood lymphocytes. *Journal of Physiology*. 1950;3:335-346.
25. Antoni FA. Hypothalamic control of adrenocorticotropin secretion: Advances since the discovery of 41-residue corticotropin-releasing factor. *Endocrine Reviews*. 1986;7(4):351-378. doi:10.1210/edrv-7-4-351
26. Sayers G. The adrenal cortex and homeostasis. *Physiological Reviews*. 1950;30(3):243-320. doi:10.7723/antiochreview.72.3.0546
27. Habib KE, Weld KP, Rice KC, et al. Oral administration of a corticotropin-releasing hormone receptor antagonist significantly attenuates behavioral, neuroendocrine, and autonomic responses to stress in primates. *Proc Natl Acad Sci U S A*. 2000;97(11):6079-6084. doi:10.1073/pnas.97.11.6079

28. Tsigos C, Chrousos GP. Hypothalamic-pituitary-adrenal axis, neuroendocrine factors and stress. *Journal of Psychosomatic Research*. 2002;53:865-871. doi:10.1016/S0022-3999(02)00429-4
29. Huang RC. The discoveries of molecular mechanisms for the circadian rhythm: The 2017 Nobel Prize in Physiology or Medicine. *Biomedical Journal*. 2018;41(1):5-8. doi:10.1016/j.bj.2018.02.003
30. Roenneberg T, Mewes M. Circadian clocks-the fall and rise of physiology. *Molecular Cell Biology*. 2005;6:965-971. www.nature.com/reviews/molcellbio
31. Vitaterna M, Takahashi JS, Turek FW. Overview of Circadian Rhythms. *Alcohol Research & Health*. 2001;25(2):85-93. doi:10.1057/9780230360051
32. Pittendrigh CS. Circadian Rhythms and the Circadian Organization of Living Systems. *Cold Spring Harb Symp Quant Biol*. 1960;25:159-184.
33. Konopka RJ, Benzer S. Clock Mutants of *Drosophila melanogaster*. *Proc Natl Acad Sci U S A*. 1971;68(9):2112-2116. doi:10.1073/pnas.68.9.2112
34. Reppert SM, Weaver DR. Comparing Clockworks: Mouse versus Fly. *Journal of Biological Rhythms*. 2000;15(5):357-364.
35. Zehring WA, Wheeler DA, Reddy P, et al. P-Element Transformation with period Locus DNA Restores Rhythmicity to Mutant, Arrhythmic *Drosophila melanogaster*. *Cell*. 1984;39(1):369-376.
36. Yoo SH, Yamazaki S, Lowrey PL, et al. PERIOD2::LUCIFERASE real-time reporting of circadian dynamics reveals persistent circadian oscillations in mouse peripheral tissues. *PNAS*. 2004;101(15):5339-5346. doi:10.1073/pnas.0308709101
37. Reddy AB, Maywood ES, Karp NA, et al. Glucocorticoid signaling synchronizes the liver circadian transcriptome. *Hepatology*. 2007;45(6):1478-1488. doi:10.1002/hep.21571
38. Almon RR, Yang E, Lai W, et al. Relationships between circadian rhythms and modulation of gene expression by glucocorticoids in skeletal muscle. *American Journal of Physiology - Regulatory Integrative and Comparative Physiology*. 2008;295(4). doi:10.1152/ajpregu.90399.2008
39. Bering T, Hertz H, Rath MF. Rhythmic Release of Corticosterone Induces Circadian Clock Gene Expression in the Cerebellum. *Neuroendocrinology*. 2020;110(7-8):604-615. doi:10.1159/000503720
40. Dickmeis T. Glucocorticoids and the circadian clock. *Journal of Endocrinology*. 2009;200(1):3-22. doi:10.1677/JOE-08-0415
41. Woodruff ER, Chun LE, Hinds LR, Spencer RL. Diurnal corticosterone presence and phase modulate clock gene expression in the male rat prefrontal cortex. *Endocrinology*. 2016;157(4):1522-1534. doi:10.1210/en.2015-1884
42. Vagnerová K, Ergang P, Soták M, et al. Diurnal expression of ABC and SLC transporters in jejunum is modulated by adrenalectomy. *Comparative Biochemistry and Physiology*. 2019;226(August):108607. doi:10.1016/j.cbpc.2019.108607

43. Patke A, Young MW, Axelrod S. Molecular mechanisms and physiological importance of circadian rhythms. *Nature Reviews Molecular Cell Biology*. 2020;21(2):67-84. doi:10.1038/s41580-019-0179-2
44. Aryal RP, Kwak PB, Tamayo AG, et al. Macromolecular Assemblies of the Mammalian Circadian Clock. *Molecular Cell*. 2017;67(5):770-782. doi:10.1016/j.molcel.2017.07.017
45. Zhang R, Lahens NF, Ballance HI, Hughes ME, Hogenesch JB. A circadian gene expression atlas in mammals: Implications for biology and medicine. *PNAS*. 2014;111(45):16219-16224. doi:10.1073/pnas.1408886111
46. Noya SB, Colameo D, Brüning F, et al. The forebrain synaptic transcriptome is organized by clocks but its proteome is driven by sleep. *Science (1979)*. 2019;366(6462). doi:10.1126/science.aav2642
47. Nicolaidis NC, Charmandari E, Chrousos GP, Kino T. Circadian endocrine rhythms: The hypothalamic-pituitary-adrenal axis and its actions. *Ann N Y Acad Sci*. 2014;1318(1):71-80. doi:10.1111/nyas.12464
48. Udo R, Hamada T, Horikawa K, et al. The role of Clock in the plasticity of circadian entrainment. *Biochemical and Biophysical Research Communications*. 2004;318:893-898. doi:10.1016/j.bbrc.2004.04.113
49. Jud C, Schmutz I, Hampf G, Oster H, Albrecht U. A guideline for analyzing circadian wheel-running behavior in rodents under different lighting conditions. *Biological Procedures Online*. 2005;7(1):101-116. doi:10.1251/bpo109
50. Karatsoreos IN, Bhagat S, Bloss EB, Morrison JH, McEwen BS. Disruption of circadian clocks has ramifications for metabolism, brain, and behavior. *Proc Natl Acad Sci U S A*. 2011;108(4):1657-1662. doi:10.1073/pnas.1018375108
51. Legates TA, Altimus CM, Wang H, et al. Aberrant light directly impairs mood and learning through melanopsin-expressing neurons. *Nature*. 2012;491:594-598. doi:10.1038/nature11673
52. Lefta M, Wolff G, Esser KA. *Circadian Rhythms, the Molecular Clock, and Skeletal Muscle*. Vol 96.; 2011. doi:10.1016/B978-0-12-385940-2.00009-7.Circadian
53. Sousa-Pinto A, Castro-Correta J. Light Microscopic Observations on the Possible Retinohypothalamic Projection in the Rat. *Experimental Brain Research*. 1970;11:515-527.
54. Stephan FK, Zucker I. Circadian rhythms in drinking behavior and locomotor activity of rats are eliminated by hypothalamic lesions. *Proc Natl Acad Sci U S A*. 1972;69(6):1583-1586. doi:10.1073/pnas.69.6.1583
55. Moore RY, Eichler VB. Loss of a circadian adrenal corticosterone rhythm following suprachiasmatic lesions in the rat. *Brain Research*. 1972;42(1):201-206. doi:10.1016/0006-8993(72)90054-6

56. Evans JA, Suen TC, Callif BL, et al. Shell neurons of the master circadian clock coordinate the phase of tissue clocks throughout the brain and body. *BMC Biology*. 2015;13(43):1-15. doi:10.1186/s12915-015-0157-x
57. Freedman MS, Lucas RJ, Soni B, et al. Regulation of Mammalian Circadian Behavior by Non-rod, Non-cone, Ocular Photoreceptors. *Science (1979)*. 1999;284:502-504. www.sciencemag.org
58. Hattar S, Liao HW, Takao M, Berson DM, Yau KW. Melanopsin-containing retinal ganglion cells: Architecture, projections, and intrinsic photosensitivity. *Science (1979)*. 2002;295(5557):1065-1070. doi:10.1126/science.1069609
59. Kofuji P, Mure LS, Massman LJ, Purrier N, Panda S, Engeland WC. Intrinsically photosensitive retinal ganglion cells (ipRGCs) are necessary for light entrainment of peripheral clocks. *PLoS ONE*. 2016;11(12):1-23. doi:10.1371/journal.pone.0168651
60. Meijer JH, Schwartz WJ. In Search of the Pathways for Light-Induced Pacemaker Resetting in the Suprachiasmatic Nucleus. *Journal of Biological Rhythms*. 2003;18(3):235-249. doi:10.1177/0748730403253370
61. Travnickova-Bendova Z, Cermakian N, Reppert SM, Sassone-Corsi P. Bimodal regulation of mPeriod promoters by CREB-dependent signaling and CLOCK/BMAL1 activity. *Proc Natl Acad Sci U S A*. 2002;99(11):7728-7733. doi:10.1073/pnas.102075599
62. Hastings MH, Maywood ES, Brancaccio M. Generation of circadian rhythms in the suprachiasmatic nucleus. *Nature Reviews Neuroscience*. 2018;19:453-469. doi:10.1038/s41583-018-0026-z
63. Patton AP, Chesham JE, Hastings MH. Combined pharmacological and genetic manipulations unlock unprecedented temporal elasticity and reveal phase-specific modulation of the molecular circadian clock of the mouse suprachiasmatic nucleus. *Journal of Neuroscience*. 2016;36(36):9326-9341. doi:10.1523/JNEUROSCI.0958-16.2016
64. Liu AC, Welsh DK, Ko CH, et al. Intercellular Coupling Confers Robustness against Mutations in the SCN Circadian Clock Network. *Cell*. 2007;129:605-616. doi:10.1016/j.cell.2007.02.047
65. Colwell CS. Linking neural activity and molecular oscillations in the SCN. *Nature Reviews Neuroscience*. 2011;12(10):553-569. doi:10.1038/nrn3086
66. Webb AB, Angelo N, Huettner JE, Herzog ED. Intrinsic, nondeterministic circadian rhythm generation in identified mammalian neurons. *Proceedings of the National Academy of Sciences*. 2009;106(38):16493-16498. www.pnas.org/cgi/content/full/
67. Fernandez DC, Chang YT, Hattar S, Chen SK. Architecture of retinal projections to the central circadian pacemaker. *Proc Natl Acad Sci U S A*. 2016;113(21):6047-6052. doi:10.1073/pnas.1523629113
68. Varadarajan S, Tajiri M, Jain R, et al. Connectome of the suprachiasmatic nucleus: New evidence of the core-shell relationship. *eNeuro*. 2018;5(5):1-14. doi:10.1523/ENEURO.0205-18.2018

69. Aton SJ, Colwell CS, Harmar AJ, Waschek J, Herzog ED. Vasoactive intestinal polypeptide mediates circadian rhythmicity and synchrony in mammalian clock neurons. *Nature Neuroscience*. 2005;8(4):476-483. doi:10.1038/nn1419
70. Gamble KL, Allen GC, Zhou T, McMahon DG. Gastrin-releasing peptide mediates light-like resetting of the suprachiasmatic nucleus circadian pacemaker through cAMP response element-binding protein and Per1 activation. *Journal of Neuroscience*. 2007;27(44):12078-12087. doi:10.1523/JNEUROSCI.1109-07.2007
71. Hamnett R, Crosby P, Chesham JE, Hastings MH. Vasoactive intestinal peptide controls the suprachiasmatic circadian clock network via ERK1/2 and DUSP4 signalling. *Nature Communications*. 2019;10(1):1-17. doi:10.1038/s41467-019-08427-3
72. Gizowski C, Zaelzer C, Bourque CW. Clock-driven vasopressin neurotransmission mediates anticipatory thirst prior to sleep. *Nature*. 2016;537:685-688. doi:10.1038/nature19756
73. Santoso P, Nakata M, Ueta Y, Yada T. Suprachiasmatic vasopressin to paraventricular oxytocin neurocircuit in the hypothalamus relays light reception to inhibit feeding behavior. *Am J Physiol Endocrinol Metab*. 2018;315:478-488. doi:10.1152/ajpendo.00338.2016.-Light
74. Ono D, Mukai Y, Hung CJ, Chowdhury S, Sugiyama T, Yamanaka A. The mammalian circadian pacemaker regulates wakefulness via CRF neurons in the paraventricular nucleus of the hypothalamus. *Science Advances*. 2020;6:1-14. doi:10.1126/SCIADV.ABD0384
75. Watts AG, Swanson LW, Sanchez-Watts G. Efferent projections of the suprachiasmatic nucleus: I. Studies using anterograde transport of Phaseolus vulgaris leucoagglutinin in the rat. *Journal of Comparative Neurology*. 1987;258:204-229. doi:10.1002/cne.902580204
76. Sylvester CM, Krout KE, Loewy AD. Suprachiasmatic nucleus projection to the medial prefrontal cortex: A viral transneuronal tracing study. *Neuroscience*. 2002;114(4):1071-1080. doi:10.1016/S0306-4522(02)00361-5
77. Kalsbeek A, van der Vliet J, Buijs RM. Decrease of endogenous vasopressin release necessary for expression of the circadian rise in plasma corticosterone: A reverse microdialysis study. *Journal of Neuroendocrinology*. 1996;8:299-307. doi:10.1046/j.1365-2826.1996.04597.x
78. Kalsbeek A, Buijs RM, Engelmann M, Wotjak CT, Landgraf R. In vivo measurement of a diurnal variation in vasopressin release in the rat suprachiasmatic nucleus. *Brain Research*. 1995;682:75-82. doi:10.1016/0006-8993(95)00324-J
79. Kalsbeek A, van Heerikhuize JJ, Wortel J, Buijs RM. A diurnal rhythm of stimulatory input to the hypothalamo-pituitary- adrenal system as revealed by timed intrahypothalamic administration of the vasopressin V1 antagonist. *Journal of Neuroscience*. 1996;16(17):5555-5565. doi:10.1523/jneurosci.16-17-05555.1996
80. Wotjak CT, Kubota M, Liebsch G, et al. Release of vasopressin within the rat paraventricular nucleus in response to emotional stress: A novel mechanism of regulating

- adrenocorticotrophic hormone secretion? *Journal of Neuroscience*. 1996;16(23):7725-7732. doi:10.1523/jneurosci.16-23-07725.1996
81. Jones JR, Chaturvedi S, Granados-Fuentes D, Herzog ED. Circadian neurons in the paraventricular nucleus entrain and sustain daily rhythms in glucocorticoids. *Nature Communications*. 2021;12(1):1-15. doi:10.1038/s41467-021-25959-9
 82. Nader N, Chrousos GP, Kino T. Interactions of the Circadian CLOCK System and the HPA Axis. *Trends Endocrinol Metab*. 2010;21(5):1-19. doi:10.1016/j.tem.2009.12.011.Interactions
 83. Chou TC, Scammell TE, Gooley JJ, Gaus SE, Saper CB, Lu J. Critical Role of Dorsomedial Hypothalamic Nucleus in a Wide Range of Behavioral Circadian Rhythms. *Journal of Neuroscience*. 2003;23(33):10691-10702.
 84. Keim SR, Shekhar A. The effects of GABA(A) receptor blockade in the dorsomedial hypothalamic nucleus on corticotrophin (ACTH) and corticosterone secretion in male rats. *Brain Research*. 1996;739:46-51. doi:10.1016/S0006-8993(96)00810-4
 85. Shimon Amir, Elaine Waddington Lamont, Barry Robinson and JS. A Circadian Rhythm in the Expression of PERIOD2 Protein Reveals a Novel SCN-Controlled Oscillator in the Oval Nucleus of the Bed Nucleus of the Stria Terminalis. *Journal of Neuroscience*. 2004;24(4):781-790. doi:10.1523/JNEUROSCI.4488-03.2004
 86. Reddy TE, Gertz J, Crawford GE, Garabedian MJ, Myers RM. The Hypersensitive Glucocorticoid Response Specifically Regulates Period 1 and Expression of Circadian Genes. *Molecular and Cellular Biology*. 2012;32(18):3756-3767. doi:10.1128/mcb.00062-12
 87. Cheon S, Park N, Cho S, Kim K. Glucocorticoid-mediated Period2 induction delays the phase of circadian rhythm. *Nucleic Acids Research*. 2013;41(12):6161-6174. doi:10.1093/nar/gkt307
 88. Balsalobre A, Brown SA, Marcacci L, et al. Resetting of circadian time in peripheral tissues by glucocorticoid signaling. *Science (1979)*. 2000;289(5488):2344-2347. doi:10.1126/science.289.5488.2344
 89. Kamagata M, Ikeda Y, Sasaki H, et al. Potent synchronization of peripheral circadian clocks by glucocorticoid injections in PER2::LUC-Clock/Clock mice. *Chronobiology International*. 2017;34(8):1067-1082. doi:10.1080/07420528.2017.1338716
 90. Balsalobre A, Marcacci L, Schibler U. Multiple signaling pathways elicit circadian gene expression in cultured Rat-1 fibroblasts. *Current Biology*. 2000;10(20):1291-1294. doi:10.1016/S0960-9822(00)00758-2
 91. So AYL, Bernal TU, Pillsbury ML, Yamamoto KR, Feldman BJ. Glucocorticoid regulation of the circadian clock modulates glucose homeostasis. *PNAS*. 2009;106(41):17582-17587. doi:10.1073/pnas.0909733106
 92. Soták M, Bryndová J, Ergang P, et al. Peripheral circadian clocks are diversely affected by adrenalectomy. *Chronobiology International*. 2016;33(5):520-529. doi:10.3109/07420528.2016.1161643

93. Pácha J, Sumová A. Circadian regulation of epithelial functions in the intestine. *Acta Physiologica*. 2013;208(1):11-24. doi:10.1111/apha.12090
94. Vetter C, Scheer FAJL. Circadian Biology: Uncoupling Human Body Clocks by Food Timing. *Current Biology*. 2017;27(13):R656-R658. doi:10.1016/j.cub.2017.05.057
95. le Minh N, Damiola F, Tronche F, Schütz G, Schibler U. Glucocorticoid hormones inhibit food-induced phase-shifting of peripheral circadian oscillators. *The EMBO Journal*. 2001;20(24):7128-7136. doi:10.1093/emboj/20.24.7128
96. Rosenfeld P, van Eekelen JAM, Levine S, de Kloet ER. Ontogeny of the Type 2 glucocorticoid receptor in discrete rat brain regions: an immunocytochemical study. *Developmental Brain Research*. 1988;42:119-127.
97. Liška K, Sládek M, Houdek P, et al. High Sensitivity of the Circadian Clock in the Hippocampal Dentate Gyrus to Glucocorticoid- and GSK3-Beta-Dependent Signals. *Neuroendocrinology*. 2022;112(4):384-398. doi:10.1159/000517689
98. Lamont EW, Robinson B, Stewart J, Amir S. The central and basolateral nuclei of the amygdala exhibit opposite diurnal rhythms of expression of the clock protein Period2. *Proc Natl Acad Sci U S A*. 2005;102(11):4180-4184. doi:10.1073/pnas.0500901102
99. Segall LA, Milet A, Tronche F, Amir S. Brain glucocorticoid receptors are necessary for the rhythmic expression of the clock protein, PERIOD2, in the central extended amygdala in mice. *Neuroscience Letters*. 2009;457(1):58-60. doi:10.1016/j.neulet.2009.03.083
100. DeFelipe J. The dendritic spine story: An intriguing process of discovery. *Frontiers in Neuroanatomy*. 2015;9:1-13. doi:10.3389/fnana.2015.00014
101. Yuste R. The discovery of dendritic spines by Cajal. *Frontiers in Neuroanatomy*. 2015;9:1-6. doi:10.3389/fnana.2015.00018
102. Peters A, Kaiserman-Abramof IR. The small pyramidal neuron of the rat cerebral cortex. The perikaryon, dendrites and spines. *American Journal of Anatomy*. 1970;127(4):321-355. doi:10.1002/aja.1001270402
103. Holtmaat AJGD, Trachtenberg JT, Wilbrecht L, et al. Transient and Persistent Dendritic Spines in the Neocortex In Vivo. *Neuron*. 2005;45(2):279-291. doi:10.1016/j.neuron.2005.01.003
104. Fifková E, van Harreveld A. Long-lasting morphological changes in dendritic spines of dentate granular cells following stimulation of the entorhinal area. *Journal of Neurocytology*. 1977;6(2):211-230. doi:10.1007/BF01261506
105. Desmond NL, Levy WB. Changes in the postsynaptic density with long-term potentiation in the dentate gyrus. *Journal of Comparative Neurology*. 1986;253(4):476-482. doi:10.1002/cne.902530405
106. Bhatt DH, Zhang S, Gan WB. Dendritic spine dynamics. *Annual Review of Physiology*. 2009;71:261-282. doi:10.1146/annurev.physiol.010908.163140

107. Parnass Z, Tashiro A, Yuste R. Analysis of spine morphological plasticity in developing hippocampal pyramidal neurons. *Hippocampus*. 2000;10(5):561-568. doi:10.1002/1098-1063(2000)10:5<561::AID-HIPO6>3.0.CO;2-X
108. Gan WB, Kasthuri N, Yang G. Spine Plasticity. *Encyclopedia of Neuroscience*. Published online 2009:321-327. doi:10.1016/B978-008045046-9.00362-4
109. John C. Fiala, Marcia Feinberg, Viktor Popov KMH. Synaptogenesis Via Dendritic Filopodia in Developing Hippocampal Area CA1. *Ear Nose Throat J*. 1998;18(21):8900-8911. doi:10.1177/014556131609500604
110. Chen CC, Lu J, Zuo Y. Spatiotemporal dynamics of dendritic spines in the living brain. *Frontiers in Neuroanatomy*. 2014;8(28):1-7. doi:10.3389/fnana.2014.00028
111. Allen Reference Atlas - Mouse Brain [brain atlas]. atlas.brain-map.org
112. Nicoll RA. A Brief History of Long-Term Potentiation. *Neuron*. 2017;93:281-290. doi:10.1016/j.neuron.2016.12.015
113. Bliss TVP, Cooke SF. Long-term potentiation and long-term depression: A clinical perspective. *Clinics*. 2011;66(S1):3-17. doi:10.1590/S1807-59322011001300002
114. Bosch M, Castro J, Saneyoshi T, Matsuno H, Sur M, Hayashi Y. Structural and molecular remodeling of dendritic spine substructures during long-term potentiation. *Neuron*. 2014;82:444-459. doi:10.1016/j.neuron.2014.03.021
115. Zhou Q, Homma KJ, Poo MM. Shrinkage of dendritic spines associated with long-term depression of hippocampal synapses. *Neuron*. 2004;44(5):749-757. doi:10.1016/j.neuron.2004.11.011
116. Tatsuya Hayama, Jun Noguchi, Satoshi Watanabe, Noriko Takahashi, Akiko Hayashi-Takagi, Graham C R Ellis-Davies, Masanori Matsuzaki and HK. GABA promotes the competitive selection of dendritic spines by controlling local Ca²⁺ signaling. *Nat Neurosci*. 2013;16(10):1409-1416. doi:10.1038/nn.3496.GABA
117. Castañeda P, Muñoz M, García-Rojo G, et al. Association of N-cadherin levels and downstream effectors of Rho GTPases with dendritic spine loss induced by chronic stress in rat hippocampal neurons. *Journal of Neuroscience Research*. 2015;93(10):1476-1491. doi:10.1002/jnr.23602
118. Perez-Cruz C, Simon M, Flügge G, Fuchs E, Czéh B. Diurnal rhythm and stress regulate dendritic architecture and spine density of pyramidal neurons in the rat infralimbic cortex. *Behavioural Brain Research*. 2009;205(2):406-413. doi:10.1016/j.bbr.2009.07.021
119. Wohleb ES, Terwilliger R, Duman CH, Duman RS. Stress-Induced Neuronal Colony Stimulating Factor 1 Provokes Microglia-Mediated Neuronal Remodeling and Depressive-like Behavior. *Biological Psychiatry*. 2018;83(1):38-49. doi:10.1016/j.biopsych.2017.05.026
120. Horchar MJ, Wohleb ES. Glucocorticoid receptor antagonism prevents microglia-mediated neuronal remodeling and behavioral despair following chronic unpredictable

- stress. *Brain, Behavior, and Immunity*. 2019;81(February):329-340. doi:10.1016/j.bbi.2019.06.030
121. Radley JJ, Sisti HM, Hao J, et al. Chronic behavioral stress induces apical dendritic reorganization in pyramidal neurons of the medial prefrontal cortex. *Neuroscience*. 2004;125(1):1-6. doi:10.1016/j.neuroscience.2004.01.006
 122. Radley JJ, Rocher AB, Miller M, et al. Repeated stress induces dendritic spine loss in the rat medial prefrontal cortex. *Cerebral Cortex*. 2006;16(3):313-320. doi:10.1093/cercor/bhi104
 123. Morales-Medina JC, Sanchez F, Flores G, Dumont Y, Quirion R. Morphological reorganization after repeated corticosterone administration in the hippocampus, nucleus accumbens and amygdala in the rat. *Journal of Chemical Neuroanatomy*. 2009;38:266-272. doi:10.1016/j.jchemneu.2009.05.009
 124. Allen TA, Fortin NJ. The evolution of episodic memory. *Proc Natl Acad Sci U S A*. 2013;110(SUPPL2):10379-10386. doi:10.1073/pnas.1301199110
 125. Reul JM, de Kloet ER. Two receptor systems for corticosterone in rat brain: Microdistribution and differential occupation. *Endocrinology*. 1985;117(6):2505-2511. doi:10.1210/endo-117-6-2505
 126. Ikeda M, Hojo Y, Komatsuzaki Y, et al. Hippocampal spine changes across the sleep-wake cycle: Corticosterone and kinases. *Journal of Endocrinology*. 2015;226(2):M13-M27. doi:10.1530/JOE-15-0078
 127. Vyas A, Mitra R, Shankaranarayana Rao BS, Chattarji S. Chronic stress induces contrasting patterns of dendritic remodeling in hippocampal and amygdaloid neurons. *Journal of Neuroscience*. 2002;22(15):6810-6818. doi:10.1523/jneurosci.22-15-06810.2002
 128. Komatsuzaki Y, Hatanaka Y, Murakami G, et al. Corticosterone induces rapid spinogenesis via synaptic glucocorticoid receptors and kinase networks in hippocampus. *PLoS ONE*. 2012;7(4). doi:10.1371/journal.pone.0034124
 129. Liston C, Cichon JM, Jeanneteau F, Jia Z, Chao M v, Gan WB. Circadian glucocorticoid oscillations promote learning-dependent synapse formation and maintenance. *Nat Neurosci*. 2013;16(6):698-705. doi:10.1038/nn.3387
 130. Yuen EY, Liu W, Karatsoreos IN, Feng J, McEwen BS, Yan Z. Acute stress enhances glutamatergic transmission in prefrontal cortex and facilitates working memory. *Proc Natl Acad Sci U S A*. 2009;106(33):14075-14079. doi:10.1073/pnas.0906791106
 131. Yuen EY, Wei J, Liu W, Zhong P, Li X, Yan Z. Repeated Stress Causes Cognitive Impairment by Suppressing Glutamate Receptor Expression and Function in Prefrontal Cortex. *Neuron*. 2012;73(5):962-977. doi:10.1016/j.neuron.2011.12.033.Repeated
 132. Qiao H, Li MX, Xu C, Chen H bin, An SC, Ma XM. Dendritic Spines in Depression: What We Learned from Animal Models. *Neural Plasticity*. 2016;2016:1-26. doi:10.1155/2016/8056370

133. Sunanda, Rao MS, Raju TR. Effect of chronic restraint stress on dendritic spines and excrescences of hippocampal CA3 pyramidal neurons-a quantitative study. *Brain Research*. 1995;694:312-317. doi:10.1016/0006-8993(95)00822-8
134. Hayashi Y, Koyanagi S, Kusunose N, et al. The intrinsic microglial molecular clock controls synaptic strength via the circadian expression of cathepsin S. *Scientific Reports*. 2013;3:1-7. doi:10.1038/srep02744
135. Chaudhury D, Wang LM, Colwell CS. Circadian regulation of hippocampal long-term potentiation. *Journal of Biological Rhythms*. 2005;20(3):225-236. doi:10.1177/0748730405276352
136. Wardlaw SM, Phan TX, Saraf A, Chen X, Storm DR. Genetic disruption of the core circadian clock impairs hippocampus-dependent memory. *Learning and Memory*. 2014;21(9):498.
137. Liston C, Cichon JM, Jeanneteau F, Jia Z, Chao M v., Gan WBB. Circadian glucocorticoid oscillations promote learning-dependent synapse formation and maintenance. *Nature Neuroscience*. 2013;16(6):698-705. doi:10.1038/nn.3387
138. Liston C, Cichon JM, Jeanneteau F, Jia Z, Chao M v., Gan WB. Circadian glucocorticoid oscillations promote learning-dependent synapse formation and maintenance. *Nature Neuroscience*. 2013;16(6):698-705. doi:10.1038/nn.3387
139. Myers B, McKlveen JM, Morano R, et al. Vesicular glutamate transporter 1 knockdown in infralimbic prefrontal cortex augments neuroendocrine responses to chronic stress in male rats. *Endocrinology*. 2017;158(10):3579-3591. doi:10.1210/en.2017-00426
140. Jessica M. McKlveen, Brent Myers, Jonathan N. Flak, Jana Bundzikova, Matia B. Solomon, Kim B. Seroogy and JPH. Role of Prefrontal Cortex Glucocorticoid Receptors in Stress and Emotion. *Biol Psychiatry*. 2013;74(9):672-679. doi:10.1016/j.biopsych.2013.03.024.Role
141. Heck AL, Thompson MK, Uht RM, Handa RJ. Sex-dependent mechanisms of glucocorticoid regulation of the mouse hypothalamic corticotropin-releasing hormone gene. *Endocrinology (United States)*. 2020;161(1):1-15. doi:10.1210/endo/bqz012
142. Dickmeis T. Glucocorticoids and the circadian clock. *Journal of Endocrinology*. 2009;200(1):3-22. doi:10.1677/JOE-08-0415
143. Buijs RM, la Fleur SE, Wortel J, et al. The suprachiasmatic nucleus balances sympathetic and parasympathetic output to peripheral organs through separate preautonomic neurons. *Journal of Comparative Neurology*. 2003;464(1):36-48. doi:10.1002/cne.10765
144. Ulrich-Lai YM, Arnhold MM, Engeland WC. Adrenal splanchnic innervation contributes to the diurnal rhythm of plasma corticosterone in rats by modulating adrenal sensitivity to ACTH. *American Journal of Physiology - Regulatory Integrative and Comparative Physiology*. 2005;290(4):1128-1135. doi:10.1152/ajpregu.00042.2003
145. Abe K, Kroning J, Greer MA, Critchlow V. Effects of destruction of the suprachiasmatic nuclei on the circadian rhythms in plasma corticosterone, body temperature, feeding and plasma thyrotropin. *Neuroendocrinology*. 1979;29(2):119-131. doi:10.1159/000122913

146. Perez-Cruz C, Simon M, Flügge G, Fuchs E, Czéh B. Diurnal rhythm and stress regulate dendritic architecture and spine density of pyramidal neurons in the rat infralimbic cortex. *Behavioural Brain Research*. 2009;205(2):406-413. doi:10.1016/j.bbr.2009.07.021
147. Liston C, Cichon JM, Jeanneteau F, Jia Z, Chao M v., Gan WB. Circadian glucocorticoid oscillations promote learning-dependent synapse formation and maintenance. *Nature Neuroscience*. 2013;16(6):698-705. doi:10.1038/nn.3387
148. Woodruff ER, Chun LE, Hinds LR, et al. Coordination between prefrontal cortex clock gene expression and corticosterone contributes to enhanced conditioned fear extinction recall. *eNeuro*. 2018;5(6). doi:10.1523/ENEURO.0455-18.2018
149. Hindson BJ, Ness KD, Masquelier DA, et al. High-throughput droplet digital PCR system for absolute quantitation of DNA copy number. *Analytical Chemistry*. 2011;83(22):8604-8610. doi:10.1021/ac202028g
150. Miotke L, Lau BT, Rumma RT, Ji HP. High sensitivity detection and quantitation of DNA copy number and single nucleotide variants with single color droplet digital PCR. *Analytical Chemistry*. 2014;86:2618-2624. doi:10.1021/acs.analchem.5b00061
151. Pinheiro LB, Coleman VA, Hindson CM, et al. Evaluation of a droplet digital polymerase chain reaction format for DNA copy number quantification. *Analytical Chemistry*. 2012;84:1003-1011. doi:10.1021/ac202578x
152. Oyola MG, Portillo W, Reyna A, et al. Anxiolytic effects and neuroanatomical targets of estrogen receptor- β (ER β) activation by a selective ER β agonist in female mice. *Endocrinology*. 2012;153(2):837-846. doi:10.1210/en.2011-1674
153. Heck AL, Handa RJ. Androgens drive sex biases in hypothalamic corticotropin-releasing hormone gene expression after adrenalectomy of mice. *Endocrinology*. 2019;160(7):1757-1770. doi:10.1210/en.2019-00238
154. Weiser MJ, Foradori CD, Handa RJ. Estrogen receptor beta activation prevents glucocorticoid receptor-dependent effects of the central nucleus of the amygdala on behavior and neuroendocrine function. *Brain Research*. 2010;1336:78-88. doi:10.1016/j.brainres.2010.03.098
155. Gerfen CR, Economo MN, Chandrashekar J. Long Distance Projections of Cortical Pyramidal Neurons. *Journal of Neuroscience*. 2018;96(9):1467-1475. doi:10.1002/jnr.23978.Long
156. Shrestha P, Mousa A, Heintz N. Layer 2/3 pyramidal cells in the medial prefrontal cortex moderate stress induced depressive behaviors. *Elife*. 2015;4(September2015):1-24. doi:10.7554/eLife.08752
157. Gabbott PLA, Warner TA, Jays PRL, Salway P, Busby SJ. Prefrontal cortex in the rat: Projections to subcortical autonomic, motor, and limbic centers. *Journal of Comparative Neurology*. 2005;492(2):145-177. doi:10.1002/cne.20738
158. Radley JJ, Rocher AB, Rodriguez A, et al. Repeated Stress Alters Dendritic Spine Morphology in the Rat Medial Prefrontal Cortex. *Journal of Comparative Neurology*. 2008;507(1):1141-1150. doi:10.1002/cne

159. Liston C, Miller MM, Goldwater DS, et al. Stress-induced alterations in prefrontal cortical dendritic morphology predict selective impairments in perceptual attentional set-shifting. *Journal of Neuroscience*. 2006;26(30):7870-7874. doi:10.1523/JNEUROSCI.1184-06.2006
160. Anderson RM, Johnson SB, Lingg RT, Hinz DC, Romig-Martin SA, Radley JJ. Evidence for Similar Prefrontal Structural and Functional Alterations in Male and Female Rats following Chronic Stress or Glucocorticoid Exposure. *Cerebral Cortex*. 2020;30(1):353-370. doi:10.1093/cercor/bhz092
161. Nava N, Treccani G, Alabsi A, et al. Temporal dynamics of acute stress-induced dendritic remodeling in medial prefrontal cortex and the protective effect of desipramine. *Cerebral Cortex*. 2017;27(1):694-705. doi:10.1093/cercor/bhv254
162. Radley JJ, Anderson RM, Hamilton BA, Alcock JA, Romig-Martin SA. Chronic stress-induced alterations of dendritic spine subtypes predict functional decrements in an hypothalamo-pituitary-adrenal-inhibitory prefrontal circuit. *Journal of Neuroscience*. 2013;33(36):14379-14391. doi:10.1523/JNEUROSCI.0287-13.2013
163. Russell AL, Miller L, Yi H, Keil R, Handa RJ, Wu TJ. Knockout of the circadian gene, *Per2*, disrupts corticosterone secretion and results in depressive-like behaviors and deficits in startle responses. *BMC Neuroscience*. 2021;22(1):1-11. doi:10.1186/s12868-020-00607-y
164. Dallmann R, Touma C, Palme R, Albrecht U, Steinlechner S. Impaired daily glucocorticoid rhythm in *Per1Brd* mice. *Journal of Comparative Physiology A: Neuroethology, Sensory, Neural, and Behavioral Physiology*. 2006;192(7):769-775. doi:10.1007/s00359-006-0114-9
165. Netser S, Meyer A, Magalnik H, et al. Distinct dynamics of social motivation drive differential social behavior in laboratory rat and mouse strains. *Nature Communications*. 2020;11:1-19. doi:10.1038/s41467-020-19569-0
166. Whishaw IQ, Tomie JA. Of Mice and Mazes: Similarities Between Mice and Rats on Dry Land But Not Water Mazes. *Physiology & Behavior*. 1996;60(5):1191-1197.
167. Routh BN, Johnston D, Harris K, Chitwood RA. Anatomical and electrophysiological comparison of CA1 pyramidal neurons of the rat and mouse. *Journal of Neurophysiology*. 2009;102:2288-2302. doi:10.1152/jn.00082.2009
168. Sierra-Mercado D, Padilla-Coreano N, Quirk GJ. Dissociable roles of prelimbic and infralimbic cortices, ventral hippocampus, and basolateral amygdala in the expression and extinction of conditioned fear. *Neuropsychopharmacology*. 2011;36(2):529-538. doi:10.1038/npp.2010.184
169. Vidal-Gonzalez I, Vidal-Gonzalez B, Rauch SL, Quirk GJ. Microstimulation reveals opposing influences of prelimbic and infralimbic cortex on the expression of conditioned fear. *Learning & Memory*. 2006;13(6):728-733. doi:10.1101/lm.306106
170. Radley JJ, Arias CM, Sawchenko PE. Regional differentiation of the medial prefrontal cortex in regulating adaptive responses to acute emotional stress. *Journal of Neuroscience*. 2006;26(50):12967-12976. doi:10.1523/JNEUROSCI.4297-06.2006

171. Myers B, McKlveen JM, Morano R, et al. Vesicular glutamate transporter 1 knockdown in infralimbic prefrontal cortex augments neuroendocrine responses to chronic stress in male rats. *Endocrinology*. 2017;158(10):3579-3591. doi:10.1210/en.2017-00426
172. Wallace T, Schaeuble D, Pace SA, et al. Sexually divergent cortical control of affective-autonomic integration. *Psychoneuroendocrinology*. 2021;129:1-14. doi:10.1016/j.psyneuen.2021.105238
173. Schaeuble D, Packard AEB, McKlveen JM, et al. Prefrontal Cortex Regulates Chronic Stress-Induced Cardiovascular Susceptibility. *J Am Heart Assoc*. 2019;8(24):e014451. doi:10.1161/JAHA.119.014451
174. Pace SA, Christensen C, Schackmuth MK, et al. Infralimbic cortical glutamate output is necessary for the neural and behavioral consequences of chronic stress. *Neurobiology of Stress*. 2020;13:100274. doi:10.1016/j.ynstr.2020.100274
175. Wioland H, Guichard B, Senju Y, et al. ADF/Cofilin Accelerates Actin Dynamics by Severing Filaments and Promoting Their Depolymerization at Both Ends. *Current Biology*. 2017;27:1956-1967.e7. doi:10.1016/j.cub.2017.05.048
176. Larsson C. Protein kinase C and the regulation of the actin cytoskeleton. *Cellular Signalling*. 2006;18:276-284. doi:10.1016/j.cellsig.2005.07.010
177. Nadella KS, Saji M, Jacob NK, Pavel E, Ringel MD, Kirschner LS. Regulation of actin function by protein kinase A-mediated phosphorylation of Limk1. *EMBO Reports*. 2009;10(6):599-605. doi:10.1038/embor.2009.58
178. Mendoza MC, Vilela M, Juarez JE, Blenis J, Danuser G. ERK reinforces actin polymerization to power persistent edge protrusion during motility. *Science Signaling*. 2015;8(377):1-21. doi:10.1126/scisignal.aaa8859
179. Zuloaga DG, Zuloaga KL, Hinds LR, Carbone DL, Handa RJ. Estrogen receptor β expression in the mouse forebrain: age and sex differences. *J Comp Neurol*. 2014;522(2):358-371. doi:10.1002/cne.23400
180. Seale J v., Wood SA, Atkinson HC, et al. Gonadectomy reverses the sexually divergent patterns of circadian and stress-induced hypothalamic-pituitary-adrenal axis activity in male and female rats. *Journal of Neuroendocrinology*. 2004;16(6):516-524. doi:10.1111/j.1365-2826.2004.01195.x
181. Shors TJ, Chua C, Falduto J. Sex differences and opposite effects of stress on dendritic spine density in the male versus female hippocampus. *Journal of Neuroscience*. 2001;21(16):6292-6297. doi:10.1523/jneurosci.21-16-06292.2001
182. Milad MR, Igoe SA, Lebron-Milad K, Novales JE. Estrous cycle phase and gonadal hormones influence conditioned fear extinction. *Neuroscience*. 2009;164:887-895. doi:10.1016/j.neuroscience.2009.09.011
183. United States Department of Labor. Job Flexibilities and Work Schedules Summary. Occupational Outlook Handbook. Published 2019. Accessed April 16, 2022. <https://www.bls.gov/news.release/flex2.nr0.htm>

184. Abbott SM, Malkani RG, Zee PC. Circadian disruption and human health: A bidirectional relationship. *Eur J Neurosci.* 2020;51(1):567-583. doi:10.1111/ejn.14298.Circadian
185. Lee A, Myung SK, Cho JJ, Jung YJ, Yoon JL, Kim MY. Night shift work and risk of depression: Meta-analysis of observational studies. *Journal of Korean Medical Science.* 2017;32(7):1091-1096. doi:10.3346/jkms.2017.32.7.1091
186. Manenschijn L, van Kruysbergen RGPM, de Jong FH, Koper JW, van Rossum EFC. Shift work at young age is associated with elevated long-term cortisol levels and body mass index. *Journal of Clinical Endocrinology and Metabolism.* 2011;96(11):1862-1865. doi:10.1210/jc.2011-1551
187. Harris A, Waage S, Ursin H, Hansen ÅM, Bjorvatn B, Eriksen HR. Cortisol, reaction time test and health among offshore shift workers. *Psychoneuroendocrinology.* 2010;35:1339-1347. doi:10.1016/j.psyneuen.2010.03.006
188. Brown DL, Feskanich D, Sánchez BN, Rexrode KM, Schernhammer ES, Lisabeth LD. Rotating night shift work and the risk of ischemic stroke. *American Journal of Epidemiology.* 2009;169(11):1370-1377. doi:10.1093/aje/kwp056
189. Karlsson B, Knutsson A, Lindahl B. Is there an association between shift work and having a metabolic syndrome? Results from a population based study of 27 485 people. *Occupational and Environmental Medicine.* 2001;58(11):747-752. doi:10.1136/oem.58.11.747
190. Wyse CA, Celis Morales CA, Graham N, et al. Adverse metabolic and mental health outcomes associated with shiftwork in a population-based study of 277,168 workers in UK biobank*. *Annals of Medicine.* 2017;49(5):411-420. doi:10.1080/07853890.2017.1292045
191. Manohar S, Thongprayoon C, Cheungpasitporn W, Mao MA, Herrmann SM. Associations of rotational shift work and night shift status with hypertension: A systematic review and meta-analysis. *Journal of Hypertension.* 2017;35(10):1929-1937. doi:10.1097/HJH.0000000000001442
192. Torquati L, Mielke GI, Brown WJ, Kolbe-Alexander T. Shift work and the risk of cardiovascular disease. A systematic review and meta-analysis including dose-response relationship. *Scandinavian Journal of Work, Environment and Health.* 2018;44(3):229-238. doi:10.5271/sjweh.3700
193. Monk TH, Buysse DJ. Exposure to shift work as a risk factor for diabetes. *Journal of Biological Rhythms.* 2013;28(5):356-359. doi:10.1177/0748730413506557
194. Zhang S, Wang Y, Wang Z, et al. Rotating night shift work and non-Alcoholic fatty liver disease among steelworkers in China: A cross-sectional survey. *Occupational and Environmental Medicine.* 2020;77(5):333-339. doi:10.1136/oemed-2019-106220
195. Tynes T, Hannevik M, Andersen A, Vistnes AI, Haldorsen T. Incidence of breast cancer in Norwegian female radio and telegraph operators. *Cancer Causes and Control.* 1996;7(2):197-204. doi:10.1007/BF00051295

196. Davis S, Mirick DK, Stevens RG. Shift work, light at night and risk of breast cancer. *J Natl Cancer Inst.* 2006;93(20):1557-1562. doi:10.1093/occmed/kql078
197. Rouch I, Wild P, Ansiau D, Marquie JC. Shiftwork experience, age and cognitive performance. *Ergonomics.* 2005;48(10):1282-1293. doi:10.1080/00140130500241670
198. Folkard S, Tucker P. Shift work, safety and productivity. *Occupational Medicine.* 2003;53(2):95-101. doi:10.1093/occmed/kqg047
199. Walker WH, Walton JC, DeVries AC, Nelson RJ. Circadian rhythm disruption and mental health. *Translational Psychiatry.* 2020;10(1). doi:10.1038/s41398-020-0694-0
200. Vadnie CA, McClung CA. Circadian Rhythm Disturbances in Mood Disorders: Insights into the Role of the Suprachiasmatic Nucleus. *Neural Plasticity.* 2017;2017:1-28. doi:10.1155/2017/1504507
201. Het S, Ramlow G, Wolf OT. A meta-analytic review of the effects of acute cortisol administration on human memory. *Psychoneuroendocrinology.* 2005;30:771-784. doi:10.1016/j.psyneuen.2005.03.005
202. Meuret AE, Rosenfield D, Bhaskara L, et al. Timing matters: Endogenous cortisol mediates benefits from early-day psychotherapy. *Psychoneuroendocrinology.* 2016;74:197-202. doi:10.1016/j.psyneuen.2016.09.008
203. Pace-Schott EF, Spencer RMC, Vijayakumar S, et al. Extinction of Conditioned Fear is Better Learned and Recalled in the Morning than in the Evening. *Journal of Psychiatric Research.* 2013;47(11):1776-1784. doi:10.1016/j.jpsychires.2013.07.027. Extinction

LIST OF ABBREVIATIONS

ACC	Anterior cingulate cortex
ACTH	Adrenocorticotrophic Hormone
ADX	Adrenalectomy
AMPA/AMPAr	α -amino-3-hydroxy-5-methyl-4-isoxazolepropionic acid receptor
ANOVA	Analysis of variance
AVP	Arginine vasopressin
BA	Brodmann area
BLA	Basolateral amygdala
Bmal1	Brain and muscle Arnt-like protein-1
BMI	Bicuculline methiodide
BNSTov	Oval nucleus of the bed nucleus of the stria terminalis
CA	Cornu ammonis
Ca ²⁺	Calcium
CAM	Calmodulin
CAM-Kinase	Calmodulin-dependent protein kinase
CCG	clock-controlled gene
CEA	Central nucleus of the amygdala
ChR2	Channelrhodopsin-2
CK	Casein kinase
CLOCK	Circadian locomotor output cycles kaput
CORT	Corticosterone
CREB	Cyclic-AMP response element binding protein
CRH	Corticotropin releasing hormone

Cry	Cryptochrome
CTb	Cholera toxin beta subunit
ddPCR	Droplet digital PCR
DEX	Dexamethasone
DMH	Dorsomedial nucleus of the hypothalamus
E-Box	Enhancer Box
ELISA	Enzyme-linked immunosorbent assay
EPSC	Excitatory postsynaptic current
EPSP	Excitatory postsynaptic potential
ERK	Extracellular signal-related kinase
F-actin	Filamentous actin
GABA	γ -Aminobutyric acid
GC	Glucocorticoid
GNRH	Gonadotropin releasing hormone
GR	Glucocorticoid receptor
GRE	Glucocorticoid response element
GRP	Gastrin-releasing peptide
HPA	Hypothalamic-pituitary-adrenal
IHC	Immunohistochemistry
IL	Infralimbic Area
ipRGC	intrinsically photosensitive retinal ganglion cell
JNK	c-Jun N-terminal kinase
L:D	Light:Dark
LIMK	LIM kinase
LTD	Long-term depression

LTP	Long-term potentiation
LUC	Luciferase
MUS	Muscimol
NAc	Nucleus accumbens
NGS	Normal goat serum
NMDA/NMDAr	<i>N</i> -methyl-D-aspartate receptor
OT	Oxytocin
OVLT	Organum vasculosum lamina terminalis
PBS	Phosphate buffered saline
PBST	Phosphate buffered saline with 0.1% triton-X
Per	Period (gene)
PFC	Prefrontal cortex
PKA	Protein kinase A
PKC	Protein kinase C
PL	Prelimbic Area
PRV	Pseudorabies virus
PSD	Postsynaptic Density
PTSD	Posttraumatic stress disorder
PVN	Paraventricular Nucleus
PVT	Paraventricular thalamic nucleus
qPCR	Quantitative PCR
RIA	Radioimmunoassay
SCN	Suprachiasmatic Nucleus
SEM	Standard error of the mean
siRNA	Small interfering RNA

SON	Supraoptic Nucleus
V1AR	AVP receptor 1
Veh	Vehicle
vGlut1	Vesicular glutamate transporter 1
VIP	Vasoactive intestinal peptide
vmPFC	Ventromedial prefrontal cortex
VO	Ventrorobital cortex
VPAC2	Vasoactive intestinal peptide receptor 2